# Application of the Finite Element Method in the Human Spine Biomechanics

**by**

**Iman Zafarparandeh**

**A Thesis Submitted to the**

**Graduate School of Science and Engineering**

**in Partial Fulfillment of the Requirements for**

**the Degree of**

**Doctor of Philosophy**

**in**

**Department of Mechanical Engineering**

**Koc University**

**May 2015**

We are not machines exploring the universe, we are people and we are taking that ability to adapt, and that ability to understand and the ability to take our own self–perception to a new place.

Chris Hadfield

To

my Mom and Dad

my sisters, Sima and Mina

# Abstract:

Since its development in the mid 20th Century, the finite element (FE) method has shown to be a reliable tool, not only in mechanical engineering, but also in other fields such as electronics, or thermodynamics. In biomechanics, the principles of continuum mechanics and constitutive equations so far successfully applied to plastics, metals, and rubbers, have demonstrated their potential to reproduce general behaviors of the musculoskeletal system, when coupled to finite element models. The main of goal of the present thesis is to develop accurate FE models of the human cervical and the lumbar spine. A novel method was suggested to construct an integrated interface between the discs and the vertebrae. Hexahedral element was used to mesh the discs and vertebrae. Truss elements were used to simulate the ligaments. The exact geometry was obtained from CT scan data. All the main features of the human spine were modeled; vertebrae, intervertebral discs, and ligaments. Pure moments were used in simulations and lower part of each models were constrained in all directions. The predicted motion responses of both models were compared with the published in vitro studies in the literature and they were in good agreement. The effect change in the geometry of the cervical spine on the biomechanical parameters was studied. An FE model with the symmetry assumption in the mid-sagittal plane was developed using the CT data similar to the accurate cervical model. The reason to use such assumption is the numerous FE models in the literature symmetry approximation. The comparison of the biomechanical parameters showed that the symmetric model produces reasonable results and using the symmetry assumption reduce the modeling time. Different types of instruments were applied to both the cervical and the lumbar models. The effect of the

instruments on the kinematic, range of motion (ROM), and kinetic, intradiscal pressure (IDP), facet load (FL), and ligament stress (LS), parameters of the cervical and the lumbar spine were investigated. The instruments included total disc replacement (TDR), posterior dynamic stabilization (PDS), fusion, interspinous fusion, and sacroiliac wings. Design modifications were suggested after comparing the biomechanical behavior of the instrumented models with intact models.

**Özet:**

Ortalarında 20. yüzyılda gelişimi bu yana, sonlu elemanlar (FE) yöntemi makine mühendisliği, fakat aynı zamanda elektronik veya termodinamiğin gibi diğer alanlarda sadece güvenilir bir aracı olarak görülmüştür. Biyomekanik olarak, sürekli mekaniği ve bünye denklemleri ilkeleri bugüne kadar başarıyla, plastik, metal ve kauçuk uygulanan sonlu elemanlar modelleri birleştiğinde kas-iskelet sistemi, genel davranışları çoğaltmak kendi potansiyellerini ortaya koymuştur. Mevcut tezin hedefi temel insan servikal ve lomber doğru FE modelleri geliştirmektir. Yeni bir metot diskler ve omur arasında entegre bir arayüz yapısı önerilmiştir. Hexahedral eleman diskleri ve omurları örgü için kullanılmıştır. Kafes elemanları bağ simüle etmek için kullanıldı. Tam geometri CT taraması verilerinden elde edilmiştir. İnsan omurga tüm temel özellikleri modellenmiştir; vertebra, intervertebral diskler ve ligament. Saf anlar simülasyonlar kullanıldı ve her modellerin alt kısmı her yöne kısıtlı bulundu. Her iki modelin tahmin hareket cevapları literatürde yayınlanmış in vitro çalışmalar ile karşılaştırılmış ve onlar iyi anlaşma vardı. biyomekanik parametreler üzerine servikal geometri etkisi değişikliği çalışılmıştır. Mid-sagital düzlemde simetri varsayımı ile FE modeli doğru servikal modeline benzer BT verileri kullanılarak geliştirildi. Böyle varsayımı kullanmak için bir neden edebiyat simetri yaklaşımı çok sayıda FE modelleri. Biyomekanik parametrelerin karşılaştırılması simetrik modeli makul sonuçlar üretir ve simetri varsayımı modelleme süresini azaltmak kullanarak gösterdi. Araç türleri, servikal ve bel modelleri hem uygulanmıştır. Hareket (EHA) kinematik, dizi araçların etkisi ve kinetik, intradiskal basıncı (IDP), faset yükü (FL), ve ligament stres (LS), servikal ve lomber parametreleri araştırıldı. araçlar, toplam disk replasmanı (TDR), posterior dinamik stabilizasyon (PDS), füzyon, interspinöz füzyon ve sakroiliak kanatları dahil. Tasarım

değişiklikleri sağlam modelleri ile Araçlı modellerin biyomekanik davranışını karşılaştırarak sonra önerilmiştir.

## Acknowledgments

I express my most sincere gratitude to my advisor, Dr. Deniz Erbulut for his continuous guidance throughout my PhD program. His advice and support during my research work and compilation of my thesis were invaluable. I was able to learn a lot from his vast expanse of knowledge.

I would like to express my special thanks to Dr. Fahir Ozer for his guidance in my research. The knowledge he shared and the counsel he provided were immensely helpful. I also thank Dr. Demircan Canadinc for serving on my thesis committee and his guidance in making this report better.

Special thanks to the Neurosurgery Department in American Hospital and Algoritma Company that provided the financial support during my study for fulfilling my research.

My graduate studies would not have been the same without the social and academic challenges provided by all of my friends that I made during my stay in Koc University. A special thanks to Araz Bateni, Farhad Ghorbani, Ali Aleali, Ahad Khaleghi, and many others.

## Table of Contents

# List of Figures

# List of Tables

# Introduction

## 1. Motivation for research

Clinical studies, animal and cadaver models, and mathematical simulations have advanced the under- standing of normal, diseased, and injured conditions of the cervical spine. Clinical studies have assessed treatment outcomes, quantified injury rate, and identified influencing factors for injury susceptibility and severity. Animal and cadaveric models have quantified the external angular rotation biomechanical response to a wide variety of external loadings. However, it is not possible to directly measure internal responses such as stress and strain in experimental or animal models. Internal tissue responses may be decisive variables in predicting the pathology of cervical spondylosis and other disease conditions. Mathematical simulations have the greatest advantage in this area. The finite element method is capable of quantifying both external and internal responses to mechanical loading. FE models allow, in effect, "surrogate experiments," characterized by absolute repeatability. They enable the user to vary parameter and observe any resulting changes in the final outcome. FE models go beyond experiments, in that they often provide estimation of parameters that cannot be measured experimentally. The results from FE models can suggest crucial experiments that should be undertaken.

## 2. Research objective and approach

The goal of the present research was to develop accurate FE models of the cervical and the lumbar spine. The accurate geometry was obtained from CT data provided by the American Hospital in Istanbul. The CT data were processed in MIMICS software and the surface definition of the vertebrae

and discs were generated. The hexahedral mesh was created on the vertebrae and discs in IA-FEMESH. The material properties, load, and boundary conditions were added into the ABAQUS software. Pure moments were used in simulations and the predicted range of motion (ROM) was compared to the in vitro studies in the literature.

After validating the models, different types of instruments were applied to the models. The instruments were designed in SOLIDWORKS software. Tetrahedral mesh was generated on the instruments. Necessary surgery before adding the instrument was simulated by removing the target elements. All steps of the instrumentation were performed with the recommendations of the surgeons.

# Chapter 1:

## Application of the Finite Element Method in Spinal Implant Design and Manufacture[1]

[1]Iman Zafarparandeh, Ismail Lazoglu, Application of the Finite Element Method in Spinal Implant Design and Manufacture, Book Chapter, In: The Design and Manufacture of Medical, Woodhead Publishing, Pages 153-183, October 2012.

## 1. Introduction to Finite Element Method

In a general view, a numerical model is a combination of large number of mathematical equations that depends on computers to find an approximate solution to the underlying physical problem. Thus, a numerical model can be considered a particular instance of a mathematical model, which is in physics, the way we represent a theory ([1]; [2]). Because of representing complex systems, numerical models are utilized to simulate and study a large range of problems in biomechanics ranging from classical structural analysis and mass transport, to fluid mechanics, etc. In the field of biomechanics and related research, one of the biggest challenge is the uncertain material properties and complex micro and macro-geometry of the biological tissues taken into account in analysis. On the other side, the validity of the tools themselves, such as finite element method, is achieved when they are used correctly. It was 1922 that the finite element method was suggested for the first time by Richard Courant, but at that time lack of computers was a barrier for taking the advantage of the method ([3]). During the 1950s to 1960s the finite element method found noticeable popularity in solving engineering problems but this technique was introduced to

spine in 1970 with thorax modeling and then the vertebral column in 1973 ([4]). Nowadays, analyzing the stress and the load transfer in the biomechanics of the human spine is feasible by means of the finite element method which itself is the result of continuous advancements in computer technology.

The development cycle of medical devices is complex involving several steps. These steps include clinician/engineer teams conducting prototype design, animal trials, clinical trials, multi-centre trials, obtaining regulatory approval, and conducting postmarketing surveillance. Use of non-linear finite element analysis and simulation can be critical at the prototype stage to explore the functionality of proposed design concepts and manufacturing methods, and to perform "what-if" material sensitivity analyses. In fact, the balance of simulation-versus-experimental-modelling is particularly important, and making this decision requires knowledge of the capabilities of finite element analysis. Reducing experiments may be particularly an issue if animal experiments are required where an objective is to reduce the number of animals used. Finite element modelling and simulation is playing an increasing role in medical device regulation, and may be submitted as part of the information regarding design functionality to regulatory bodies ([5]; [6]; [7]; [8]). The role of computer simulation as part of the preoperative planning process is still in its preliminary stage, and finite element modelling may have a key role to play in this.

## 2. General Aspects of FEM

A finite element model has three aspects; the geometric representation, the material representation (constitutive laws) and, the boundary conditions (loading and restraints).

One aspect of finite element modelling that is clearly essential for future developments is the use of geometric data from medical images to create finite element models that are anatomically accurate. In the case of the spine, the geometry can be transferred e.g. from computed tomographs (Figure 1), magnetic resonance images, from the visual human project ([9]). The material properties of the spine components vary strongly and are mostly only available from in vitro studies ([10]; [11]). The elastic modulus of the nucleus pulposus may be 100 kPa while that of the cortical bone of the vertebra may have a value of 10 GPa. Unfortunately, experimentally determined material values vary strongly in the literature even for the same structure. Thus, it is not sufficient to adopt a certain literature value and then assume that the results can be generalized. As shown in Figure 2 similar to other numerical methods, finite element method allows us to analyze the problem by splitting it to numerous finite elements and simulating the behavior of each of them under the certain boundary conditions. By using these elements, the modeling of complex irregular geometries as in biomedical cases is feasible ([12]).

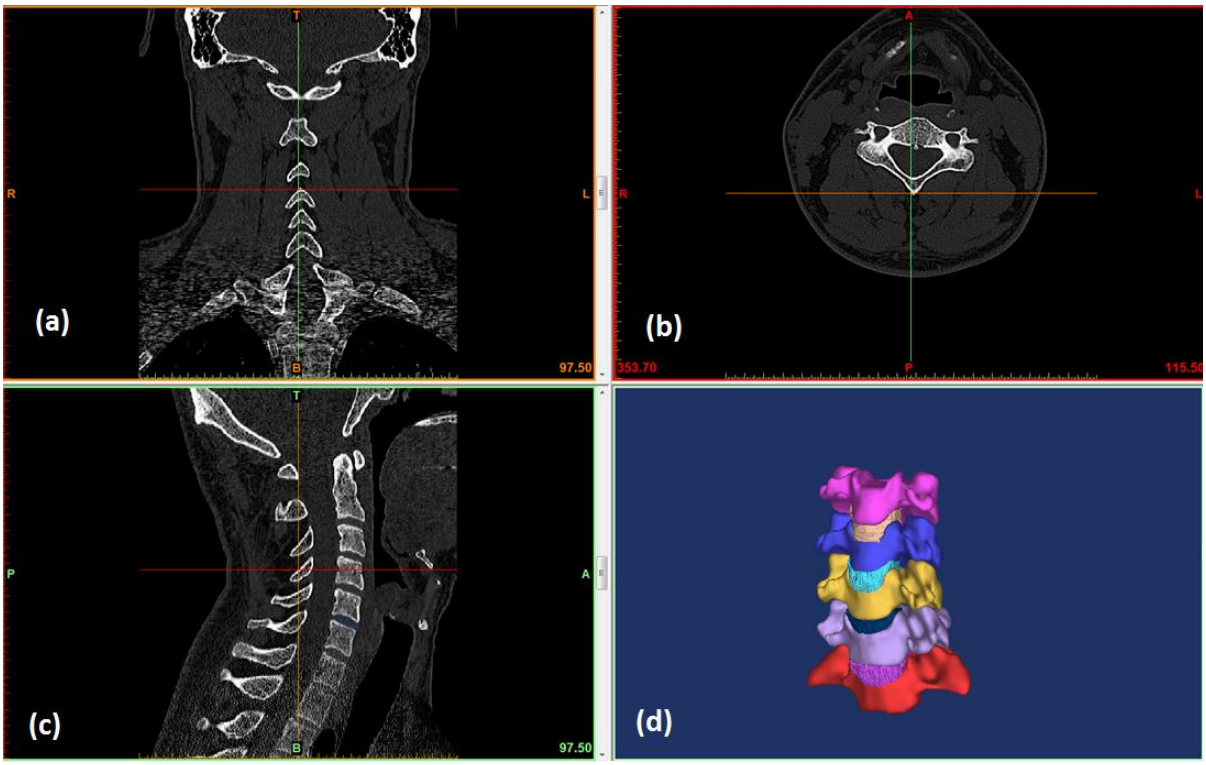


**Figure 1: Computer Tomography scans of the cervical spine of a patient; (a) front view, (b) top view, (c) right view and (d) 3-D STL model of the whole cervical spine.**

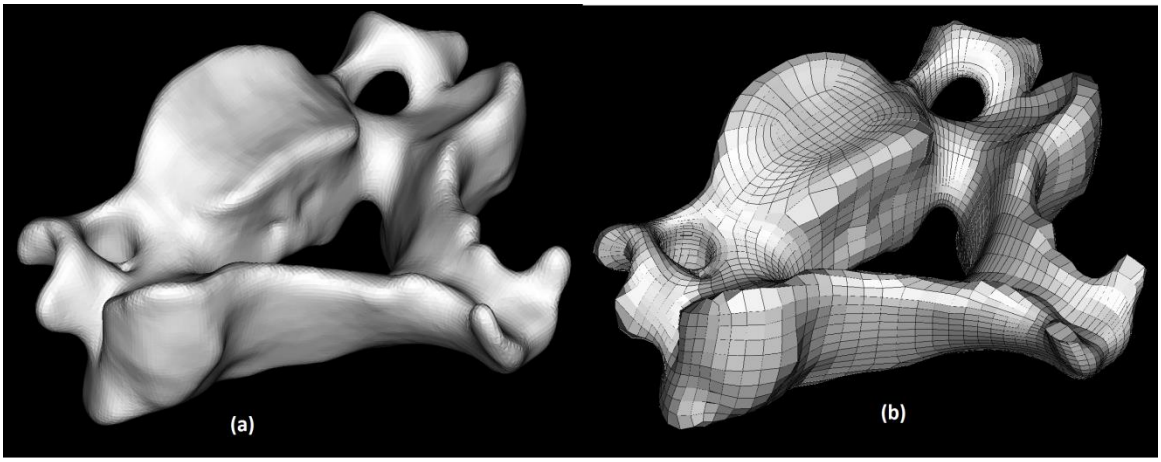


**Figure 2: Splitting the STL model to numerous finite elements for C5; (a) the STL model, (b) the meshed model.**

## 3. Parts of the finite element model of spine

The finite element model of the spine is consisted of several major components; vertebrae, intervertebral discs and ligaments. For each component the material property and the type of element being used as well as other parameters, which are explained in the following, differ completely.

### 3.1 Vertebra

The vertebral body has several key features that should be considered in its simulation. From the material point of view there are two different parts: cortical shell and cancellous core, while on the geometry side there are vertebral body and posterior part ([13]; [14, 15]). The cortical shell surrounds the cancellous core which is made up of a lattice of trabecular struts. In the FE model, the cancellous part is considered for the vertebral body and the left part is considered as the cortical shell, Figure 3. The material properties of these two parts of vertebra are similar to some extent. Furthermore, in some literature, vertebrae are considered as rigid bodies comparing to other soft tissues in the spine ([15]).

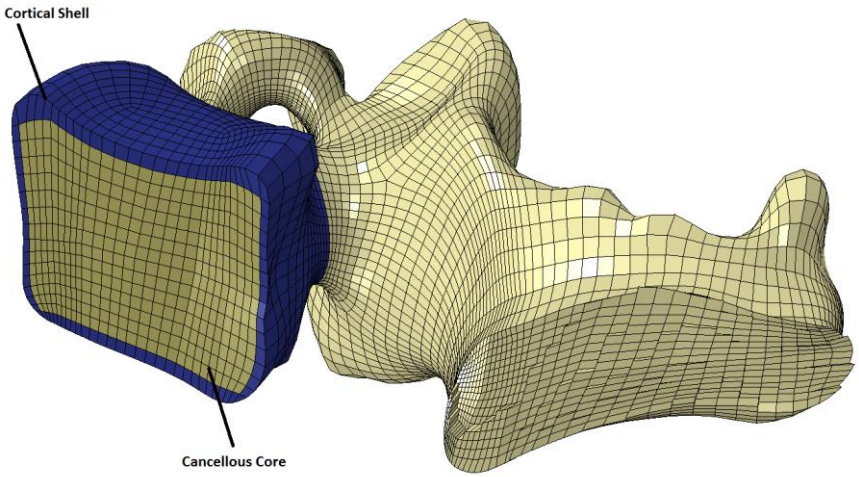

**Figure 3: Cancellous core and cortical shell for assigning the material properties shown on the section view of C5 meshed model.**

Geometry is usually achieved from the surface representation of the anatomical structure data. Nowadays, the most common source of geometric data is subject-specific medical imaging, typically computed tomography (CT). A surface extraction step is required to find the STL format of the surface which can be done by several available softwares in the market. This technique allows the researcher to select the parameters based on the subject specific (age, gender, pathology, and etc). Use of quantitative computed tomography (QCT) also provides additional information regarding bone density and structure. Material property formulation is defined based on the complexity of the problem being considered. In some cases the vertebrae are modeled as rigid bodies when the behavior of the soft tissues is pointed out and the degrees of freedom is greatly reduced, also the solution time ([16]). The common simplified model for the bone is a homogenous isotropic elastic material.

Finite element models of the vertebra can be divided into those whose geometry matches that of a particular in vitro specimen and those which have generic geometries representing an average vertebra. Vertebral models may be fall in to two categories. Generic models of vertebrae have been developed from anatomical measurements for various purposes ([17]; [18]; [19]). In these models the geometry is fully parameterised, allowing for straight-forward regeneration of try is lost. However, the cubic mesh resolution is commonly much lower than that of the source images, allowing for a lower number of elements. A clear advantage of voxel-based vertebral models is the simplicity of the mesh generation process. In order to maintain the straight-forward mesh generation, the cortical surfaces of these

models are commonly rough. Also, the endplates are flat, corresponding to the three-dimensional voxel faces. Recent models have built on the voxel-meshing foundation and used mesh smoothing on the surface to improve the geometric fit. The initial mesh is generated from the image voxels, creating hexahedral elements. The surface is then smoothed by converting to tetrahedral elements where necessary. This method allows for anatomical cortical shell and endplate shape in specimen-specific models.

Vertebral body models provide valuable insight into a number of aspects of the loading regime within the spine for healthy and degenerated cases. The respective load bearing roles of the cortical shell and cancellous core have been investigated, as well as the effect of bone distribution on vertebral strength. The principal clinical driver for the detailed modelling of the single human vertebra is the accurate prediction of compressive strength. Currently models are developed, and validated with, in vitro experiments. However, the longer term aim is to use the methods to predict fracture risk in vivo, replacing the current most common clinical measure of bone mineral density (BMD) taken from medical images. The most recent study to compare these methods shows that finite element based techniques are significantly more effective than pure bone BMD measures ([20]). A number of vertebral finite element models include an inhomogeneous representation of the cancellous bone structure. Consequently, they can be used to predict the location of failure by analysing the micro-strain for each element and provide a distribution of at-risk tissue. Single vertebral models have also been constructed to simulate the presence of another material within the vertebral body, such as bone cement after a vertebroplasty procedure, or a tumour in a metastatically involved spine ([19]; [21]).

### 3.2 Intervertebral Disc

The intervertebral disc is a complex structure. It is inhomogenous, anisotropic and porous. Its behaviour is governed by its biochemical as well as mechanical composition. Simulation of the disc function is therefore challenging and has led to the development of a number of different approaches to represent its behaviour.

As with the vertebral simulations, one of the major reasons for modelling the disc has been to investigate the disease state. Vertebral modelling has focused mostly on predicting strength and fracture risk. However, disc research has concentrated more on developing an understanding of the degeneration process itself, and its effects on the tissue biomechanics. As well as the natural disc tissue, a limited number of studies have also investigated treatments for degeneration. These include a parametric analysis of nucleus replacement materials ([22]). Recently, a simulation of the wear in total disc replacement devices is performed ([23]). In general, the geometry of the disc has been simplified. For example, a number of authors assumed the structure to be axisymmetric ([24]; [25]; [26, 27]) or to exhibit symmetry in either the sagittal ([28]) or sagittal and transverse planes. In any cases, the cranial and caudal surfaces of the disc have also been assumed to be flat, although a more realistic curvature has been included in some segment models ([29]). The geometric dimensions have been taken from either in vitro measurements ([25]; [28]) or medical image data such as magnetic resonance imaging (MRI) ([29]) or CT ([30]; [31]; [32]). In the latter case, some dimensions have to be assumed or interpolated because of the lack of clear differentiation between the disc tissues under X-ray imaging. In contrast to the bony spinal components, the generation of the finite element mesh of the disc morphology is relatively

straight-forward. In most cases, the element size has been approximately uniformly distributed, although in a study of the cellular micromechanical environment, ([33]) used a multi-scale approach to couple a micro-scale mesh of the cell and surrounding matrix with a macro-scale mesh of a larger tissue sample. An example of the disc model showing the layers and the nucleus is presented in Figure 4,.

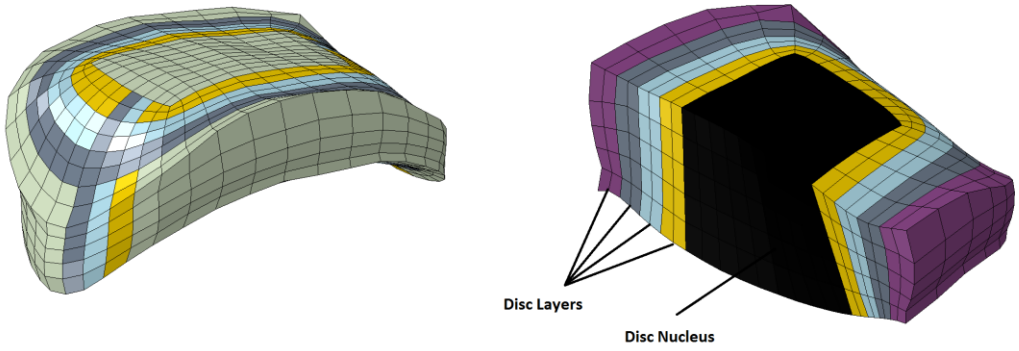


**Figure 4: FE model of the intervertebral disc and definition of the nucleus and layers.**

In recent years, increasingly complexity has been incorporated into the material models used to represent the intervertebral disc tissue, including the anisotropy of the annulus due to the collagen fibre orientation, the fluid content and fluid flow, the osmotic forces and the regional variations in tissue composition. In simulating the annulus behaviour, two methods have been commonly adopted to account for the collagen fiber orientation. Either the fiber bundles have been represented as truss or cable elements within a matrix of solid elements, or a homogenisation approach has been taken and anisotropic properties assigned to represent on the macroscale the fibre alignment within the extra-fibular matrix. A study by ([34]) compared the different approaches and found little difference between the formulations. The predicted tensile moduli of the constructed tissue were found to be consistent with values reported in the literature, but the predicted shear modulus was two

orders of magnitude greater than direct experimental measurements taken from the literature. The authors suggested the discrepancy might be because the fibres were not anchored in the experimental tests. This fact, highlights the potential for erroneous validation when finite element simulation results are compared to experimental results which do not necessarily have the same boundary conditions. Whilst anisotropic models alone may be sufficient to represent the instantaneous response of the intervertebral disc, simulation of the time-dependent response requires the inclusion of the biphasic behaviour of the tissue. Many of the models and parameters used in poroelastic simulations of the intervertebral disc have their origins in studies of articular cartilage. [35]were the first to present details of a finite element analysis of an intervertebral disc and adjacent vertebra. They modelled the problem assuming axial symmetry with linear orthotropic material properties for the disc. The same axisymmetric model was subsequently extended by assuming that the annulus had non-linear orthotropic properties, the actual values of which were derived by comparison with experimental measurements. Simon et al. (1985) first introduced poroelastic material behaviour into a finite element model of the disc. In this case, an axisymmetric model was used to simulate creep response. Both annulus and nucleus were considered as biphasic, comprising an incompressible fluid phase that saturates and flows through an elastic isotropic solid phase. Since this time, a number of authors have added further complexity to the poroelastic model.

**3.2 Ligaments**

As uniaxial structures, the role of ligaments is to resist the tensile or distractive forces. In contrast to the intervertebral discs, both the geometry and material property formulation of the ligamentous structures of the spine contribute significantly to the fidelity of the model ([36]; [37]; [38]; [39]; [40]). Material property formulation is also important for these structures, although they are often treated as simple elastic beam elements. A standard beam formulation for these elements imposes nonphysiologic loading during compression, and tension only cable elements are preferred when using discrete elements to represent the ligaments. Alternatively, both shell elements and volumetric elements have also been used, with cross-sectional properties based on values from representative cadaveric specimens or from the literature. Linear, bi-linear, and nonlinear elastic properties have been used with each of these element formulations, Figure 5.

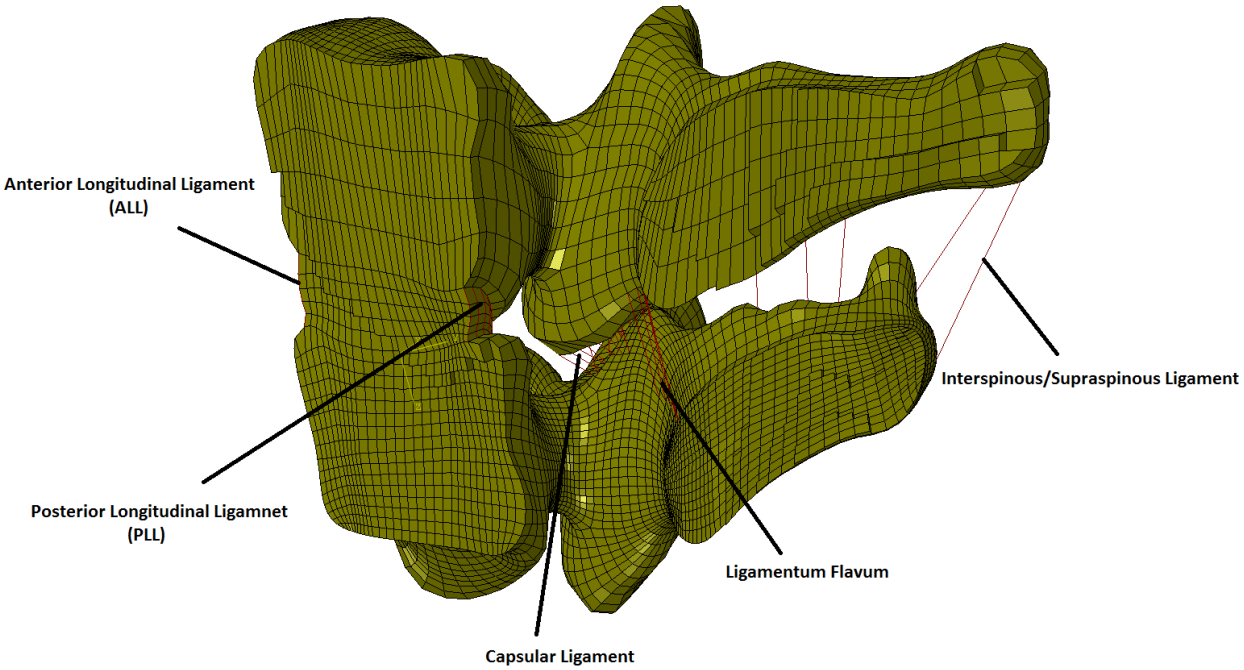

**Figure 5: Using cable elements to represent the ligaments.**

Most ligaments contain an inherent tensile in situ strain, which is evidenced by the immediate retraction observed when the ligament is cut ([41]). However, there is some disagreement regarding whether this is indeed the case in the spinal ligaments ([36]; [37]). It appears that the magnitude of this prestrain is relatively small and can possibly be ignored in most finite element simulations of the spine.

## 4. Verification

In extreme synthesis, verification is about solving the equations right; validation is about solving the right equations ([42]). A verified code yields the correct solution to benchmark problems of known solution (analytic or numeric), but does not necessarily guarantee that it will accurately represent complex biomechanical problems (American Institute of Aeronautics and Astronautics, 1998). From this definition, it is clear that verification must precede validation. The need for validation is obviated if the numerical implementation of the proposed model is not accurate in its own right. Verification is composed of two categories, code and calculation verification. Code verification ensures the mathematical model and solution algorithms are working as intended. Typically the numerical algorithms are in the framework of finite-difference or finite-element (FE) methods, in which discretized domains are solved iteratively until the convergence criteria are met. The assessment of numerical error has been studied extensively and is suggested to follow a hierarchy of test problems. This includes comparison to exact analytical solutions (most

accurate, but least likely to exist for complex problems), semi-analytic solutions with numerical integration of ordinary differential equations, and highly accurate numerical solutions to partial differential equations describing the problem domain. An example of code verification is found in [43], where a transversely isotropic hyperelastic constitutive model implementation was verified against an analytical solution for the case of equibiaxial stretch. The code was capable of predicting stresses to within less than 3 of an analytical solution, thus verifying the code performance. Note that this was a limited test of applicability and does not mean the model could accurately predict other responses that were not independently verified.

Calculation verification focuses on errors arising from the discretization of the problem domain. Errors can arise from the discretization of both the geometry and analysis time and should be verified independently. A common way to characterize the discretization error in the FE method is via a mesh convergence study. A mesh is considered too coarse if subsequent refinement of the mesh results in predictions that are substantially different (i.e. solution does not asymptote). The consequence of incomplete mesh convergence is that the problem will generally be too “stiff” in comparison to an analytical solution, and increasing the number of elements will “soften” the FE solution. Studies of spinal segments have suggested that a change of less than of 5% in the solution output is adequate to ensure mesh convergence is complete. Mesh convergence is documented in the literature due to the prevalence in finite-element studies, and it is recommended for all discretized analyses ([44]; [45]; [46]).

## 5. Validation

Validation is the process of ensuring that a computational model accurately represents the physics of the real world system ([47]). While some consider validation of natural systems to be impossible, the engineering viewpoint suggests the "truth" about the system is a statistically meaningful prediction that can be made for a specific set of boundary conditions. This does not suggest that in vitro experimental validation (in a controlled laboratory environment) represents the in-vivo case since the boundary conditions are likely impossible to mimic. It means that if a simplified model cannot predict the outcome of a basic experiment, it is probably not suited to simulate a more complex system, Figure 6.

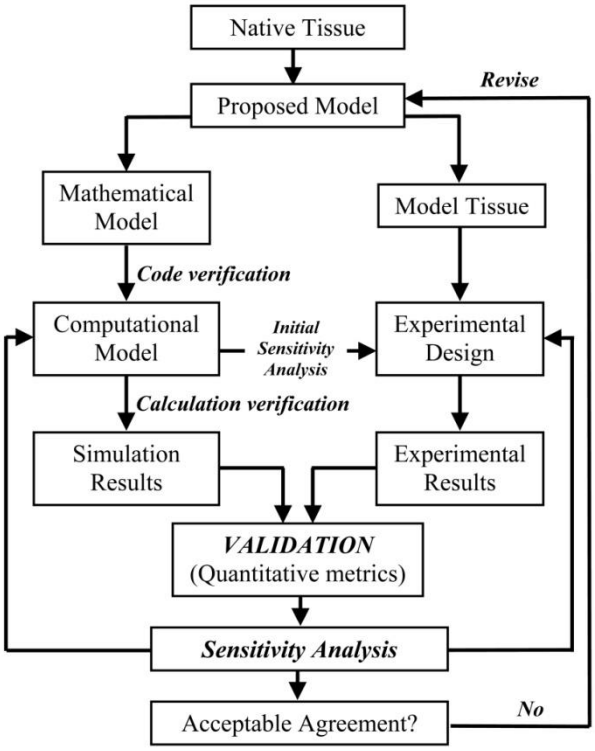


**Figure 6: Flow of the verification and validation in biomechanics, [48].**

A general validation methodology is to determine the outcome variables of interest and prioritise them based on their relative importance. Oberkampf suggests using the PIRT

(Phenomenon Identification and Ranking Table) ([49]). The PIRT guidelines scale each variable based on its impact within the system and determine if the model adequately represents the phenomena in question. It then identifies if existing experimental data are able to validate the model or if additional experiments are required. Finally, PIRT provides a framework to assess validation metrics which quantify the predictive capability of the model for the desired outcome variable. The central question is one of time, cost and the complexity of the experiments needed to validate the simulation and the ramifications of erroneous conclusions. Other queries may be about the most appropriate model to represent the physical system or a simpler model which satisfies the needs.

The two predominant types of validation are direct and indirect ([50]). Direct validation performs experiments on the quantities of interest, from basic material characterizations to hierarchal systems analysis. Though they may seem trivial, the most basic validation experiments are often the most beneficial as they provide fundamental confidence in the model's ability to represent constituents of the system. The goal is to produce an experiment that closely matches a desired simulation so each material property and boundary condition can be incorporated. Limitations include the reproduction of the physical scale or an inability to generate data for the specific model output that is most desired. Typically, these relate to the regeneration of the complex boundary conditions associated with in-vivo systems as quantified by in vitro experiments. Indirect validation utilizes experimental results that cannot be controlled by the user, such as from the literature or results of clinical studies. Experimental quality control, sources of error, and the degree of variability are typically not known if the data are not collected by the analyst. Indirect validation is clearly less favored than direct validation, but may be unavoidable.

The required experiments may be cost prohibitive, difficult to perform, or may simply be unable to quantify the value that is sought by the model.

An important consideration during the validation phase is directly related to the subject-specific nature of biological modeling. Subject-specific experimental validation studies are entitled to a higher measure of confidence than statistically significant experimental studies of different subjects. Obviously, this entitlement is only true when the methodology and results are rigorously examined. The large variation in material and geometric considerations between individuals warrant such considerations. Despite this advantage, it is difficult to perform subject-specific validation experiments and most models are validated against published experimental data from different subjects. The standard error measurements associated with these studies are usually high, due to the intersubject differences, making validation of gross kinematics difficult. As such, more rigorous (and more difficult) validation is obtained by comparing results that depend on both kinematic and material considerations, such as end plate strains and intervertebral disc pressures.

## 6. Application of the FEM in implant design

Analyzing medical device designs to improve performance in medical implants presents a unique challenge to engineers and clinicians. Unlike products created for use outside the body, medical implants are difficult to test in a realistic environment. Products are validated in increasingly lifelike scenarios, including computer models such as those described throughout this chapter, as well as experimental testing and clinical investigational trials. Nonetheless, despite best efforts by both regulatory agencies and industry, device failures

can and do occur. Medical device failures in the spine are especially risky to the patients, due to the close proximity of these devices to the central nervous system and its associated structures. Thus, when an implanted device fails there is a strong motivation to determine the cause of failure, so that present and future design efforts can be improved.

Disc degeneration is a natural procedure of ageing and characterized by changes in the morphology and biochemistry of the disc ([51]). The biologic changes of disc degeneration are associated with back pain and other spinal disorders, such as disc herniation, spondylolisthesis, facet arthropathy, and spinal stenosis. Currently, there is no effective method that can reverse or even retard disc degeneration. However, many different strategies are used for the treatment of the degenerated disc, which are classified into two broad areas: nonsurgical and surgical. Surgical treatment is normally performed only after a specific pathoanatomic condition has been identified as the cause of the patient's symptoms and is an option for patients who have failed to respond to conservative treatment. For a relative slight degeneration patient, a dynamic stabilization device can be considered, while fusion and disc replacement will be used for severe cases. Fusion consists of distraction and surgical immobilization of a joint, in this case of a functional spine unit (FSU), to alleviate pain and prevent mechanical instability. Disc displacement consists of the implantation of an artificial disc in order to alleviate pain by restoring relevant functionalities of the degenerated intervertebral disc (IVD). The clinical efficacy and biomechanical features of the implants used for disc degeneration scan be evaluated through short- or long-term follow-up observation, in vitro and in vivo experiments and computational simulations.

As implant for non-fusion treatment, the objective of disc replacement and dynamic stabilization are both to restore the normal spinal kinematics and load transmission among the spinal segments as in a normal intact spine. The primary difference between them is that the disc prosthesis is a load bearing structure as opposed to the load sharing nature of the dynamic stabilization devices.

### 6.1 Disc replacement

Using a L3-S1 model, ([52]) tested the effects of a mobile core type artificial disc (Charité artificial disc) across the implanted and adjacent segments, Figure 7. The model was subjected to 400-N axial compression and pure moments that produced the overall rotation of the L3-S1 Charité model equal to the intact case. By inserting the disc into the L5-S1 segment, it was found that Charité artificial disc placement slightly increases motion at the implanted level, with a resultant increase in facet loading when compared to the adjacent segments, while the motions and loads decrease at the adjacent levels. In the study of [53], a new designed composite device with a similar structure to a natural lumbar disc was evaluated with a L3–L5 model under compression, flexion, extension and axial rotation. Comparing with the intact model, the implanted model was found to be much stiffer. It was also predicted that the prosthesis significantly affects the stress distribution within the adjacent vertebrae, but not the stress magnitude, which may induce bone remodeling.

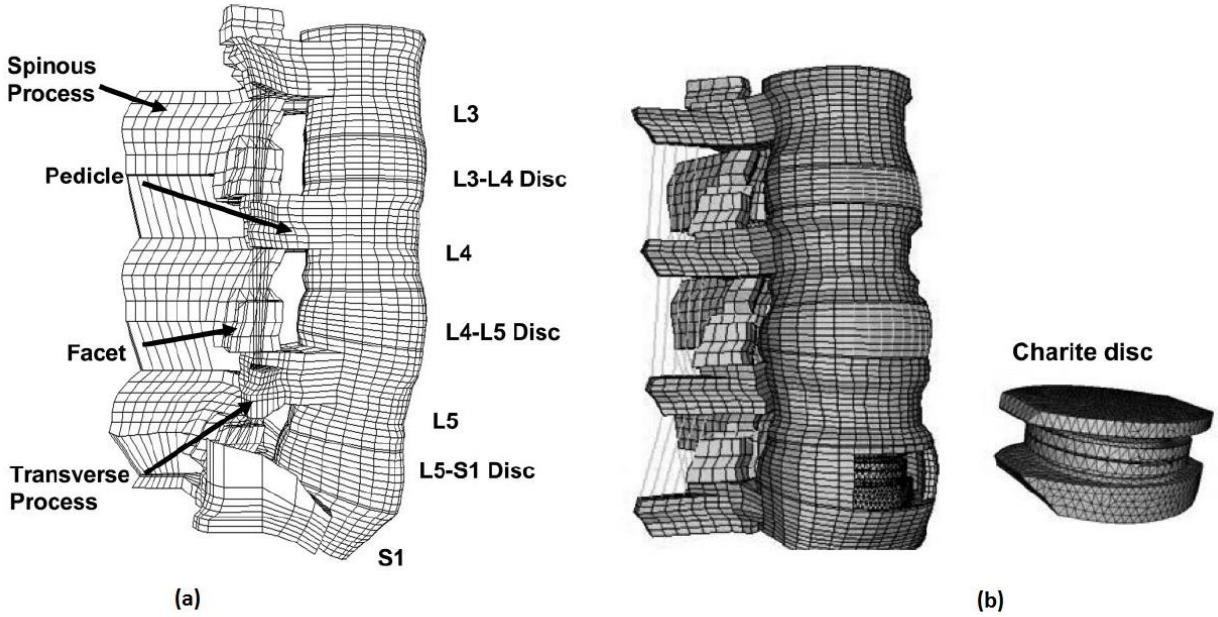


**Figure 7: FE model of the lumbar spine, L3-S1 segment, (a) In-tact model, (b) Charité disc model placed at the L5-S1.**

In the study of [54],a ball-and-cup-type artificial disc (Sofamor Danek) implanted into a L3–L4 model via an anterior approach was evaluated for the effect of its position on the biomechanics of the posterior spinal elements (including the facet joints, pedicles, and lamina) and on the vertebral bodies. Under 800N axial compression, implanted models with an anteriorly placed artificial disc exhibited facet loads 2.5 times greater than loads observed with the intact model, whereas posteriorly implanted models predicted no facet loads in compression. Implanted models with a posteriorly placed disc exhibited greater flexibility than the intact and implanted models with anteriorly placed discs. Restoration of the anterior longitudinal ligament reduced pedicle stresses, facet loads, and extension rotation to nearly intact levels. The models suggest that, by altering placement of the artificial disc in the anteroposterior direction, a surgeon can modulate motion-segment flexural stiffness and posterior load-sharing, even though the specific disc replacement

design has no inherent rotational stiffness. [55], also found the importance of artificial disc position. Using a L1–L5 model, they examined how the mechanical behavior of the lumbar spine is affected by the height and position of a ProDisc prosthesis. The disc position was varied by up to 2mm in both an anterior and posterior direction, and three different disc heights were investigated. The results showed that implant position strongly influences intersegmental rotation for the loading cases of standing and flexion, a disc height 2mm in excess of the normal disc space increases intersegmental rotation at implant level during standing and extension. Furthermore, they also found that for a disc replacement, the values for intersegmental rotation are closer to those for the intact spine when lateral portions of the anulus are not removed. A perfect reconstruction of the ALL would help to restore the biomechanics to normal.

**6.2 Dynamic stabilization**

The various dynamic stabilization systems described in the literature are all posterior implant. In the study of [56],the biomechanical compatibility of a U-shaped interspinous device was evaluated using a L4–L5 model by comparing the motions of the healthy, the nucleotomized and the implanted model under compression, flexion, extension and lateral bending, Figure 8. The results showed that the implant was able to achieve their main design purpose, which is to diminish the forces acting on the apophyseal joints. In another study, the biomechanical behavior of the implanted motion segment with Dynesys under physiological loading conditions was assessed by [57], Figure 9. The predicted results showed that the stiffness of the treated motion segment was considerably increased under

flexion and extension, especially under torsion, which was so high that non-physiological biomechanical response was observed. In addition, they found that general functionality of the Dynesys was independent on the applied preload forces.

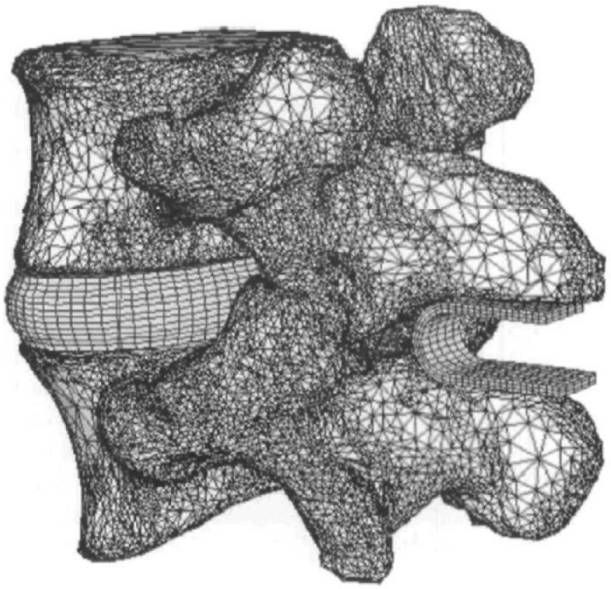

**Figure 8: The FE model of the L4-L5 lumbar motion segment with implanted interspinous device.**

The effect of a posterior dynamic implant adjacent to a rigid spinal fixator on the biomechanical on the mechanical behavior at the corresponding level was studied by [58],using a L1–L5 model. After studying a healthy lumbar spine for comparison, a rigid fixator and a bone graft were inserted at L2/L3. Healthy and degenerated discs were assumed at the adjacent level, i.e. L3/L4. An additional paired dynamic posterior fixator was then implemented at level L3/L4. The loading cases of walking, extension, flexion and axial rotation were simulated. The results showed that anterior interbody fusion in combination with a rigid fixator has only a minor effect on intersegmental rotation, intradiscal pressure and facet joint force at the adjacent level. A dynamic implant reduces intersegmental rotation for walking, extension and flexion as well as facet joint forces for

axial rotation at its insertion level. Intradiscal pressure is not markedly reduced by a dynamic implant. The results do not support the assumption that disc loads are significantly reduced by a dynamic implant. For axial rotation, however, dynamic fixation devices do reduce the force in the facet joint. In another study of the same group, the effect of a bilateral posterior dynamic implant on the mechanical behavior of the lumbar spine was compared to a rigid fixator using same L1–L5 model. The implant was assumed to be the straight longitudinal rod with a diameter of 5 mm. The stiffness of the longitudinal rod was varied between 1 and 83,000 N/m.min discrete steps, while the latter value represents the material of rigid fixator. The results showed that a stiffness of the implant greater than 1000 N/mm has only a minor effect on intersegmental rotation. The mechanical effects of a dynamic implant are similar to those of a rigid fixation device, except after distraction, when intradiscal pressure is considerably lower for rigid than for dynamic implants. Thus, the results of this study demonstrate that a dynamic implant does not necessarily reduce axial spinal loads compared to an uninstrumented spine. The difference in the mechanical effect of a paired posterior dynamic or rigid implant is smaller than often expected.

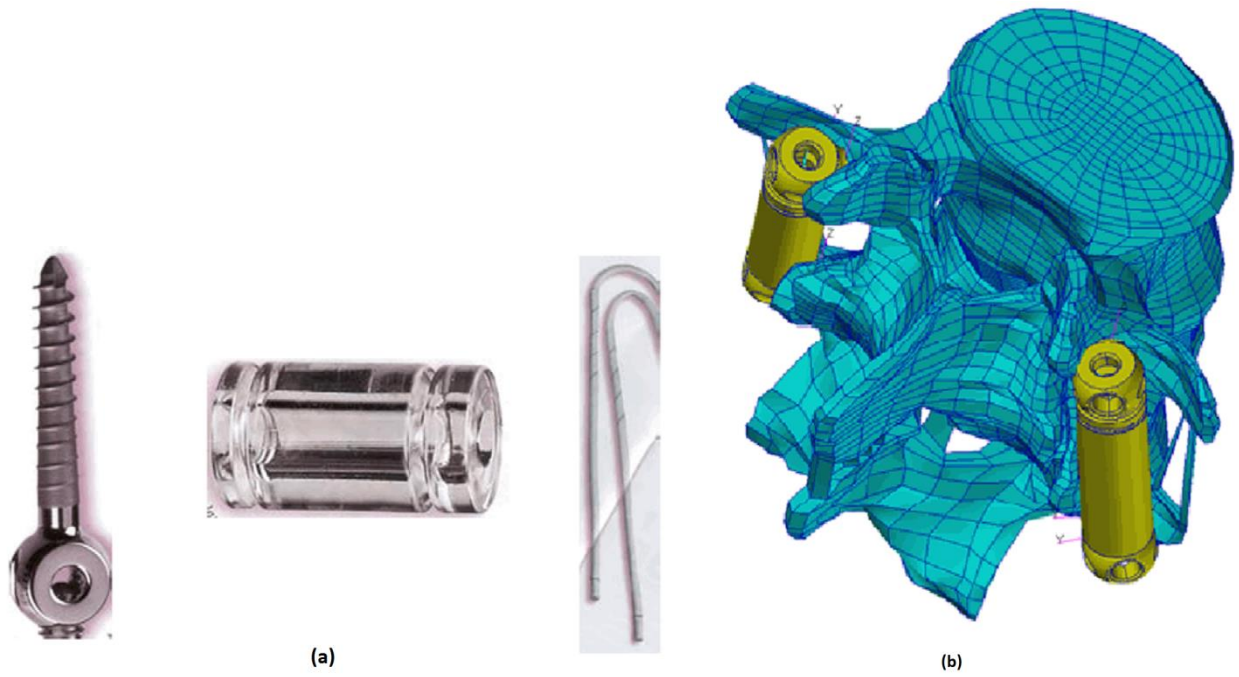


**Figure 9: FE model for the Dynesys system developed by, (a) Components of the Dynesys system, (b) Implanted L2-L3 segment.**

## 7. Conclusions

Real advances have been made in the field of finite element modelling of the spine since the first models were developed over three decades ago. This progress has only been possible because of parallel advances in computational power, imaging technology and experimental techniques, all of which are likely to develop further in the future. In a typical FE study for examination of any specific spinal implant, a detailed FE model of related spinal motion segments, single or multi-, will firstly be developed and validated as reference to simulate the segments under normal (healthy) condition. Next, the healthy model will be modified by removing a certain part of the spine structure and inserting the implant following the medical instruction to represent the segment under instrumented condition. The effect of the implant can then be evaluated by comparing the results of the healthy model and instrumented model under various physiological loadings. It is accordingly essential that

the developed FE intact spine model being accurate enough to reflect the motion of the simulated segments and internal loadings shared among various components in reality.

Cautious incorporation of new technologies, with adequate consideration of model sensitivity and validation, will allow us to generate more efficient and accurate simulations. This will enable the development of spinal simulation tools that fulfil their potential for preclinical evaluation and patient assessment.

## 8 . References


[1] Wheeldon JA, Stemper BD, Yoganandan N, Pintar FA. Validation of a finite element model of the young normal lower cervical spine. Annals of biomedical engineering 2008; 36: 1458-1469.

[2] Kumaresan S, Yoganandan N, Pintar FA, Maiman DJ. Finite element modeling of the cervical spine: role of intervertebral disc under axial and eccentric loads. Med Eng Phys 1999; 21: 689-700.

[3] Hurwitz A, Courant R. Vorlesunger über Allgemeine Funcktionen Theorie. . Grundlehren der mathematischer Wissenschaften 1922; 3.

[4] Liu Y, Ray G. A Finite Element Analysis of Wave Propagation in the Human Spine. Technical Report F33615-72-C-1212 1973; Wright Patterson A.F.B. Fairborn, OH.

[5] Crawford R. Finite element models predict in vitro vertebral body compressive strength better than quantitative computed tomography. Bone 2003; 33: 744-750.

[6] Zhang QH, Teo EC, Ng HW, Lee VS. Finite element analysis of moment-rotation relationships for human cervical spine. J. of biomechanics 2006; 39: 189-193.

[7] Maurel N, Lavaste F, Skalli W. A three-dimensional parameterized finite element model of the lower cervical spine. Study of the influence of the posterior articular facets. J. of biomechanics 1997; 30: 921-931.

[8] Zhang QH, Teo EC. Finite element application in implant research for treatment of lumbar degenerative disc disease. Medical Engineering & Physics 2008; 20: 1246-1256.

[9] Sairyo K, Goel VK, Masuda A, Vishnubhotla S, Faizan A, Biyani A, Ebraheim N, Yonekura D, Murakami R-I, Terai T. Three dimensional finite element analysis of the pediatric lumbar spine. Part II: biomechanical change as the initiating factor for pediatric isthmic spondylolisthesis at the growth plate. European spine J. 2006; 15: 930-935.

[10] Schmidt H, Shirazi-Adl A, Galbusera F, Wilke H-J. Response analysis of the lumbar spine during regular daily activities--a finite element analysis. J. of biomechanics 2010; 43: 1849-1856.

[11] Yoganandan N, Kumaresan S, Pintar Fa. Biomechanics of the cervical spine Part 2. Cervical spine soft tissue responses and biomechanical modeling. Clinical biomechanics 2001; 16: 1-27.

[12] Kallemeyn Na, Tadepalli SC, Shivanna KH, Grosland NM. An interactive multiblock approach to meshing the spine. Computer methods and programs in biomedicine 2009; 95: 227-235.

[13] Kallemeyn N, Gandhi A, Kode S, Shivanna K, Smucker J, Grosland NM. Validation of a C2-C7 cervical spine finite element model using specimen-specific flexibility data. Medical Engineering and Physics 2010; 32: 482-489.

[14] Teo EC, Ng HW. Evaluation of the role of ligaments, facets and disc nucleus in lower cervical spine under compression and sagittal moments using finite element method. Medical engineering & physics 2001; 23: 155-164.

[15] Del Palomar aP, Calvo B, Doblaré M. An accurate finite element model of the cervical spine under quasi-static loading. J. of biomechanics 2008; 41: 523-531.

[16] Shirazi-Adl A, Parnianpour M. Load-bearing and stress analysis of the human spine under a novel wrapping compression loading. Clin Biomech 2000; 15: 718-725.

[17] Overaker DW, Langrana NA, Cuitino AM. Finite element analysis of vertebral body mechanics with a nonlinear microstructural model for the trabecular core. . J Biomechanical Engineering 1999; 121: 542-550.

[18] Higgins KB, Sindall DR, Cuitino AM, Langrana NA. Biomechanical alterations in intact osteoporotic spine due to synthetic augmentation: finite element investigation. J Biomechanical Engineering 2007; 129: 575-585.

[19] Whyne CM, Hu SS, Lotz JC. Burst fracture in the metastatically involved spine: development, validation, and parametric analysis of a three-dimensional poroelastic finite-element model. . Spine 2003; 28: 652-660.

[20] Buckley JM, Loo K, Motherway J. Comparison of quantitative computed tomography-based measures in predicting vertebral compressive strength. Bone 2007; 40: 767-774.

[21] Tschirhart CE, Nagpurkar A, Whyne CM. Effects of tumor location, shape and surface serration on burst fracture risk in the metastatic spine. J Biomechanics 2004; 37: 653-660.

[22] Meakin JR, Reid JE, Hukins DW. Replacing the nucleus pulposus of the intervertebral disc. Clinical biomechanics 2001; 16: 560-565.

[23] Rawlinson JJ, Punga KP, Gunsallus KL, Bartel DL, Wright TM. Wear simulation of the ProDisc-L disc replacement using adaptive finite element analysis. J Neurosurgery Spine 2007; 7: 165-173.

[24] Simon BR, Wu JS, Carlton MW, Evans JH, Kazarian LE. Structural models for human spinal motion segments based on a poroelastic view of the intervertebral disk. J. Biomechanical Engineering 1985; 107: 327-335.

[25] Schroeder Y, Wilson W, Huyghe JM, Baaijens F. Osmoviscoelastic finite element model of the intervertebral disc. Eurpean Spine J. 2006; 15: 361-371.

[26] Ferguson SJ, Ito K, Nolte LP. Fluid flow and convective transport of solutes within the intervertebral disc. J. Biomechanics 2004; 37: 213-221.

[27] Espino DM, Meakin JR, Hukins DWL, Reid JE. Stochastic finite element analysis of biological systems: comparison of a simple intervertebral disc model with experimental results. Computer Methods in Biomechanics and Biomedical Engineering 2003; 6: 243-248.

[28] Argoubi M, Shirazi-Adl A. Poroelastic creep response analysis of a lumbar motion segment in compression. J. Biomechanics 1996; 29: 1331-1339.

[29] Schmidt H, Heuer F, Simon U, Kettler A, Rohlmann A, Claes L, Wilke H-J. Application of a new calibration method for a three-dimensional finite element model of a human lumbar annulus fibrosus. Clinical biomechanics 2006; 21: 337-344.

[30] Lu YM, Hutton WC, Gharpuray VM. Can variations in intervertebral disc height affect the mechanical function of the disc? Spine 1996; 21: 2208-2216.

[31] Natarajan RN, Andersson GB. The influence of lumbar disc height and cross-sectional area on the mechanical response of the disc to physiologic loading. Spine 1999; 18: 1873-1881.

[32] Fagan MJ, Julian S, Siddall DJ, Mohsen AM. Patient-specific spine models. Part 1: finite element analysis of the lumbar intervertebral disc—a material sensitivity study. Proceeding of Institute of Mechanical Engineering [H] 2002; 216: 299-314.

[33] Baer AE, Laursen TA, Guilak F, Setton LA. The micromechanical environment of intervertebral disc cells determined by a finite deformation, anisotropic, and biphasic finite element model. J Biomechanical Engineering 2003; 125: 1-11.

[34] Yin L, Elliott DM. A homogenization model of the annulus fibrosus. J. Biomechanics 2005; 38: 1674-1684.

[35] Belytschko T, Kulak RF, Schultz AB. Finite element stress analysis of an intervertebral disc. J. Biomechanics 1974 7: 277-285.

[36] Brolin K, Halldin P. Development of a Finite Element Model of the Upper Cervical Spine and a Parameter Study of Ligament Characteristics. Spine 2004; 29: 376-385.

[37] Hukins DW, Kirby MC, Sikoryn TA, Aspden RM, Cox AJ. Comparison of Structure, Mechanical Properties, and Functions of Lumbar Spinal Ligaments. Spine 1990; 15: 787–795.

[38] Panjabi MM, Goel VK, Takata K. Physiologic Strains in the Lumbar Spinal Ligaments: An In Vitro Biomechanical Study. Spine 1982; 7: 192-203.

[39] Przybylski GJ, Patel PR, Carlin GJ, Woo SL. Quantitative Anthropometry of the Subatlantal Cervical Longitudinal Ligaments. Spine 1998; 23: 893-898.

[40] Zander T, Rohlmann A, Klockner C, Bergmann G. Influence of Graded Facetectomy and Laminectomy on Spinal Biomechanics. Eurpean Spine J. 2003; 12: 427–434.

[41] Weiss JA, Gardiner JC, Ellis BJ, Lujan TJ, Phatak NS. Three-dimensional finite element modeling of ligaments: technical aspects. Medical engineering & physics 2005; 27: 895-861.

[42] Editorial. Extracting clinically relevant data from finite element simulations. Clinical Biomechanics 2005; 20: 451-454.

[43] Ionescu I, Weiss JA, Guilkey J, Cole M, Kirby RM, Berzins M. Ballistic injury simulation using the material point method. Stud Health Technol Inform 2006; 119: 228-233.

[44] Villa T, Migliavacca F, Gastaldi D, Colombo M, Pietrabissa R. Contact stresses and fatigue life in a knee prosthesis: comparison between in vitro measurements and computational simulations. J. Biomechanics 2004; 37: 45-53.

[45] Anderson AE, Peters CL, Tuttle BD, Weiss JA. Subject-specific finite element model of the pelvis: development, validation and sensitivity studies. J. Biomechanical Engineering 2005; 3: 364-373.

[46] Ellis BJ, Debski RE, Moore SM, McMahon PJ, Weiss JA. Methodology and sensitivity studies for finite element modeling of the inferior glenohumeral ligament complex. J. Biomechanics 2007; 40: 603-612.

[47] Oberkampf WL, Trucano TG, Hirsch C. Verification, Validation, and Predictive Capability in Computational Engineering and Physics. Sandia National Laboratories 2003: 3-78.

[48] Henninger HB, Reese SP, Anderson AE, Weiss JA. Validation of Computational Models in Biomechanics. Proc Inst Mech Eng H 2010; 224: 801-812.

[49] Wilson GE, Boyack BE. The role of the PIRT process in experiments, code development and code applications associated with reactor safety analysis. Nuclear Engineering and Design 1998; 186: 23-37.

[50] Jones AC, Wilcox RK. Finite element analysis of the spine: Towards a framework of verification, validation and sensitivity analysis. Medical Engineering & Physics 2008; 30: 1287–1304.

[51] Cassinelli EH, Hall RA, Kang JD. Biochemistry of intervertebraldiscdegeneration and the potential for gene therapy applications. The Spine J. 2001; 1: 205-214.

[52] Goel VK, Grauer JN, Patel TC, Biyani A, K S, S V, Matyas A, Cowgill I, Shaw M, Long R, Dick D, Panjabi MM, Serhan H. Effects of Charite´ Artificial Disc on the Implanted and Adjacent Spinal Segments Mechanics Using a Hybrid Testing Protocol. Spine 2005; 30: 2755–2764.

[53] Noailly J, Lacroix D, Planell JA. Finite Element Study of a Novel Intervertebral Disc Substitute. Spine 2005; 30: 2257-2264.

[54] Dooris AP, Goel VK, Grosland NM, Gilbertson LG, Wilder DG. Load-sharing between anterior and posterior elements in a lumbar motion segment implanted with an artificial disc. . Spine 2001; 26: 122-129.

[55] Rohlmann A, Zander T, Bergmann G. Effect of total disc replacement with ProDisc on intersegmental rotation of the lumbar spine. Spine 2005; 30: 738-743.

[56] Vena P, Franzoso G, Gastaldi D, Contro R, Dallolio V. A finite element model of the L4-L5 spinal motion segment: biomechanical compatibility of an interspinous device. Computer Methods in Biomechanics and Biomedical Engineering 2005; 8: 7-16.

[57] Eberlein R, Holzapfel GA, Schulze-Bauer CAJ. Assessment of a spinal implant by means of advanced FE modeling of intact human intervertebral discs. Fifth World Congress on Computational Mechanics. 2002.

[58] Zander T, Rohlmann A, Burra NK, Bergmann G. Effect of a posterior dynamic implant adjacent to a rigid spinal fixator. Clinical Biomechanics 2006; 21: 767-774.

## Chapter 2:

## Development of a finite element model of the cervical spine[1]

[1]I. Zafarparandeh, D. Erbulut, I. Lazoglu, and A. F. Ozer. Development of a finite element model of the human cervical spine. Turkish Neurosurgery, 24: 312-318, 2014.

### 1. Introduction

The cervical region is a frequent site of injury in the spinal column. Most of the injuries are soft tissue and are caused by automobile accidents. To understand the underlying mechanisms of injury and dysfunction, biomechanical models are introduced as versatile tools. These models can be helpful in prevention, diagnosis, and treatment of clinical problems. Finite element (FE) model is one of the critical biomechanical models that provides basic insights into the workings of the cervical spine. Physical models, *in vitro* models and *in vivo* models are the other available biomechanical models to obtain important information regarding cervical spine biomechanics in response to various treatments. However, these models in comparison to the FE models suffer from their inability to predict the internal response of the cervical spine, for instance, localized stress and strain fields [1]. Continuous advancements in numerical techniques as well as computer technology has made the finite element method a strong tool in human spine biomechanics. Finite element modeling gives researchers different points of view of the spine biomechanics, that is, stress analysis, load sharing under normal, pathologic, and stabilized conditions, and the design of anthropomorphic test devices [2]. In order to

achieve reliable results, it is crucial to use accurate anatomy, material properties, boundary and loading conditions and validation against appropriate experimental data.

In earlier FE models, the cervical column is a combination of simple rigid masses connected by beam and spring elements representing intervertebral discs, ligaments, facet joints and muscles [3, 4]. The simple rigid masses considered for vertebrae do not produce realistic results. Thereafter, detailed FE models were suggested by researchers, [5-8]. In 1996, Yoganandan et al. [5] proposed a detailed three-dimensional FE model of C4-C6 segment, considering all the important anatomic features such as the facet articulation surfaces and uncinate processes. They used close-up computed tomography scans to create an anatomically accurate geometry for vertebrae. The model was validated against the published *in vitro* experimental results under axial compression only. The models proposed till 1998 suffered from inability to predict correct biomechanical response in complex loading modes, including axial rotation and lateral bending. In 1998, Goel et al. [6] developed a C5-C6 motion segment of cervical spine and it was validated in all of the loading modes for the first time in the literature, including axial rotation and lateral bending. Nonlinear ligament definition, fully composite intervertberal disc, fluid nucleus and Luschka's joint were included in this model. In another study, Teo et al. [7] in 2001 developed a three-dimensional FE model C4-C6 to study the role of ligaments, facets and disc nucleus on instability. Their model used digitizing technique to obtain the accurate geometry of each single vertebra. The model assumed symmetry about the mid-sagittal

plane. The validation was done in three load configurations including, axial compression, flexion and extension.

Abovementioned proposed models had the ability to predict the internal stresses, strains and biomechanical responses under complex loading modes. However, these models consisted of either one or two spinal motion segments, or they did not consider all features of the cervical spine. Therefore, the proposed models were insufficient to provide realistic response of the physical multi-levels (more than two levels) of the spinal column [9].

Based on type of the FE analysis in cervical spine biomechanics, static or dynamic, the necessity of considering the full cervical or multi-segment models were defined by researchers [9]. In dynamic simulation, vertebrae are usually considered as rigid bodies that are connected by discs and ligaments which are modeled as springs. Those dynamic models included the skull and all vertebrae and discs [10-12]. On the other hand, models that are proposed for static simulation consider more details in geometry and material properties of the cervical spine [5, 8, 13, 14]. However, these models do not include all segments of the cervical spine. Thereafter, full cervical spine FE models were proposed by several investigators [9, 15-17] for static analysis. In 2006, Zhang et al. [9] developed a comprehensive FE model of C0-C7 cervical spine and head. They validated the mode under 1.0 Nm pure moment applied on the skull in different directions i.e. flexion, extension, axial rotation and lateral bending. All the important spinal components, such as cortical bone,

cancellous bone, posterior elements, disc annulus, disc nucleus and endplate were appropriately simulated.

The objective of this chapter is to review the recent advancements in FE modeling of the cervical spine. The structure of the chapter is based on the procedure of FE modeling of the cervical spine. The cervical spine FE modeling procedure consists of the following steps: construction of vertebra, intervertebral disc and ligaments, assigning material properties and boundary conditions and validation with different *in vitro* studies.

## 2. FE model of cervical spine

In general, the FE model of any structure consists of a finite number of "elements" which interact at their points of attachment, called "nodes". By using these elements, the modeling of complex irregular geometries, as in biomedical cases, is feasible. In the FE model of the cervical spine, different types of elements with different geometric forms (bars, plates, blocks, etc.) may be used to represent the components of cervical spine [18].

A finite element model is composed of three aspects: the geometric representation, the material representation (constitutive laws) and the boundary conditions (loading and restraints). Firstly, it is favorable to define the actual geometry of the cervical spine as closely as possible. One of the techniques known as Computed Tomography (CT) is commonly used in providing the appropriate three-dimensional bone details of the spine.

Using CT data enables a subject based on the specific requirements of the problem [5, 6, 15, 16, 19, 20]. Alternative to CT technique, direct digitization of dried or embalmed cadaveric bones can provide excellent geometric fidelity at the cost of large time [7, 9, 14, 21-24]. Another major concern in FE modeling of the spine is the material properties of the spinal components which vary broadly, even for a specific structure. They are mostly available from *in-vitro* studies [25]. Finally, applying the boundary conditions similar to *in-vitro* studies prepare the model for simulation.

**2.1. Model geometry and mesh**

The first step in FE modeling of the cervical spine is obtaining the geometry of all different components. The geometry of the cervical spine may be defined by three different groups, including vertebrae, intervertebral discs, and ligaments and facet joints. This type of division is based on the functionality of each spinal component. There have been different methods introduced in the literature to generate the geometry of each group. The geometry of the vertebrae may be obtained through CT scan data while discs are usually created as solid volumes filling the space between two vertebrae. Ligaments are modeled based on their origin and insertion. Facet joints modeling depend on the type of the element being used. Generally, geometry construction and mesh generation are two interdependent steps. In some cases, the spinal component is modeled by using the appropriate mesh type without geometry constructions.

Vertebra geometry is the most complicated part in model construction. It consists of many free form surfaces such as facet surfaces and the surface where the disc is located. These free form surfaces increase the time required to generate the mesh. Vertebrae meshing time

varies and depends on the type of the mesh. There are two common element types used for spinal models. Tetrahedral elements are easier to generate on the curvy surfaces of vertebrae but they have limitations due to the inability in simulating appropriate material properties [26]. Hexahedral elements, eight-node "brick" elements, are accepted as the preferred element type for three-dimensional nonlinear analysis [27]. However, this type of element is computationally expensive to solve and can cause discontinuities in edges if sufficient surface smoothing is not well enough. Zhang et al. [9] obtained the vertebrae geometry using flexible digitizer from an embalmed 68-year old cadaveric specimen (C1-C7). They used eight-node "brick" elements for vertebrae, Fig. 1. Del Palomar et al. [15] used computed tomography scan data of a 48-year old man to construct the three-dimensional surface geometry of the cervical vertebrae. The vertebrae were considered rigid bodies, thus only the exterior surfaces of the vertebrae were meshed using surface elements (triangles and quadrilaterals), Fig. 2. Panzer et al. [17, 28, 29] used 3D dataset available in literature [30] to construct the geometry of the full cervical spine. They compared the vertebrae geometry with the existing anatomical studies. Three-dimensional hexagonal elements were used to generate mesh on cancellous bone, while cortical bone and endplates of the vertebrae were meshed with two-dimensional quadrilateral elements, Fig. 3. Kallemeyn et al. [16, 27] proposed mesh generation methods using multi-block techniques to ease the procedure required to create FE model of cervical spine with only hexahedral elements. They obtained the geometry of vertebrae from a 74-year old male cadaver specimen, Fig. 4. Ha [31] developed three-dimensional FE model of the C3-C6 cervical segment using computed tomography. The CT scan data was used to construct non-uniform rational B-splines (NURBS) CAD surfaces of the vertebrae. He used eight-node shell

elements for cortical bone and twenty-node solid elements for the cancellous bone, Fig. 5. Reviewing the recent FE model of the cervical spine reveals that CT scan data is trustworthy and easily obtainable source for constructing the geometry of vertebrae. Furthermore, researchers are putting more effort to generate hexahedral elements on the complex geometry of the vertebrae.

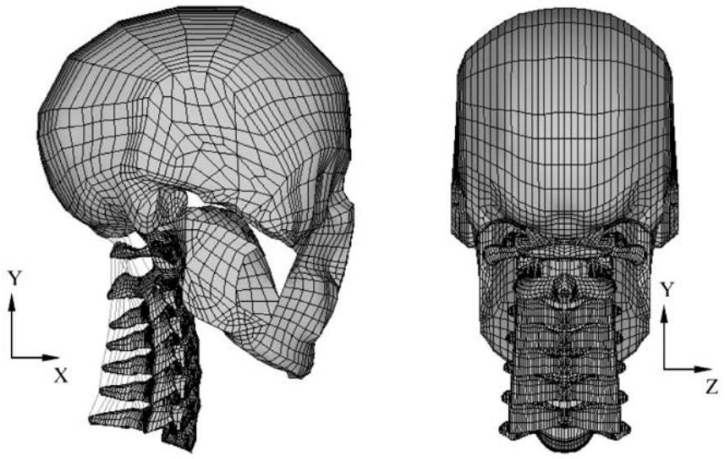


**Figure 10: Finite element model of full cervical spine proposed by Zhang et al.**

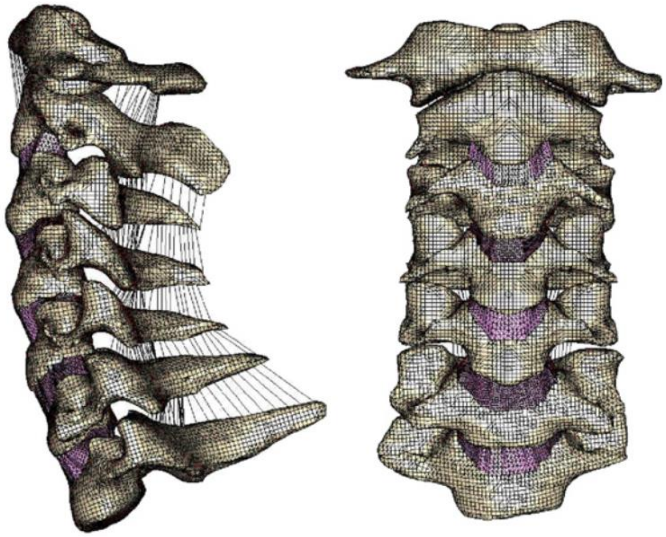

**Figure 11: Three-dimensional finite element model of cervical spine proposed by Del Palomar et al.**

Generally, the geometry of discs are created after the obtaining the geometry of vertebrae. Intervertebral discs are modeled as solid volumes that fill the space between two vertebrae while not exceeding the outer boundary of the vertebral bodies. Several studies, [9, 15, 28, 31], defined the geometry of discs based on the anterior and posterior thickness reported in the literature [32]. Kallemeyn et al. [27] generated the mesh between two vertebrae without creating surface geometry of discs. Hexahedral element is the most common type of element being used to generate mesh on discs [9, 16, 28, 31, 33] while tetrahedral elements have also been used [15, 34].

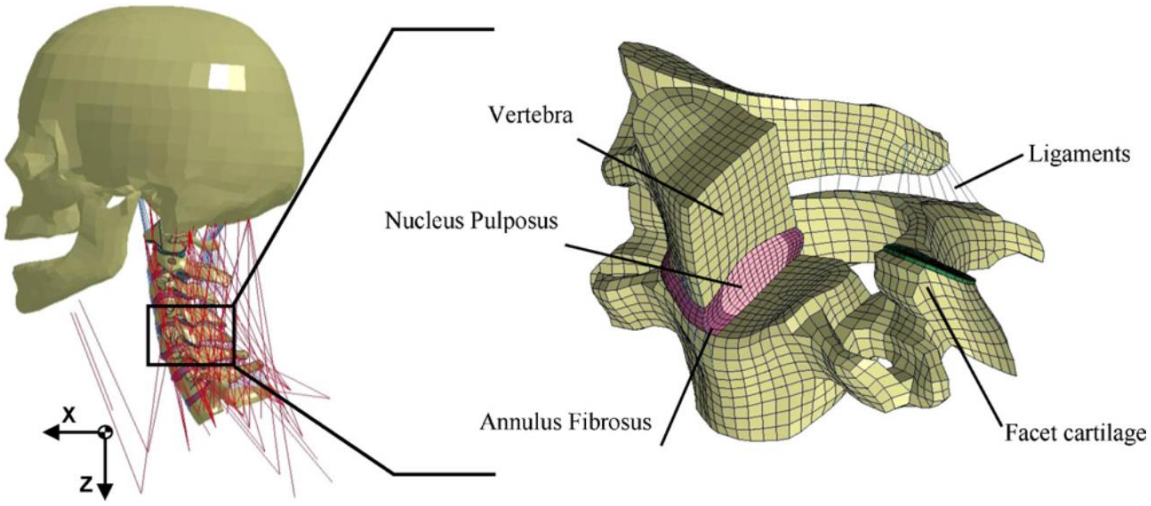


**Figure 12: Finite element model of full cervical spine used for studying frontal crash**

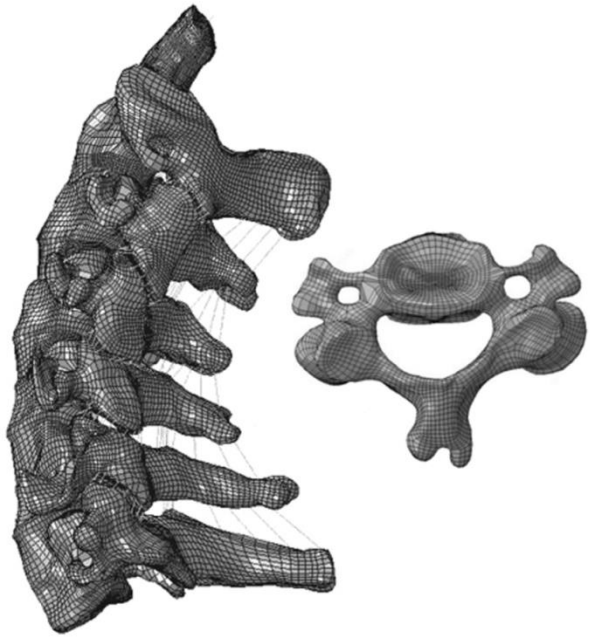

**Figure 13: Finite element model of full cervical spine used for studying frontal crash**

The geometry of ligaments are defined based on their origin/insertion, length and cross-sectional area [25]. In general, the proposed ligament models use the same geometric properties as published before [35-38]. Five different groups of ligaments are considered in FE modeling of cervical spine: anterior longitudinal ligament (ALL), posterior longitudinal

ligament (PLL), ligamentum flavum (LF), interspinous ligament (ISL) and capsular ligament (CL). Different types of elements have been used in simulating the behavior of ligaments, including spring or cable and membrane types. Del Palomar et al. [15], Kallemeyn et al. [16, 27] and Goel et al. [6] used 3D truss elements acting only under tension. Zhang et al. [9] used two-node link elements which only permitted axial force transmission.

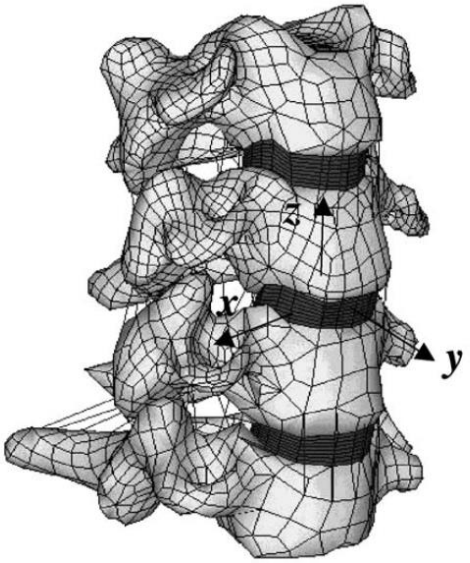


**Figure 14: Finite element model of lower cervical spine proposed by Ha**

The last part in creating geometry and mesh for FE model of the cervical spine is modeling of the facet or zygapophysial joints. The anatomy of this joint is composed of three parts including cartilage, synovial membrane and synovial fluid. The space between the two cartilage is usually defined by sliding or gap elements [6, 19]. In some FE models, facet joints are treated as surface-to-contact problem [9, 27, 31]. Panzer et al. [28] used a

squeeze-film-bearing model to represent the synovial fluid. They used hexagonal elements to simulate the articular cartilage.

### 2.2. Material properties

The second most important aspect of a finite element model is the definition of material properties of the individual components. Non-homogeneity, anisotropy and material nonlinearities are prevalent within the cervical structure, though in some instances, linear assumptions may be appropriate in the simulation. As an example, linear models has been used to determine the sites of crack initiation during vertebral collapse [39]. The material property data on the human cervical spine are developed through controlled laboratory experiments. The wide variation in material properties used in finite element models generally arises from the inherent biologic variability in experimental work. This variation causes inconsistency between material definition in FE model and cadaver experiments.

To assign the material properties, the vertebra mesh is divided into four different groups based on the mineral density of the bone. These groups are cortical bone, cancellous bone, posterior part and endplates. In most of the FE models, the isotropic elastic model is used to simulate the material properties of all four parts of vertebra [6, 7, 9, 14, 16, 21-23, 27, 31, 40]. Panzer et al. [28], used orthotropic elastic material model for the cancellous bone to consider the increase in stiffness in the superior-inferior direction than in transverse direction due to the trabecular structure. Del Palomar et al. [15] modeled the vertebrae as rigid bodies, since they focused on soft tissue response in their model.

Definition of intervertebral disc draws many complications in finite element modeling of cervical spine. The complex geometry of intervertebral disc consists of annulus fibrosus and nucleus pulposus. The annulus part is reinforced with collagen fibers while the nucleus part is composed of fluid material. Various material models have been proposed for modeling the discs structure. One of the accurate FE models focusing on intervertebral disc material modeling was proposed by Del Palomar et al. [15]. To model the annulus, they used a strain energy function with two family of fibers proposed previously [41] and adjusted the material parameters to the experimental results of Ebara et al. [42]. To model the nucleus, they used a hyperelastic incompressible Neo-Hookean model. Panzer et al. [28] used the isotropic material strain-energy function proposed by Hill (1978) [43] representing the annulus. Five pairs of quadrilateral layers were embedded in the annulus representing the fibers. The nucleus was modeled using the fluid elements. Teo et al. [7] modeled the intervertebral disc as three layers: two layers (superior and inferior) of 0.5 thickness as the endplates and the encasing middle layer of intervertebral disc consisting of annulus and nucleus. The simple isotropic elastic model was used to represent the material property of both annulus and nucleus.

As uniaxial structures, role of ligaments is to resist the tensile or distractive forces. They are often treated as simple elastic beam elements. A standard beam formulation for these elements imposes non-physiologic loading during compression, and tension only cable elements are preferred [7, 9, 15, 27].

### 2.3. Boundary and loading conditions

The last step in creating an FE model of the cervical spine after constructing the model geometry and mesh, and assigning material properties to each spinal component, is defining the appropriate boundary conditions. Generally, boundary conditions are specified on the superior and inferior ends of the FE model. In order to achieve this boundary condition, every node laying on the inferior surface of the lowermost vertebra is restrained to have zero displacement. In quasi-static studies, an axial compressive load is applied on the superior part of the model to represent the weight of skull [9]. Other types of loading including tension, compression, shear, flexion, extension, lateral bending and axial rotation can be applied on the superior of the uppermost vertebra and follower load that simulates the body weight may be applied to each vertebrae [2].

## 3. Validation

The validation process is the last step in FE analysis after creating the model. The goal of validation is to assess the capability of the FE model in predicting model response in practical issues. This assessment is made by comparing the predictive results of the model and cadaver experiments. The required experimental data for validation of FE model of the cervical spine can be obtained from the reported *in-vitro* or cadaveric studies. There is a large variety of *in vitro* studies available in the literature [44-48].

## 5. References

[1] Panjabi MM. Cervical spine models for biomechanical research. Spine 1998; 23(24): 2684-2699.

[2] Yoganandan N, Kumaresan S, Voo L, Pintar FA. Finite element application in human cervical spine modeling. Spine 1996; 21(15): 1824-1834.

[3] Chang H, Gilbertson LG, Goel VK, Winterbottom JM, Clark CR, Patwartdhan A. Dynamic response of the occipitoatlanto-axial (C0-C1-C2) complex in right axial rotation. Journal of Orthopaedic Research 1992; 10: 446-453.

[4] Coffee MS, Edwards WT, Hayes WC, White AAI. Biomechanical properties and strength of the human cervical spine. Transactions of ASME Bioengineering Division 1987; 3: 71-72.

[5] Yoganandan N, Kumaresan S, Voo L, Pintar FA, Larson SJ. Finite element modeling of the C4-C6 cervical spine unit. Med Eng Phys 1996; 18: 569-574.

[6] Goel VK, Clausen JD. Prediction of load sharing among spinal components of a C5-C6 motion segment using finite element approach. Spine 1998; 23(6): 684-691.

[7] Teo E-C, Ng H-W. Evaluation of the role of ligaments, facets and disc nucleus in lower cervical spine under compression and sagittal moments using finite element method. Med Eng Phys 2001; 23: 155-164.

[8] Maurel N, Lavaste F, Skalli W. A three-dimensional parametrized finite element model of the lower cervical spine. Study of the influence of the posterior articular facets. J Biomech 1997; 30(9): 921-931.

[9] Zhang QH, Teo E-C, Ng H-W, Lee VS. Finite element analysis of moment-rotation relationships for human cervical spine. J Biomech 2006; 39: 189-193.

[10] Camacho DL, Nightingale RW, Myers BS. Surface friction in near-vertex head and neck impact increases risk of injury. Journal of biomechanics 1999; 32: 293-301.

[11] Meyer F, Bourdet N, Deck C, Willinger R, Raul JS. Human Neck Finite Element Model Development and Validation against Original Experimental Data. Stapp car crash journal 2004; 48: 177-206.

[12] Stemper BD, Kumaresan S, Yoganandan N, Pintar FA. Head-neck finite element model for motor vehicle inertial impact: material sensitivity analysis. Biomedical Sciences Instrumentation 2000; 39: 189-193.

[13] Clausen JD, Goel VK, Traynelis VC, Scifert J. Unicinate process and Luschka joints influence the biomechanics of cervical spine: quantification using a finite element model of the C4-C5 segment. . J Orthop Res 1997; 15: 342-347.

[14] Ng H-W, Teo E-C. Nonlinear finite element analysis of the lower cervical spine (C4-C6) under axial loading. Journal of Spinal Disorders 2001; 14: 201-210.

[15] del Palomar AP, Calvo B, Doblaré M. An accurate finite element model of the cervical spine under quasi-static loading. J Biomech 2008; 41: 523-531.

[16] Kallemeyn N, Gandhi A, Kode S, Shivanna K, Smucker J, Grosland N. Validation of a C2-C7 cervical spine finite element model using specimen-specific flexibility data. Med Eng Phys 2010; 32: 482-489.

[17] Panzer BM, Fice BJ, Cronin SD. Cervical spine response in frontal crash. Med Eng Phys 2011; 33: 1147-1159.

[18] Goel VK, Gilbertson LG. Spine update: Applications of the finite element method to thoracolumbar spinal research_ past, present, and future. Spine 1995; 20: 1719-1727.

[19] Kumaresan S, Yoganandan N, Pintar FA. Finite element modeling approaches of human cervical spine facet joint capsule. J Biomech 1998; 31: 371-376.

[20] Kumaresan S, Yoganandan N, Pintar FA, Maiman DJ. Finite element modeling of the cervical spine: role of intervertebral disc under axial and eccentric loads. Med Eng Phys 1999; 21: 689-700.

[21] Ng H-W, Teo E-C. Influence of preload magnitudes and orientation angles on the cervical biomechanics, A finite element study. J Spinal Disord Tech 2005; 18(1): 72-79.

[22] Ng H-W, Teo E-C, Lee K-K, Qiu T-X. Finite element analysis of cervical spinal instability under physiologic loading. J Spinal Disord Tech 2003; 16(1): 55-65.

[23] Teo E-C, Ng H-W. The biomechanical response of lower cervical spine under axial, flexion and extension loading using FE method. International Journal of Computer Applications in Technology 2004; 21: 8-15.

[24] Guo L-x, Teo E-c, Lee K-k, Zhang Q-h. Vibration Characteristics of the Human Spine Under Axial Cyclic Loads : Effect of Frequency and Damping. Spine 2005; 30: 631-637.

[25] Yoganandan N, Kumaresan S, Pintar FA. Biomechanics of the cervical spine Part 2. Cervical spine soft tissue responses and biomechanical modeling. Clin Biomech 2001; 16: 1-27.

[26] O'Reilly MA, Whyne CM. Comparison of computed tomography based parametric and patient-specific finite element models of the healthy and metastatic spine using a mesh-morphing algorithm. Spine 2008; 33(17): 1876-1881.

[27] Kallemeyn N, Tadepalli SC, Shivanna K, Grosland N. An interactive multiblock approach to meshing the spine. Computer Methods and Programs in Biomedicine 2009; 95: 227-235.

[28] Panzer MB, Cronin DS. C4-C5 segment finite element model development, validation, and load-sharing investigation. J Biomech 2009; 42: 480-490.

[29] Panzer MB. Numerical Modelling of the Human Cervical Spine in Frontal Impact. Mechanical Engineering 2006

[30] Deng YC, Li X, Liu Y. Modeling of the human cervical spine using finite element techniques. in Proceedings from the 43rd Stapp Car Crash Conference. 1999.

[31] Ha SK. Finite element modeling of multi-level cervical spinal segments (C3-C6) and biomechanical analysis of an elastomer-type prosthetic disc. Med Eng Phys 2006; 28: 534-541.

[32] Gilad I, Nissan M. Study of vertebra and disc geometric relations of the human cervical and lumbar spine. Spine 1986; 11(2): 154-157.

[33] Wheeldon Ja, Stemper BD, Yoganandan N, Pintar Fa. Validation of a finite element model of the young normal lower cervical spine. Annals of biomedical engineering 2008; 36: 1458-1469.

[34] Li Y, Lewis G. Influence of surgical treatment for disc degeneration disease at C5-C6 on changes in some biomechanical parameters of the cervical spine. Medical engineering & physics 2010; 32(6): 595-603.

[35] Panjabi MM, Oxland TR, Parks EH. Quantitative anatomy of cervical spine ligamnets. Part 2. Middle and lower cervical spine. Journal of Spinal Disorders 1991; 4: 277-285.

[36] Panjabi MM, Oxland TR, Parks EH. Quantitative anatomy of cervical spine ligaments. Part 1. Upper cervical spine. Journal of Spinal Disorders 1991; 4(3): 270276.

[37] Yoganandan N, Kumaresan S, Pintar FA. Geometric and mechanical properties of human cervical spine ligaments. Journal of Biomechancial Engineering 2000; 122: 623-629.

[38] Clark CR, The cervical spine. 1998: Lippincott-Raven, Philadelphia.

[39] Crawford RP, Cann CE, Keaveny TM. Finite Element Models Predict In Vitro Vertebral Body Compressive Strength Better Than Quantitative Computed Tomography. Bone 2003; 33: 744-750.

[40] Teo JCM, Chui CK, Wang ZL, Ong SH, Yan CH, Wang SC, Wong HK, Teoh SH. Heterogeneous meshing and biomechanical modeling of human spine. Medical engineering & physics 2007; 29(2): 277-290.

[41] Holzapfel GA, Nonlinear solid mechanics. 2000, New York: Wiley.

[42] Ebara S, Iatridis JC, Setton LA, Foster RJ, Mov VC, Weidenbaum M. Tensile properties of nondegenerate human lumbar annulus fibrosus. Spine 1996; 21: 452-461.

[43] Hill R. Aspects of invariance in solid mechanics. Advances in Applied Mechanics 1978; 178: 1-75.

[44] Panjabi MM, Crisco JJ, Vasavada A, Oda T, Cholewicki J, Nibu K, Shin E. Mechanical properties of the human cervical spine as shown by three-dimensional load-displacement curves. Spine 2001; 26: 2692-2700.

[45] Wheeldon JA, Pintar FA, Knowles S, Yoganandan N. Experimental flexion/extension data corridors for validation of finite element models of the young, normal cervical spine. J Biomech 2006; 39: 375-380.

[46] Nightingale RW, Carol Chancey V, Ottaviano D, Luck JF, Tran L, Prange M, Myers BS. Flexion and extension structural properties and strengths for male cervical spine segments. J Biomech 2007; 40: 535-542.

[47] Nightingale RW, Winkelstein Ba, Knaub KE, Richardson WJ, Luck JF, Myers BS. Comparative strengths and structural properties of the upper and lower cervical spine in flexion and extension. J Biomech 2002; 35: 725-732.

[48] Goel VK, Clark CR, Harris KG, Schulte KR. Kinematics of the cervical spine: effects of multiple total laminectomy and facet wiring. Journal of Orthopaedic Research 1988; 6: 611-619.

# Chapter 3:

## Application of an asymmetric finite element model of the C2-T1 cervical spine for evaluating the role of soft tissues in stability[1]

[1]D. Erbulut, I. Zafarparandeh, I. Lazoglu, and A. F. Ozer. Application of an asymmetric finite element model of the C2-T1 cervical spine for evaluating the role of soft tissues in stability. Medical Engineering & Physics, 36: 915-921, 2014.

### 1- Introduction

Decades of investigations have confirmed that most of the cervical spine injuries are related to the soft tissues. Utilizing biomechanical models, it is possible to understand the mechanisms underlying injury and dysfunction, and this understanding will lead to improved safety and protection from injury[1]. The range of experimental biomechanical data from human cervical specimens is limited, and the collection of these data requires specialized experimental equipment in certain cases. In contrast, finite element (FE) method using a computer can provide insight into the inner workings of the cervical spine[2, 3]. The major concerns with the biofidelity of human FE models are related to their geometries and material properties.

There are several popular methods available for obtaining accurate geometries of the structural components of the spine. Maurel et al.[4] used a spatial measuring machine to determine the geometry of lower cervical spine vertebrae. These authors measured the three-dimensional coordinates of 154 points spread over the surfaces of 53 dry vertebrae. Ng et al.[5] used a high-definition digitizer with 6 degrees of freedom to develop a detailed,

three-dimensional, geometrically nonlinear FE model of the human lower cervical spine (C4-C6). Yoganandan et al.[3] used two-dimensional sagittal and coronal CT images from human cadavers to obtain accurate outlines of vertebral cross-sections. In general, of these methods, the most flexible and rigorous geometric data can be obtained using the computed tomography (CT)[6]. In terms of subject-specific (age, sex and pathology) medical imaging, this technique is favorable.

Spinal segment FE models are of great interest, and they have achieved success in predicting the stability of the cervical spine under physiological loading[2, 5]. The definition of clinical spinal instability has been controversial. Stokes and Frymoyer[7] defined segmental instability as displacement that is greater than that observed in a normal structure. Panjabi[8] defined segmental instability as an abnormal range of motion in the neutral zone. *In vitro* biomechanical studies of injured cervical spines have provided some insight into the role of spinal components (discs, ligaments, and facets) in providing stability[9, 10]. Additionally, some FE models have been proposed for the investigation of the importance of the spinal components in providing stability[11-13]. Sharma et al.[13] proposed a L3-L4 lumbar segment FE model and studied the role of facets, ligaments, and their geometries in providing segmental stability. Teo et al.[12] developed a three-dimensional FE model of the C4-C6 segment to predict the roles of ligaments, facet joints, and disc nucleus on lower cervical spine instability. The results showed that ligaments, facets, and disc nucleus are crucial for preserving cervical spine motion stability. However,

until now, no comprehensive studies of the roles of ligaments, facet joints, and disc nucleus on stability that have used an asymmetric, full cervical spine FE model have been reported.

The aim of this chapter was to propose a detailed FE model of the cervical spine (C2-T1), using fine hexahedral mesh on the vertebrae and intervertebral discs. The complex asymmetric geometry of the cervical spine about the mid-sagittal plane was considered in the modeling process to obtain realistic results. The model was used to evaluate the roles of ligaments, facet joints, and discs in the stability of the cervical spine under flexion and extension loading. To validate the model with the literature, different types of loadings were applied to the model in conditions of flexion, extension, right and left lateral bending, and right and left axial rotation.

## 2. Materials and Methods

### 2.1. Model geometry

Computed tomography (CT) scan data from a healthy 35-year-old man were used to construct the three-dimensional FE model of the full cervical spine from C2 to T1. Ethical approval was given by the Institutional Ethics Board committee of the Koc University Committee on Human Research. The number of Protocol was 2012.019.IRB2.009. The CT data were processed (Fig. 15a) using medical image processing software (Mimics® Version 14.1; Materialise, Inc., Leuven, Belgium). The segmentation process was utilized to obtain the three-dimensional surface representation of each vertebra in STL format.

To construct three-dimensional surfaces of the intervertebral discs, the vertebrae were first aligned with consideration for the natural lordotic curvature of the cervical spine, as reported in the literature[14, 15]. Cervical lordosis was measured based on the four-line Cobb method between C2 to C7, which resulted in a 25-degree curvature, as shown in Fig. 15b. The measured angle was in the experimental corridor. The height and width of each vertebral body were compared with those reported by Gilad et al.[16] to ensure the accuracy of the geometry. The dimensions of the vertebrae were in the corridor of the reported dimensions. In the second step, while maintaining the natural lordotic curvature of the cervical spine, the locations of the vertebrae were adjusted to correspond to the anterior and posterior thicknesses of the discs reported by Gilad et al.[16]. The anterior and posterior thicknesses of the discs were compared with the literature[16] (Table 1). Finally, three-dimensional solid volumes were created to fill the spaces between the vertebrae to create intervertebral discs.

a)

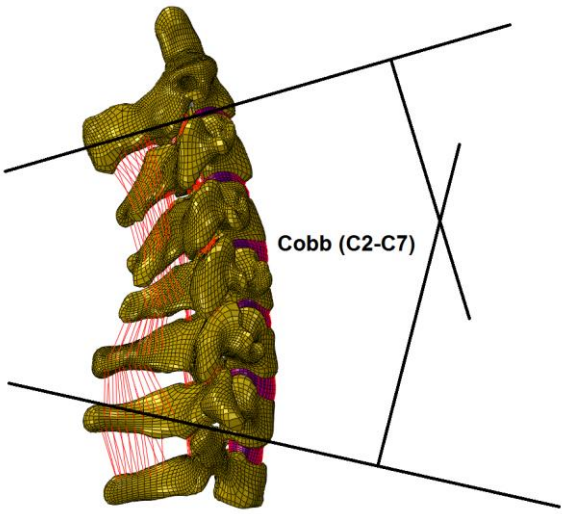


b)

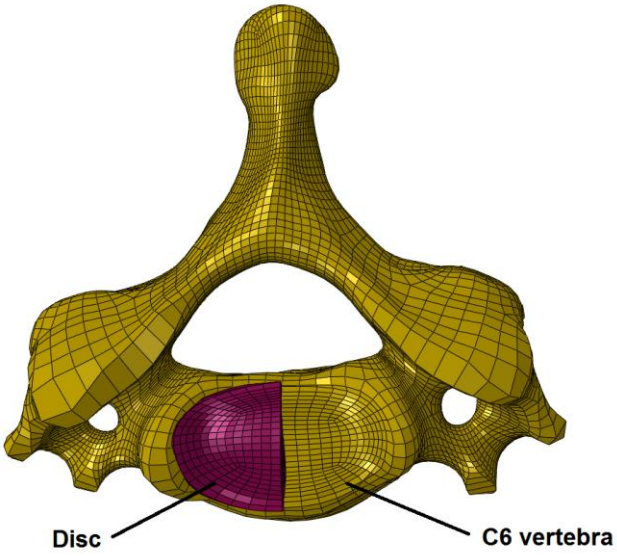


c)

**Figure 15: (a) Cervical spine CT data of a healthy 35-year-old man; (b) Three-dimensional FE model of full cervical spine (C2-T1) constructed using the multi-block approach and the measured Cobb angle for the lordosis curve; (c) The circular mesh pattern implemen**

### 2.2. Mesh creation

To reduce the effort and time required for creating the mesh on the complex geometry of the spine components, the new multi-block technique that was introduced by Kallemeyn et al.[17] was used to generate hexahedral mesh on the vertebrae and discs. The STL model of each part was separately imported into the IA-FEMESH software (University of Iowa, IA) as a three-dimensional STL surface. The blocks helped to create the volumetric hexahedral mesh of the discs and vertebrae.

After transferring the volumetric meshed parts from IA-FEMESH to ABAQUS software (ABAQUS®, Version 6.10-2; Abaqus, Inc., Providence, RI, USA), the interface of each disc and the neighboring vertebrae in each segment were merged to create the complete desired model (Fig. 15b). All cancellous, cortical and posterior parts of the vertebrae were modeled

using three-dimensional hexagonal elements (C3D8). The cortical layer was considered the outer layer of the mesh on the vertebra and had a thickness of approximately 0.5mm[18]; the bony endplate was the layer adjacent to the disc and had a thickness of approximately 0.6 mm[19]; and the cancellous bone composed the inner part. The material properties of all parts of the vertebrae were considered to be elastically isotropic.

**2.3. Intervertebral disc**

Intervertebral discs consist of two components, the nucleus pulposus and the annulus fibrosus. The annulus fibrosus consists of concentric layers of fibrous cartilage. Therefore, a circular mesh pattern was created on the disc model to simulate the concentric layers of the annulus fibrosus. The same circular mesh pattern was defined on the end plates of the vertebral bodies to merge the interfaces of the vertebrae and the discs. The circular pattern on the discs and vertebrae is depicted in Fig. 15c. The annulus fibrosus ground substance material was modeled using the Neo-Hookean hyperelastic model. The annulus also accommodated the fiber definitions in each element. The rebar option of ABAQUS was used to reinforce the layers of the annulus with fibers of ±25º in the cervical region according to the literature[2, 20]. Implementation of the "no compression" option limited the annulus fibers to resisting tension. Six different rings of hexahedral elements were layered on to the disc to integrate the nucleus. 40% of the entire disc area was dedicated to the nucleus pulposus. Incompressible fluid elements were used to simulate the fluid behavior of the nucleus.

**2.4. Ligaments**

Ligaments were modeled using three-dimensional truss elements and were constrained to act nonlinearly only during tension. A cross-sectional area was assigned for each truss element in each ligament group. The number of truss elements in each group of ligaments was chosen such that the total cross-sectional area matched the total area reported in the literature[21]. The origin and insertion locations of the ligaments used in the model were obtained from the literature[22]. For all of the segments, five different types of ligaments were considered: the anterior longitudinal ligament (ALL), the posterior longitudinal ligament (PLL), the capsular ligament (CL), the ligamentum flavum (LF), and the interspinous ligament (ISL). In each segment, 15, 15, 18, 10, and 16 truss elements were used to model the ALL, PLL, CL, LF, and ISL, respectively. These truss elements were assigned nonlinear material properties. Changes in ligament stiffness (i.e., initially low stiffness at low strains followed by increasing stiffness at higher strains) were simulated with the "hypoelastic" material designation, which allows axial stiffness to be defined as a function of axial strain[23].

The complete model consisted of 122,512 nodes and 106,547 elements that represented the various spinal structures of the cervical region, including the vertebrae, discs, and ligaments. The material properties of the various tissues used in the model (Table 2) were obtained from the literature[2, 31] and were assigned to the FE model's components.

**2.5. Facet joints**

Three-dimensional gap contact elements (GAPUNI) were utilized to simulate the facet (apophyseal) joints. These elements transfer force between nodes in a single direction as a function of the specified gap between them. The cartilaginous layer between the facet

surfaces was simulated using ABAQUS's "softened contact" parameter, which exponentially adjusts force transfer across the joint depending on the size of the gap[2, 24].

**2.6. Loads and boundary conditions**

Pure moment[19] loads were applied to the model in the three main planes and included flexion, extension, lateral bending and axial rotation. For flexion and extension, the loads tested were 0.33, 0.5, 1, 1.5, and 2 Nm. For lateral bending and axial rotation, loads of 0.3 and 1 Nm were used. For each simulation, the load was applied to a flying-node (FN) that was created 1mm above the odontoid process of C2. The nodes lying on the odontoid process of C2 were coupled with the FN to create a pure moment. All coupled nodes were constrained in all directions. During the simulations, the nodes on the inferior surface of T1 were fixed in all directions.

The roles of different soft tissues in C4-C5 segment stability were studied. The intact model was modified by excluding specified soft tissue and maintaining other soft tissues. Next, the range of motion of the modified model was compared to that of the intact model to quantify stability. The simulations were performed under 6 different conditions:

1. intact,
2. without the ISL ligament (NoISL) at C4-C5 in flexion,
3. without the LF ligament (NoLF) at C4-C5 in flexion,
4. without the PLL ligament (NoPLL) at C4-C5 in flexion,
5. without the nucleus (NoNuc) in flexion, and
6. without the facet joints (NoF) in extension.

## 2.7. Model validation

The model was compared with a number of *in vitro* studies[25-29] conducted under different loading planes in flexion/extension, right/left lateral bending, and right/left axial rotation. Furthermore, the results were compared with two recent FE models of the full cervical spine proposed by Panzer et al.[30] and Zhang et al.[31]. To verify the accuracy of the model, low-level and high-level loadings were applied to the model. Low-level loading mostly involved the disc response, and high-level loading activated the ligaments.

**Table 1: Medical, anterior and posterior distances between two vertebrae of cervical spine in a segment reported.**

| Vertebrae | Anterior (mm) | Posterior (mm) | Medial (mm) |
|---|---|---|---|
| C2-C3 | 4.87 | 4.2 | 4.53 |
| C3-C4 | 5.83 | 5.10 | 5.46 |
| C4-C5 | 6.43 | 4.27 | 5.35 |
| C5-C6 | 6.24 | 4.34 | 5.29 |
| C6-C7 | 6.73 | 5.2 | 5.96 |

**Table 2: Mechanical properties and element types of the different parts of the cervical spine model**

| Component | Element Type | Young's Modulus (MPa) | Poisson's Ratio | Cross-Sectional Area ($mm^2$) |
|---|---|---|---|---|
| Bony Structures | | | | |
| Vertebral cortical bone | Isotropic, elastic hex element | 10,000 | 0.30 | - |
| Vertebral cancellous bone | Isotropic, elastic hex element | 450 | 0.25 | - |
| Posterior bone | Isotropic, elastic hex element | 3500 | 0.25 | - |

| | | | | |
|---|---|---|---|---|
| Intervertebral disc | | | | |
| Annulus (ground) | Neo Hookean, hex element | 4.2 | 0.45 | - |
| Annulus (fiber) | Rebar | 450 | 0.3 | - |
| Nucleus | Incompressible fluid element | 1 | 0.499 | - |
| Ligaments | | | | |
| Anterior longitudinal | Tension only, truss elements | 15 (<12%) 30 (>12%) | 0.3 | 11.1 |
| Posterior longitudinal | Tension only, truss elements | 10 (<12%) 20 (>12%) | 0.3 | 11.3 |
| Ligamentumflavum | Tension only, truss elements | 5 (<25%) 10 (>25%) | 0.3 | 46.0 |
| Interspinous/supraspinous | Tension only, truss elements | 4 (20-40%) 8 (>40%) | 0.3 | 13.0 |
| Capsular | Tension only, truss elements | 7 (<30%) 30 (>12%) | 0.3 | 42.2 |
| Joint | | | | |
| Facet (apophyseal joint) | Nonlinear soft contact, GAPUNI | - | - | - |

## 3. Results

The rotation responses for each segment under sagittal moments are presented in Fig. 16. To compare the model under an expanded range of loadings, the flexion and extension experimental datasets published by Wheeldon et al.[25] and Nightingale et al.[27, 28], and the FE results of Panzer et al.[30] were selected. The simulation results were reasonable in

the experimental corridor of the selected *in vitro* studies for each segment. The nonlinear and stiffening behaviors of the cervical spine under higher loads were well predicted.

In flexion loading, the results from the intact model were stiffer than the mean values of Wheeldon et al.'s[25] experimental data in all segments by up to 55%; in the C3-C4 segment, the present model curve followed the mean experimental values well. With the exception of the C6-C7 segment, the present study results were stiffer than those of Nightingale et al.[27, 28] by up to 48%. In the C2-C3 and C3-C4 segments, the results were more flexible than those of the model proposed by Panzer et al.[30], and in the lower segments (i.e., C4-C5 and C6-C7), the results of the model were stiffer than those of Panzer et al.[30]. In C5-C6, the intact model and the model of Panzer et al.[30] predicted the same rotation response.

During extension loading, the current results were up to 48% more flexible than the mean values of Wheeldon et al.'s[25] experimental data in the C2-C3 and C3-C4 segments; in the other segments, the results were stiffer by up to 68%. In all segments other than C2-C3, the intact model results were stiffer than mean values of Nightingale et al.'s[27, 28] results by up to 50%. Similarly, the current numerical results during extension loading were stiffer than the numerical results of Panzer et al.[30].

In Figs. 17a-b, the full ranges of motion (ROMs) of lateral bending and axial rotation of the different segments are compared to the *in vitro* studies published by Panjabi et al.[26] and Traynelis et al.[29] and the FE study of Zhang et al.[31]. As the intact model was asymmetric about the mid-sagittal plane, the motion magnitudes were expected to be different for right

and left loading. Therefore, the same pure moment was applied on each right and left side separately, and the summation of those rotations was presented as the ROM.

In lateral bending, the results of the intact model and those of Zhang et al.'s[31] FE model were stiffer than the experimental corridor of Panjabi et al.[26] in all segments. However, the intact model predicted values that were closer to Panjabi et al.'s[26] study than those of the FE model of Zhang et al.[31]. The intact model predicted that the maximum rotation occurred in C4-C5 (4.89º) and that the lowest rotation occurred in C6-C7 (5.4º). The maximum and minimum values were observed at the same levels reported by Panjabi et al.[26], while Zhang et al.[31] predicted the maximum would be at C3-C4 and that the minimum would be at C6-C7.

In axial rotation, the rotation responses of the C2-C3, C4-C5, and C5-C6 segments fell in the experimental corridor of Panjabi et al.[26]; in the C3-C4 and C6-C7 segments, the intact model was more flexible. The FE results of Zhang et al.[31] were in the experimental corridor of Panjabi et al.'s[26] study only for segment C5-C6. The intact model results were in good agreement with the results of Traynelis et al. [29].

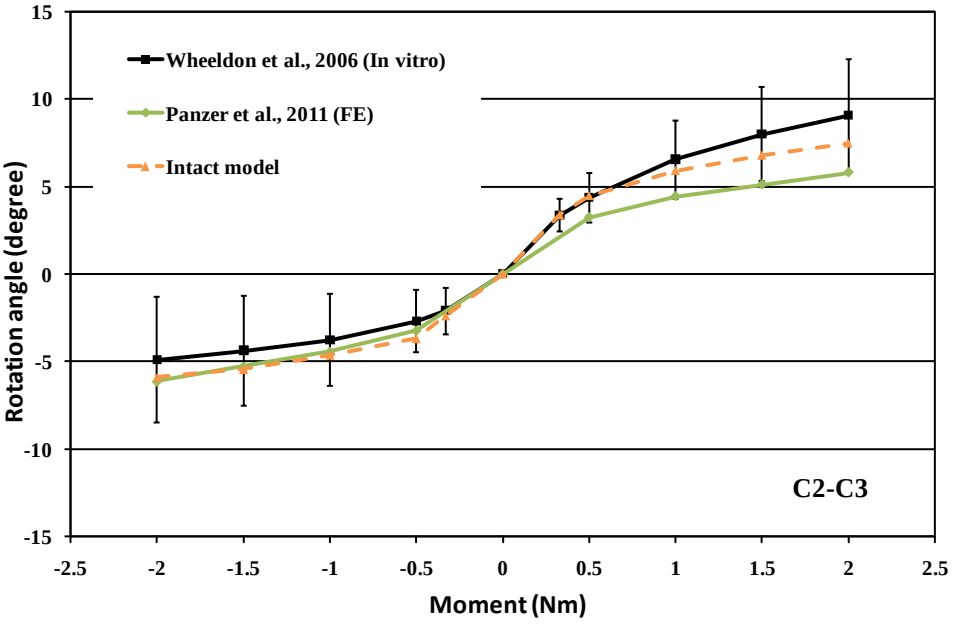
Wheeldon et al., 2006 (In vitro)
Panzer et al., 2011 (FE)
Intact model
C2-C3
Rotation angle (degree)
Moment (Nm)
15
10
5
0
-5
-10
-15
-2.5
-2
-1.5
-1
-0.5
0
0.5
1
1.5
2
2.5

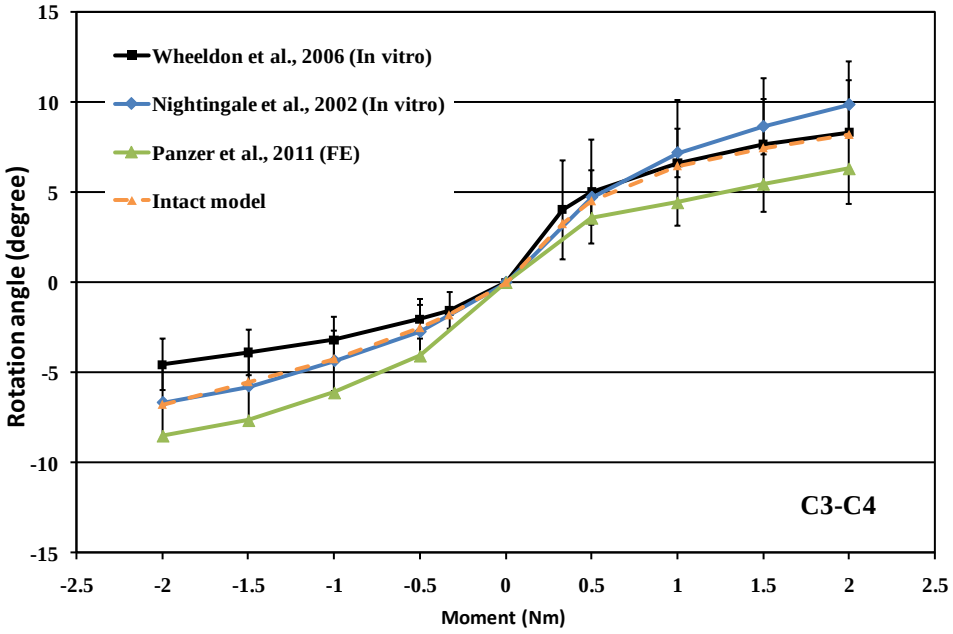
Wheeldon et al., 2006 (In vitro)
Nightingale et al., 2002 (In vitro)
Panzer et al., 2011 (FE)
Intact model
C3-C4
Rotation angle (degree)
Moment (Nm)
15
10
5
0
-5
-10
-15
-2.5
-2
-1.5
-1
-0.5
0
0.5
1
1.5
2
2.5

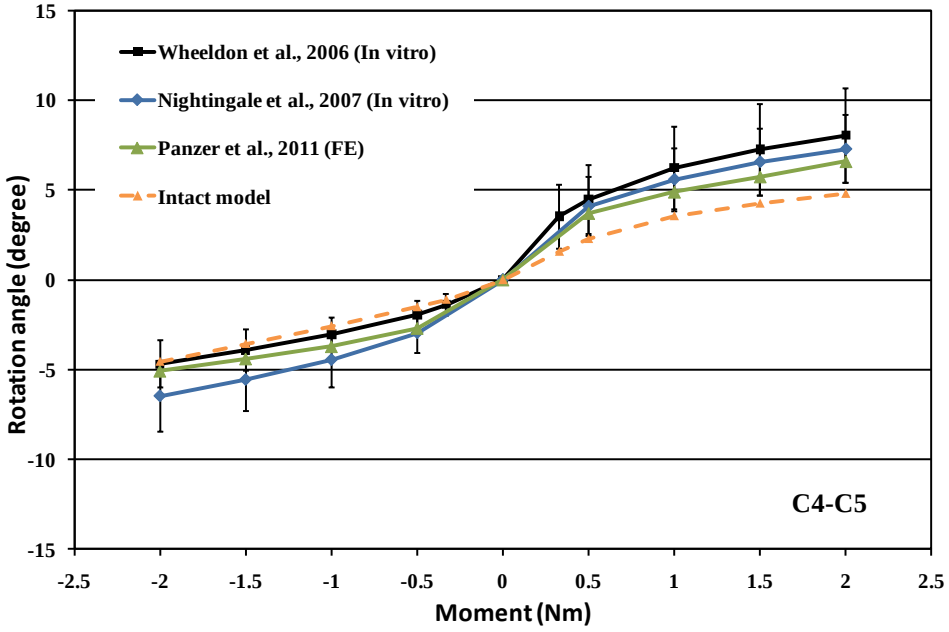
Wheeldon et al., 2006 (In vitro)
Nightingale et al., 2007 (In vitro)
Panzer et al., 2011 (FE)
Intact model
C4-C5
Rotation angle (degree)
Moment (Nm)
15
10
5
0
-5
-10
-15
-2.5
-2
-1.5
-1
-0.5
0
0.5
1
1.5
2
2.5

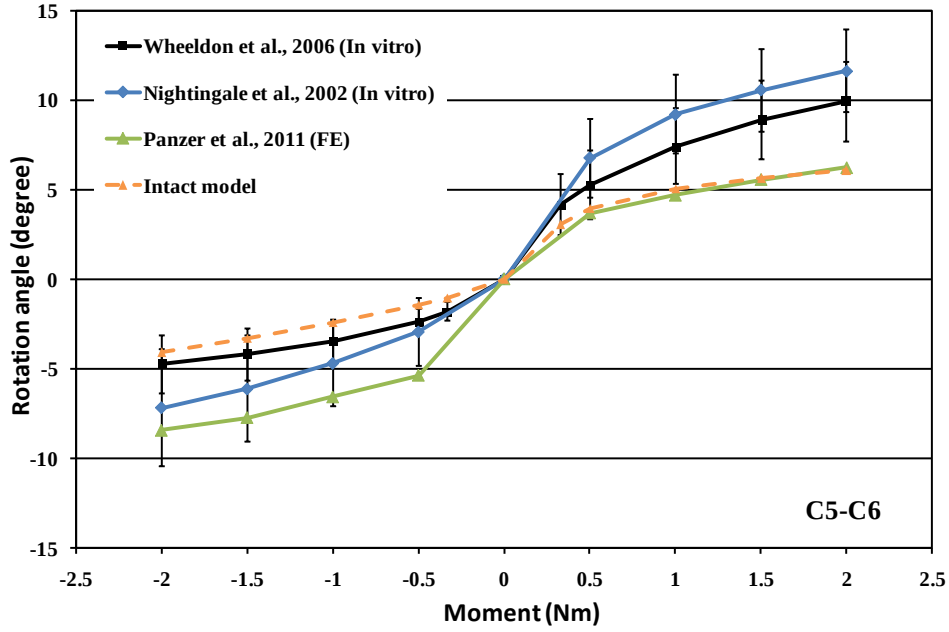
Wheeldon et al., 2006 (In vitro)
Nightingale et al., 2002 (In vitro)
Panzer et al., 2011 (FE)
Intact model
C5-C6
Rotation angle (degree)
Moment (Nm)
15
10
5
0
-5
-10
-15
-2.5
-2
-1.5
-1
-0.5
0
0.5
1
1.5
2
2.5

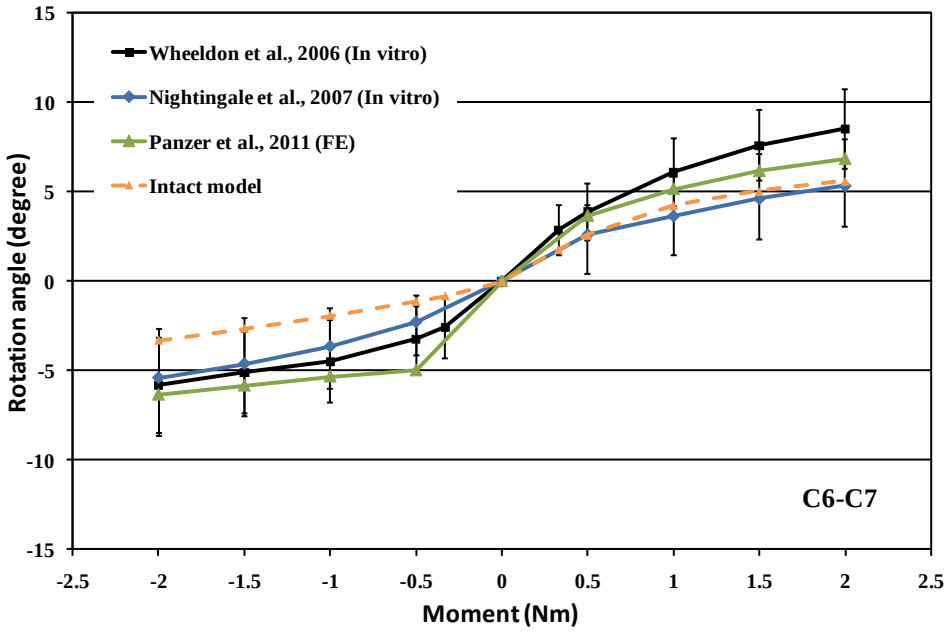


**Figure 16: Comparison of the intact model response against in vitro studies and FE models in different segments under flexion (positive) and extension (negative).**

### 3.1. Influence of ligaments

The NoISL model exhibited increases in motion of up to 66% at the 2 Nm load (Fig. 18a). The amounts of increase in motion of the NoLF and NoPLL models were as high as 1% and occurred at the 2Nm load. None of the ligaments passed the first linear zone under the considered load values.

### 3.2. Influence of facet joints

The predicted response of the NOF model during extension is presented in Fig. 18b. Changes in motion were observed for the NOF model at all load values, and the maximum change in motion (i.e., a 15% increase compared to the intact model) occurred at 0.33 Nm.

### 3.3. Influence of the Nucleus

Fig. 19 shows the motion of the NoNuc model compared to those of the intact and NoISL models during flexion. The rotation response increased by up to 75% after removing the nucleus, and the maximum value occurred at 0.33 Nm. This increase in motion was 23% for the 2 Nm load. From Fig. 19, it can be observed that from approximately the 0.5 Nm moment upward, the NoNuc model responded similar to the intact model, whereas the NoISL model responded more flexibly.

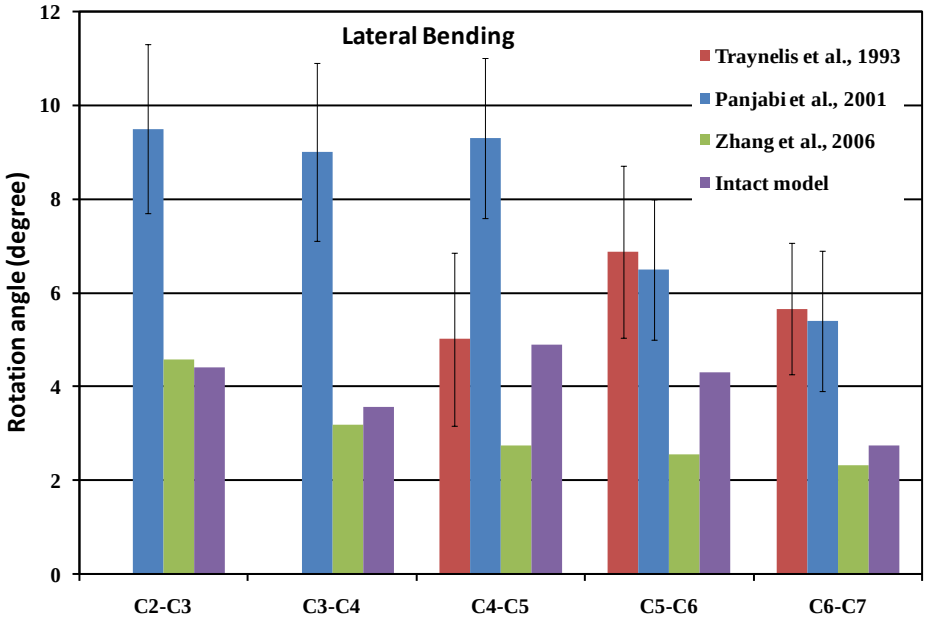

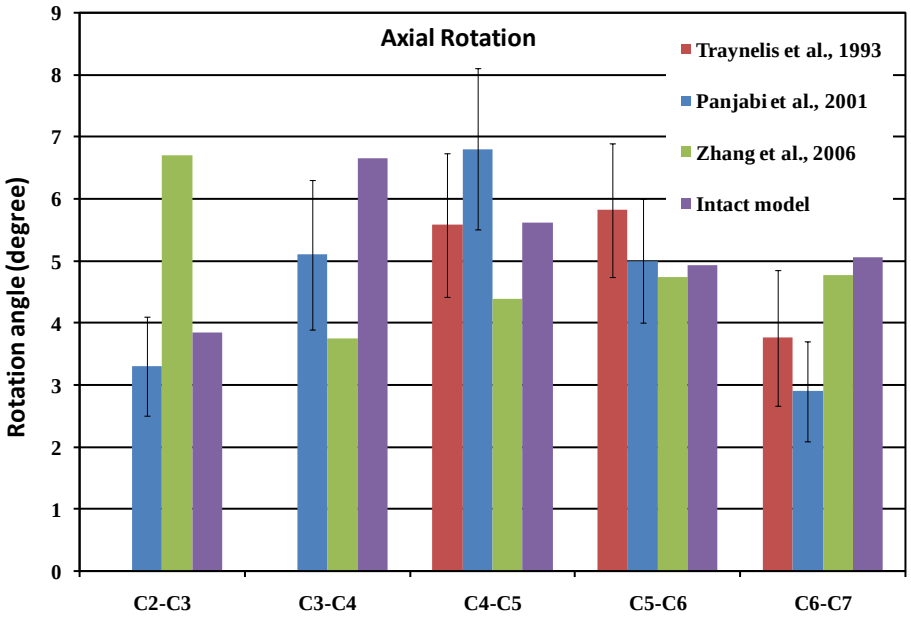


**Figure 17: Comparison of the intact model response against in vitro studies and FE models in different segments under (a) lateral bending and (b) axial rotation.**

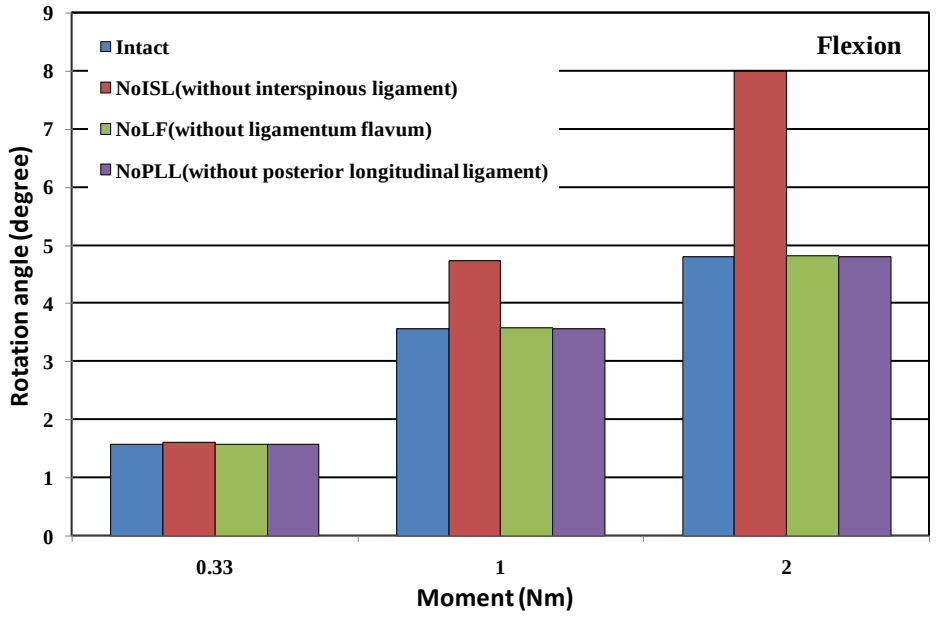

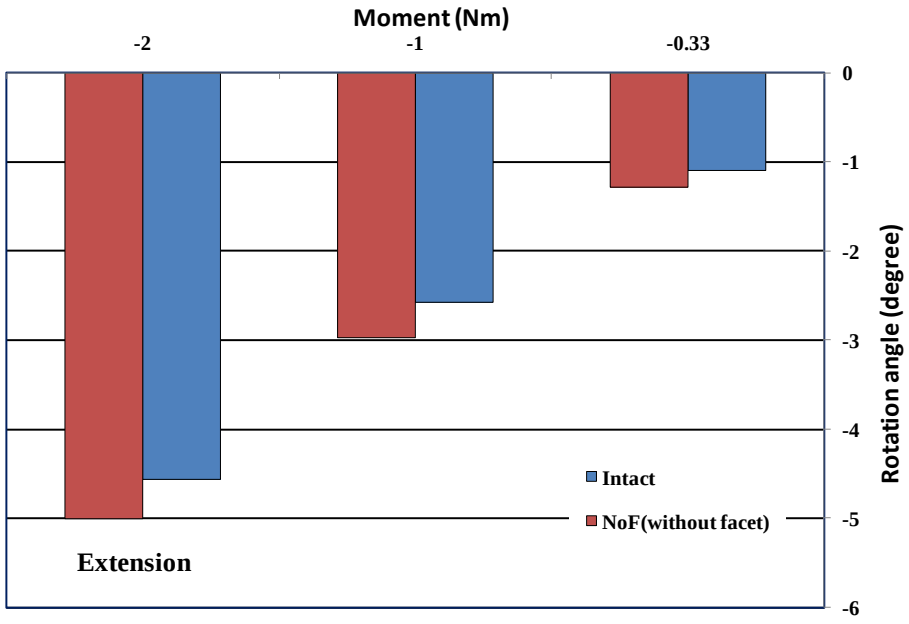


**Figure 18: (a) Influence of interspinous ligament (ISL), ligamentum flavum (LF), and posteriorlongitudinal ligament (PLL) on the stability of C4-C5 under flexion loading; (b) Influence of facet joints on the stability of C4-C5 under extension loading.**

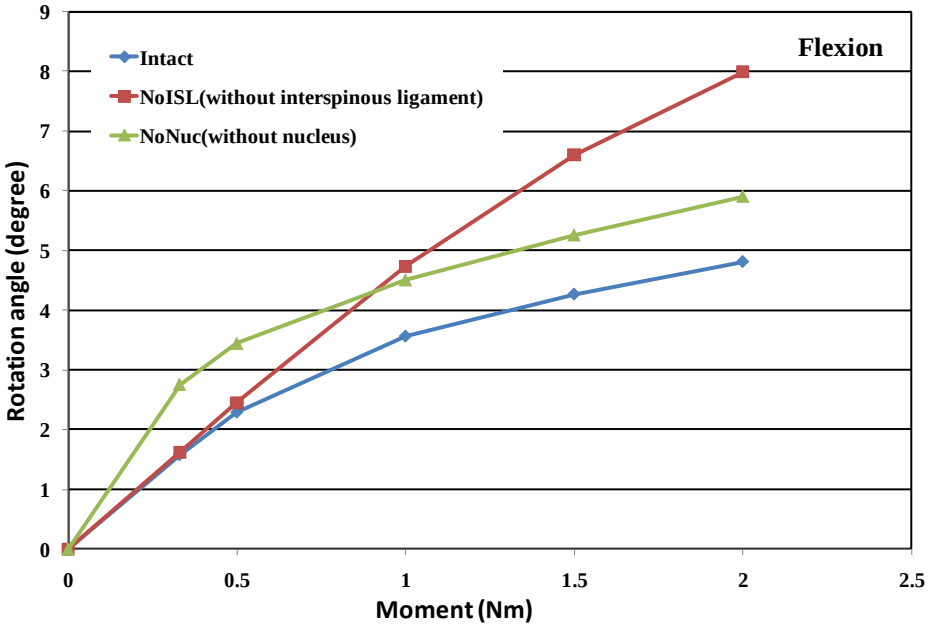


**Figure 19: Comparison of the NoISL, NoNuc, and intact models response under flexion loading.**

## 4. Discussion

The primary aim of this chapter was to use the multi-block technique to generate a fine hexahedral mesh for the whole cervical spine from C2 to T1. To obtain realistic results, the asymmetric geometry of the vertebrae and the discs about the mid-sagittal plane was considered. An accurate geometry of each vertebra was obtained from CT data, and a hexahedral mesh was generated on each vertebra and disc. In the validation step, the responses of the current FE model were compared to those of various experimental studies and proposed FE models under a wide range of loadings.

In general, the response of the intact model under different loading conditions agreed reasonably well with the reported experimental datasets in the literature. However, mostly during extension, the response of the model was stiffer in some segments and more flexible in other segments compared to the results of *in vitro* studies. We believe that the source of the inconsistencies in the extension response resulted from the orientation of the facet joints. Similar findings have been reported[25, 27, 28, 32, 33], and these studies have also suggested that facet orientations may cause differences between studies.

In the intact model, the flexion and extension curves for each segment were asymmetric at approximately zero for the intact case. The same trend was observed in the study of Wheeldon et al.[25], and the mean flexion values were higher than the extension values for all segments. Indeed, the difference in motion between flexion and extension can be explained by the asymmetric shape of the human neck on the sagittal plane and by the activation of different types of ligaments. Similar conditions were observed in Nightingale et al.'s[28] *in vitro* study. However, in another study, Nightingale et al.[27] reported that the mean values of flexion and extension were similar. The FE study of Panzer et al.[30] showed

asymmetric trends in flexion and extension, although the values for extension were higher than those for flexion in the C2-C3, C3-C4, and C5-C6 segments. In our study, the resultant flexion and extension motions of all segments agreed with the reported *in vitro* studies. Compared to the FE model of Panzer et al.[30], our FE model showed trends that were similar to those of *in vitro* studies of flexion and extension curves.

The rotation of each modified model was calculated and compared with the intact model. The results showed that the removal of the ISL affected the stability of the cervical spine to a much greater extent than the removal of other ligaments. Increasing the load increased the size of this difference. This behavior can be explained by the location of the ISL. Changes in the range of motion after excluding the PLL or LF were not noticeable. This finding proves that when the LF or PLL is omitted from the model, other ligaments can preserve the motion in all loading cases during flexion.

Facet joint simulations have been a major concern of previously proposed models of the cervical spine[2, 3, 5]. From a geometric perspective, the locations of the facet planes in our model, in contrast to most previous FE models[2, 3, 5], were not symmetric about the mid-sagittal plane. Our asymmetric cervical model caused coupled motion during extension under loading. The extent of this coupled motion was larger for higher loads. After omitting the facet joints, the amount of coupled motion was reduced. However, no change in coupled motion occurred when the ligaments were omitted from the intact model. Therefore, we conclude that the facet joints are the only component of the model responsible for coupled motion during extension loading regardless of the presence of ligaments.

The motion during flexion of the NoNuc model is presented in Fig. 5 under different loading. As seen in Fig. 19, the nucleus play the main role in preserving stability under lower loads. However, under higher loads, the ISL plays the main role in stabilizing the spine, even when the nucleus is absent.

In summary, the following key points were obtained from the FE analysis. The ISL was crucial for maintaining cervical spine stability during flexion, and the facet joints were the main contributors to stability during extension. Additionally, the nucleus provided stability under lower loads, while the ligaments provided this stability under higher loads during flexion. Future applications of our approach could be used for spine modeling.

## 5. References:


[1] Panjabi MM. Cervical spine models for biomechanical research. Spine 1998; 23(24): 2684-2699.

[2] Goel VK, Clausen JD. Prediction of load sharing among spinal components of a C5-C6 motion segment using finite element approach. Spine 1998; 23(6): 684-691.

[3] Yoganandan N, Kumaresan S, Voo L, Pintar FA, Larson SJ. Finite element modeling of the C4-C6 cervical spine unit. Med Eng Phys 1996; 18: 569-574.

[4] Maurel N, Lavaste F, Skalli W. A three-dimensional parametrized finite element model of the lower cervical spine. Study of the influence of the posterior articular facets. J Biomech 1997; 30(9): 921-931.

[5] Ng H-W, Teo E-C. Nonlinear finite element analysis of the lower cervical spine (C4-C6) under axial loading. Journal of Spinal Disorders 2001; 14: 201-210.

[6] Zafarparandeh I, Lazoglu I. Application of the finite element method in spinal implant design and manufacture, in The design and manufacture of medical devices, J.P. Davim, Editor. 2012, Woodhead Publishing.

[7] Stokes I, Frymoyer J. Segmental motion and instability. Spine 1987; 12(7): 688-691.

[8] Panjabi MM. The stabilizing system of the spine. Part II. Neutral zone and instability hypothesis. Journal of Spinal Disorders 1992; 5(4): 390-396.

[9] Panjabi MM. Clinical spinal instability and low back pain. Journal of Electromyography and Kinesiology 2003; 13(4): 371-379.

[10] Hong-Wan N, Ee-Chon T, Qing-Hang Z. Biomechanical effects of C2-C7 intersegmental stability due to laminectomy with unilateral and bilateral facetectomy. Spine 2004; 29(16): 1737-1745.

[11] Voo LM, Kumaresan S, Yoganandan N, Pintar FA, Cusick JF. Finite element analysis of cervical facetectomy. Spine 1997; 22(9): 964-969.

[12] Teo E-C, Ng H-W. Evaluation of the role of ligaments, facets and disc nucleus in lower cervical spine under compression and sagittal moments using finite element method. Med Eng Phys 2001; 23: 155-164.

[13] Sharma M, Langrana NA, Rodriguez J. Role of ligaments and facets in lumbar spinal stability. Spine 1995; 20(8).

[14] Schwab F, Lafage V, Boyce R, Skalli W, Farcy J-P. Gravity line analysis in adult volunteers: Age-related correlation with spinal parameters, pelvic parameters, and foot position. Spine 2006; 31(25): 959-967.

[15] Lafage V, Schwab F, Skalli W, Hawkinson N, Gagey P-M, Ondra S, Farcy J-P. Standing balance and sagittal plane spinal deformity: Analysis of spinopelvic and gravity line parameters. Spine 2008; 33(14): 1572-1578.

[16] Gilad I, Nissan M. Study of vertebra and disc geometric relations of the human cervical and lumbar spine. Spine 1986; 11(2): 154-157.

[17] Kallemeyn N, Tadepalli SC, Shivanna K, Grosland N. An interactive multiblock approach to meshing the spine. Computer Methods and Programs in Biomedicine 2009; 95: 227-235.

[18] Panjabi MM, Chen NC, Shin E, Wang J-L. The cortical shell architecture of human cervical vertebral bodies. Spine 2001; 26(22): 2478-2484.

[19] Pitzen T, Schmitz B, Georg T, Barbier D, Beuter T, Steudel WI, Reith W. Variation of endplate thickness in the cervical spine. Eur Spine J 2004; 13: 235-240.

[20] Clausen JD, Goel VK, Traynelis VC, Scifert J. Unicinate process and Luschka joints influence the biomechanics of cervical spine: quantification using a finite element model of the C4-C5 segment. . J Orthop Res 1997; 15: 342-347.

[21] Yoganandan N, Kumaresan S, Pintar FA. Geometric and mechanical properties of human cervical spine ligaments. Journal of Biomechancial Engineering 2000; 122: 623-629.

[22] Panjabi MM, Oxland TR, Takata K, Goel VK, duranceau J, Krag M. Articular facets of the human spine: quantitative three-dimensional anatomy. Spine 1993; 18(10): 1298-1310.

[23] Grauer JN, Biyani A, Faizan A, Kiapour A, Sairyo K, Ivanov A, Ebraheim NA, Patel TC, Goel VK. Biomechanics of two-level Charite artificial disc placement in comparison to fusion plus single-level disc placement combination. Spine J 2006; 6: 659-666.

[24] Goel VK, Grauer JN, Patel TC, Biyani A, Sairyo K, Vishnubhotla S, Matyas A, Cowgill I, Shaw M, Long R, Dick D, Panjabi MM, Serhan H. Effects of Charite aritficial disc on the implemented and adjacent spinal segments mechanics using a hybrid testing protocol. Spine 2005; 30(2755-2764).

[25] Wheeldon JA, Pintar FA, Knowles S, Yoganandan N. Experimental flexion/extension data corridors for validation of finite element models of the young, normal cervical spine. J Biomech 2006; 39: 375-380.

[26] Panjabi MM, Crisco JJ, Vasavada A, Oda T, Cholewicki J, Nibu K, Shin E. Mechanical properties of the human cervical spine as shown by three-dimensional load-displacement curves. Spine 2001; 26: 2692-2700.

[27] Nightingale RW, Carol Chancey V, Ottaviano D, Luck JF, Tran L, Prange M, Myers BS. Flexion and extension structural properties and strengths for male cervical spine segments. J Biomech 2007; 40: 535-542.

[28] Nightingale RW, Winkelstein Ba, Knaub KE, Richardson WJ, Luck JF, Myers BS. Comparative strengths and structural properties of the upper and lower cervical spine in flexion and extension. J Biomech 2002; 35: 725-732.

[29] Traynelis VC, Donaher PA, Roach RM, Goel VK. Biomechanical comparison of anterior Caspar plate and three-level posterior fixation techniques in a human cadaveric model. Journal of Neurosurgery 1993; 79: 96–103.

[30] Panzer BM, Fice BJ, Cronin SD. Cervical spine response in frontal crash. Med Eng Phys 2011; 33: 1147-1159.

[31] Zhang QH, Teo E-C, Ng H-W, Lee VS. Finite element analysis of moment-rotation relationships for human cervical spine. J Biomech 2006; 39: 189-193.

[32] Camacho D, Nightingale RW, Robinette J, Vanguri S, Coates S, Myers BS, *Experimental flexibility measurements for the development of a computational head-neck model validated for near-vertex head impcat*, in *Proceedings of the 41st Stapp Car Crash Conference*1997. p. 473-486.

[33] Panzer MB, Cronin DS. C4-C5 segment finite element model development, validation, and load-sharing investigation. J Biomech 2009; 42: 480-490.

# Chapter 4:

## Biomechanics of Posterior Dynamic Stabilization Systems [1]

[1]D. Erbulut, I. Zafarparandeh, A. F. Ozer, and Vijay K. Goel. Review article: Biomechanics of Posterior Dynamic Stabilization Systems, Advances in Orthopedics, doi: 10.1155/2013/451956, 2013.

## 1. Introduction

Low back pain is a one of the major health problems around the world. One of the leading causes of low back pain is considered to be degeneration of the intervertebral disc. Disc herniation, spondylolisthesis, spondylosis, and spinal stenosis may follow intervertebral disc degeneration. Back pain occurs when the posterior disc bulges out and impinges the nerve roots due to herniated disc. Another nerve root impingement may be seen in the condition of spinal stenosis, which is a reduction of the diameter of the spinal canal.

The treatment options of low back pain may vary depends on the severity of the case. They include conservative treatment or surgical techniques. Conservative treatments include exercise, medications, physiotherapy and rehabilitation. Surgical treatment is considered for the patient when the back pain limits their daily activities and when the condition does not respond to other therapies. Surgical methods include decompression with spinal fusion or non-fusion devices.

Spinal fusion supported by rigid instrumentation is widely used in the treatment of various spinal disorders. Since the procedure was first introduced by Albee and Hibbs in 1911, fusion has played an important role in the lumbar spine employed operations. The ideal result in performing fusion is to gain the necessary therapeutic goals with the minimal disruption of normal structure and function of the spinal column[1, 2]. However, usage of the rigid instrumentation results in a considerable amount of morbidity and of complications. Adjacent disc degeneration is reported by many investigators, known as one of the problems in fusion technique. Omitting the mobility causes the adjacent segments to be overloaded and as a result the number of interventions increases.

Considering all these reasons, the search for an alternative procedures with different concept was reinforced [3].

In recent years, posterior dynamic stabilization devices are introduced as a trustworthy alternative to fusion and gained increasing popularity. The comparable advantages of these devices to fusion include retention and protection of the intervertebral disc, earlier surgical intervention, and minimal invasive techniques. Dynamic stabilization technique is aimed for preserving motion at the treated segment. It reduces the risk of accelerated degeneration at adjacent levels which is a major concern in fusion because of the protective effects of continuing segmental motion[4, 5]. Although, dynamic stabilization has gained a lot of attention by the investigators, designing a new spinal-implant system needs a cautious approach. The fusion-implant needs to provide the stabilization until the fusion takes place; but for the dynamic stabilization systems this role should be taken throughout the lifetime [6].So far, various posterior dynamic stabilization systems have been reported in the literature that can be categorized as: 1) pedicle-based systems; 2) total facet replacement systems; 3) posterior interspinous spacers. In this chapter, biomechanical evaluation of posterior spinal implants was described and biomechanical properties of several of such devices were reviewed.

## 2. Biomechanical evaluation of dynamic spinal implants

Segmental biomechanics will be altered by the implantation. Therefore, it is crucial to evaluate biomechanical effects of implants on the treated and nontreated spinal segment(s) before clinical trials. Biomechanical evaluation of posterior dynamic stabilization systems can be accomplished by *in vivo*, *in vitro* and finite element analysis (FEA) studies. Change in decompression and stabilization parameters due to instrumentation with respect to the intact case can be assessed using spine specimen. It is the so-called *in vitro* studies that include spine specimen form human or other

species. *In vitro* studies should follow standard protocols[7]during the preparation of spine specimens and testing. Goel et al. [7]suggested that multispinal segment should be used in order to include one free functional spinal unit (FSU) on each side of the implanted segment. Desired loads are applied to the free end of the specimen and motion data is recorded accordingly. There are two loading protocols known as displacement control or flexibility control loading. The load control protocol includes force loadings such as shear, pure moment and complex loads.

FEA plays an important role in biomechanical evaluation of implants. It is helpful to determine the structural analysis of an implant, bone and interaction in between two. FE analysis gives full inside of load shearing, stresses and strain of the interested construct under loading scenarios. It provides prospective outline of needed parameters for a desired spinal implant development. These parameters cannot be determined by *in vitro* experimental studies. However, finite element model needs to be validated by *in vitro* experimental study Figure 20 depicts in vitro cadaver study and lumbar FE model.

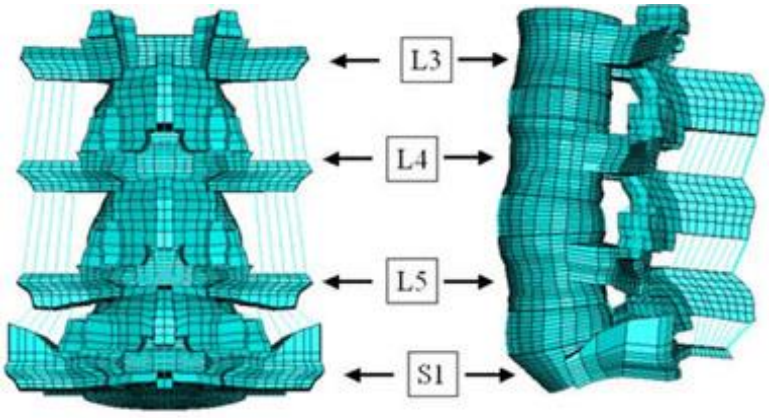


a)

b) 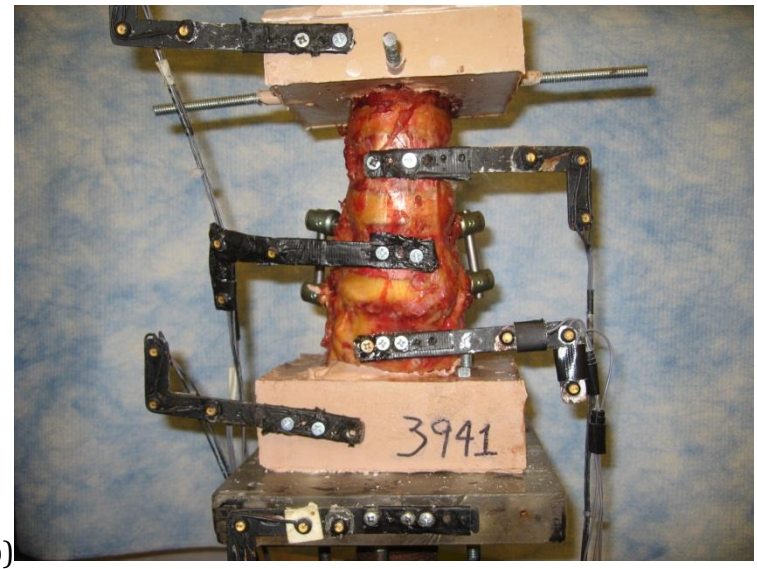


**Figure 20: a) FE model of the lumbar spine (ECORE, University of Toledo), b) the lumbar spine specimen with posterior dynamic stabilization system**

## 3. Posterior Dynamic Stabilization Systems

### 3.1. Pedicle based stabilization systems:

The Dynesys (Dynamic Neutralization System for the Spine), known as a dynamic stabilization device, is one of the alternative solutions for the degenerative lumbar disc problems, Figure 21-a. It was implanted for the first time in 1994 by Dubois et al.[8]as a pedicle screw-based system. The intention for using the Dynesys as a flexible posterior spinal fixation system is to maintain intersegmental motions or reduce them to magnitudes found in the intact spine, and reducing the negative effects on the adjacent segments. The Dynesys is a bilateral device and consists of titanium alloy pedicle screws, and polycarbonate urethane (PCU) spacers that surround tensioned polyethylene terephthalate (PET) cords [9].

Schmoels et al.[10] performed an *in vitro* study to evaluate biomechanical effect of Dynesys on the magnitudes of stabilization at the treated segment. All the six spines were tested in four stages: the intact, with the defect of the middle segment, fixation with the Dynesys, and fixation with internal fixator. The cadavers were loaded with pure moments in three motion planes i.e. flexion-extension,

lateral bending, axial rotation. The results showed that for the bridged segment, the Dynesys was able to stabilize the spine. The study showed that Dynesys allowed more flexibility to the segment than the internal fixator. In another study with the same loading conditions, Schmoels et al.[11] investigated the influence of the dynamic stabilization system (Dynesys) on the intervertebral disc which is bridged. It was observed that load bearing of the disc was slightly altered in the case of axial rotation. In flexion, both devices showed a good support of the anterior column by decreasing the intraduscal pressure but slightly below the intact level. Their results showed that the Dynesys did not show substantial differences in intradiscal pressure of the bridged disc compared to the internal fixator. Beastall et al.[12] investigated the biomechanical influence of the Dynesys on the lumbar spine. It was found that Dynesys significantly reduced motion at the bridged segment. However implantation did not affect the range of motion at the adjacent segment.

Biomechanical investigations reported that some of the posterior dynamic stabilization hada similar effect on flexion, extension and lateral bending, compared with rigid instrumentation due to dynamic implants with high stiffness [4, 9, 10, 13, 14]. Recent studies suggest that a dynamic implant with lower stiffness may be sufficient to stabilize the spinal segment[13, 15]. Dynamic implants with minimal stiffness of 45N/mm axially and 30N/mm bending are enough to reduce spinal flexibility by 30% of the intact range of motion which is considered to be optimal motion reduction [13]. Another study demonstrated that the optimal axial stiffness value of the longitudinal rods should be approximately 50N/mm for an effective pedicle screw-based dynamic implant[9].For example, studies showed that Dynesys (Dynesys-Zimmer, Minneapolis, MN),presents higher stiffness than initially expected[10, 14]. Posterior dynamic fixator with high stiffness does not allow enough mobility to the treated segment in order to have potential benefits as described above. A dynamic rod with very low axial stiffness (<200N/mm) did influence the segmental kinematics and allows more mobility [9].

Another alternative for the rigid spinal fusion is a soft or flexion stabilization technique introduced by Graf[16]. Graf Ligament (SEM Co., Mountrouge, France) is composed of titanium pedicle screws that are connected by polyester threaded bands Figure21-b. In fact, the polyester bands prevent the abnormal rotary motion and preserve the segment physiological lordosis. Biomechanical investigations have shown that the Graf system reduces the angular motion in flexion-extension without limiting the vertebral body translation in other directions. As a result, Graf system design has drawbacks in preventing the spondylolisthesis. Kanayama et al.[17]studied the efficacy of the Graf system in the treatment of the degenerative spondylolithesis. Their study included 64 patients that underwent Graf system. Based on the clinical and radiographic results, the vertebral slip could not be prevented but in 80% of the patients the lordosis was maintained.

Cosmic (Ulrich GmbH & Co.KG, Ulm, Germany) is a posterior dynamic stabilization system using pedicle screws to provide nonrigid stability for the degenerative lumbar spine. The head of the pedicle screws are hinged shape and it connects the threaded part to the screw. This composition enables the load sharing between the Cosmic and the anterior vertebral column Figure 21-c. In a study[18], 103 consecutive patients were treated with Cosmic. The results showed a considerable improvement of pain, related stability and mobility, but 10% reoperation during the follow-up was observed.

Wilke et al.[15] suggested that if one dynamic system provides 70% less range of motion compare to non-degenerated segment, it may prevent screw loosening. In addition, other studies showed a good agreement that a reduced load in the pedicle screw based dynamic stabilization system minimizes the risk of screw loosening [19]. However, studies also showed that screw loosening problem can be minimized by using hinged dynamic screws regardless of posterior stabilization systems [20, 21].

The PercuDyn (Interventional Spine Inc., Irvine, CA) is known as an extension-limiting posterior dynamic stabilization implant which is mainly a bilateral facet augmentation system, Figure 21-d. Two titanium screws anchor the device to the pedicles and a polycarbonate urethane cushion bumper resting against the inferior auricular process provides the flexibility for the dynamic posterior stabilization system[5, 22]. Masala et al. [23] conducted a study on the PercuDyn implant to evaluate the efficiency of this system as a treatment for patients with lumbar stenosis. The implantation was performed on 24 consecutive patients with lumbar stenosis. The results demonstrated that in 20 patients (83%) 1-year follow-up improvement was observed. For the all patients, including responder and nonresponder, no complications were reported regarding the device.

The Accuflex (Globus Medical, Inc) is a posterior dynamic stabilization system that achieves the flexibility from helical cuts on rod. It is categorized as a pedicle-screw based system including a dynamic rod and 6.5-mm pedicle screws made of titanium alloy, Figure21-e. The helical cut transforms the rod into semi rigid one that allows motion primarily in the flexion-extension mode. One of the advantages of the Accuflex is that it requires a technique similar to the standard pedicle screw/rod construct and due to that, the insertion can be performed by most spine surgeons[24].Reyes-sanchez et al. [25], reported the clinical outcome of a series of patients with lumbar spinal stenosis that underwent lumbar spine instrumentation with the Accuflex implant. Although, clinical benefits were observed in 83% of the patients, the failure due to fatigue in the 22.22% of the patients led to hardware removal.

BioFlex, similar to Dynesys, is a posterior dynamic stabilization system using titanium pedicle screws connected by Nitinol rods with coiling consisted of 1-2 turns, Figure 21-f. Nitinol is classified as a shape memory alloy and shows superelasticity behavior. In addition to this property, it is somewhat rigid and it can act as a tension band at the posterior spinal column. The BioFlex system

resists against excessive deformation during extension, thus it maintains the physiological range of motion[26].

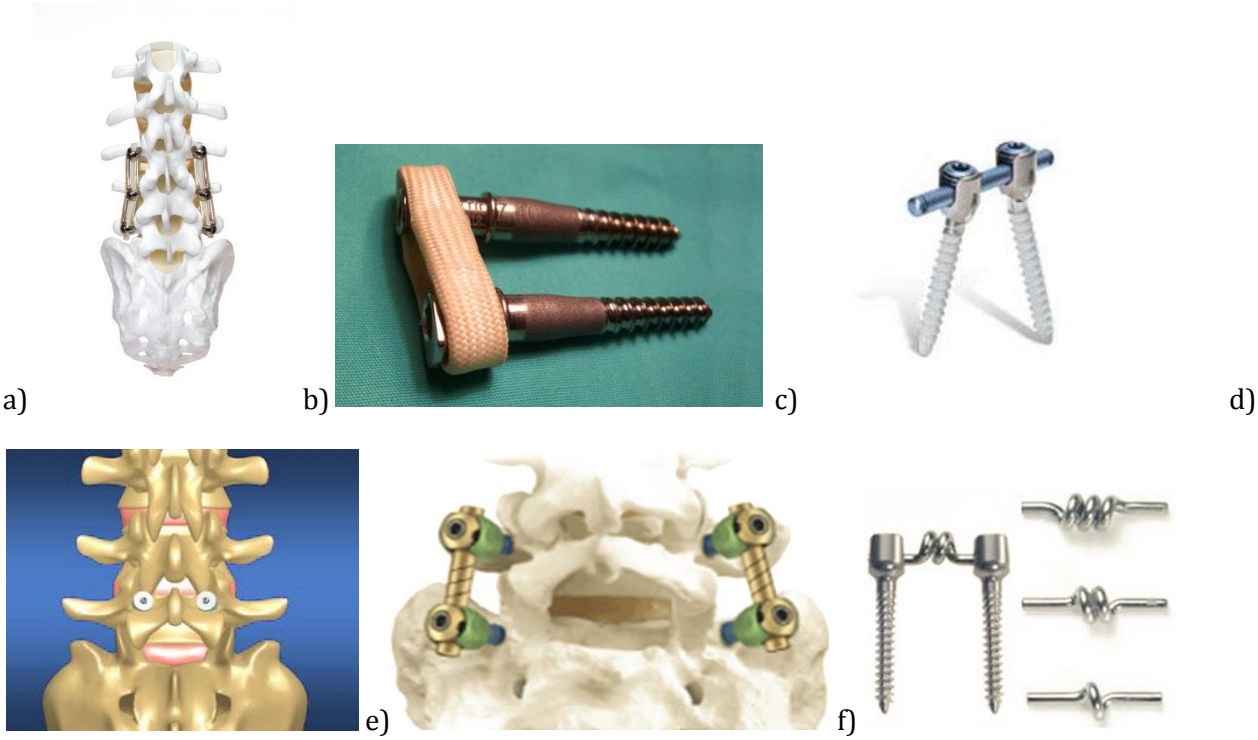

**Figure 21: Posterior dynamic stabilization systems. (a) Dynesys; (b) Graf system; (c) Precudyn (d) Cosmic (e) AccuFlex f) BioFlex**

### 3.2. Interspinous spacers

The lumbar interspinous process decompression (IPD) devices are known as trustable alternatives for the treatment of various spinal disorders. The first IPD device, X-STOP (St Francis Medical Technologies, Alameda, USA), introduced in the US for the treatment of patients with neurogenic intermittent claudication due to spinal stenosis, Figure 22-a. The major concept in the design of X-STOP is to limit the extension movement at the individual stenotic level while allowing the normal movement in all other directions of the treated and untreated level(s) [27]. Comparing to other IPD devices, X-STOP has been documented extensively in the literature. Its features include two lateral wings to prevent migration, intended to distract the discs, increase the foraminal areas, and stabilize the posterior column [5]. Lindsey et al.[28]studied the effect of X-STOP device on the kinematics of

the instrumented and adjacent levels. They tested seven lumbar spines (L2-L5) in three motion planes, flexion-extension, lateral bending, and axial rotation. The study showed that X-STOP did not affect the kinematics of the adjacent segment. Siddiqui et al.[29] studied kinematics of the lumbar spine with X-STOP device in sagittal plane at the instrumented and adjacent levels *in vivo*. They measured the disc heights, endplate angles, segmental and lumbar range of movement after implanting the X-STOP. The results showed that no significant changes were seen in disc heights, segmental and total lumbar spine movements postoperatively. They concluded that the sagittal kinematics of the lumbar spine is affected using X-STOP. Kondrashov et al.[27] performed a 4-year follow-up on 18 X-STOP subjects. Twelve patients had the X-STOP implanted at either L3-4 or L4-5 levels while the other 6 patients had the X-STOP implanted at both L3-4 and L4-5 levels. Grade I spondylolisthesis was noticed in six patients.

Coflex device (Paradigm Spine, LCC, New York, NY), formerly Interspinous 'U', is one of the dynamic interspinous implants that was first introduced by the French orthopaedic surgeon Jacques Samani as an alternative to arthrodesis, Figure 22-b. The aim of this U-shaped compressible device which is manufactured from titanium, is to unload the facet joints, restore the foraminal height and provide stability in order to improve the clinical outcome of surgery [30].

Diam implant (Medtronic, Memphis, TN) system is an interspinous spacer and it has a silicon core with a polyethylene cover[31]. Three mesh bands are designed to secure the implant: two of them are around each spinous processes and the other around the supraspinous ligament, Figure 22-c.

In mid-1980s, Sénégas introduced an interspinous implant which was a "floating system" with the purpose of avoiding the risk of loosening. The implant system consisted of a titanium spacer placed between the spinous processes of the lumbar spine. Two Dacron ligaments wrapping around the spinous processes, was considered to secure the implant. Despite the favorable results, second-generation device called Wallis (Spine Next, Bordeaux, France) was developed to improve the device

functionality(Figure 22-d). In the newer implant the polyetheretherketone (PEEK) is replaced with the titanium. Sénégas recommends that the current design of implant can be used for lumbar disc disease in the following indications: 1) discectomy for a herniated disc with a large material loss, 2) a second discectomy for recurrence of herniated disc, 3) discectomy for herniation of a transitional disc with sacralization of L5, 4) degenerative disc disease at a level adjacent to a previous, 5) isolated Modic I lesion leading to chronic low-back pain [32].

**Figure 22: Interspinous spacer: a) X-STOP, b) Coflex, c) DIAM system, d) Wallis system.**

## Conclusions

Fusion is a gold standard for low back pain treatment till date. However, there have been several complications reported clinically. These complications mainly are related to adjacent segment degeneration due to high stiffness at the stabilized segment. Alternative treatment, nonfusion stabilization systems became more and more popular in order to preserve the mobility of a motion segment and eliminate adjacent segment phenomena. Current research studies emphasize on long-term clinical evaluation of dynamic stabilization system.

On the other hand, the stiffness of the dynamic implants is a big concern due to not providing an appropriate motion range. For example, one of the so-called dynamic stabilization systems, Dynesys, performs stiffer than initially intended. Studies showed that there are no differences between rigid and dynamic stabilization systems in terms of allowing motion to the treated segment in flexion,

extension and lateral bending. Therefore, it is important to optimize the dynamic implant stiffness for a desired spinal range of motion achievement.

## 4. References


[1] White III AA, Panjabi MM, Clinical biomechanics of the spine. 1990: Lippincott-Raven.

[2] Zhang QH, Teo EC. Finite element application in implant research for treatment of lumbar degenerative disc disease. Medical engineering & physics 2008; 30(10): 1246-1256.

[3] Schwarzenbach O, Berlemann U, Stoll TM, Dubois G. Posterior dynamic stabilization systems: DYNESYS. The Orthopedic clinics of North America 2005; 36(3): 363-372.

[4] Niosi Ca, Zhu Qa, Wilson DC, Keynan O, Wilson DR, Oxland TR. Biomechanical characterization of the three-dimensional kinematic behaviour of the Dynesys dynamic stabilization system: an in vitro study. European spine journal 2006; 15(6): 913-922.

[5] Sangiorgio SN, Sheikh H, Borkowski SL, Khoo L, Warren CR, Ebramzadeh E. Comparison of three posterior dynamic stabilization devices. Spine 2011; 36(19): E1251-E1258.

[6] Molinari RW. Dynamic stabilization of the lumbar spine. Current Opinion in Orthopaedics 2007; 18(3): 215-220.

[7] Goel VK, Panjabi MM, Patwardhan AG, Dooris AP, Serhan H. Test protocols for evaluation of spinal implants. The Journal of bone and joint surgery 2006; 88-A, Suppl 2: 103-109.

[8] Dubois G, De Germay B, Schaerer NS, Fennema P. Dynamic neutralization: a new concept for restabilization of the spine, in Lumbar segmental instability., M. Szpalski, R. Gunzburg, and M.H. Pope, Editors. 1999, Lippincott Williams & Wilkins: Philadelphia. p. 233-240.

[9] Rohlmann A, Burra NK, Zander T, Bergmann G. Comparison of the effects of bilateral posterior dynamic and rigid fixation devices on the loads in the lumbar spine : a finite element analysis. European Spine Journal 2007; 16: 1223-1231.

[10] Schmoelz W, Huber JF, Nydegger T, Dipl-Ing, Claes L, Wilke HJ. Dynamic stabilization of the lumbar spine and its effects on adjacent segments: an in vitro experiment. Journal of spinal disorders & techniques 2003; 16(4): 418-423.

[11] Schmoelz W, Huber JF, Nydegger T, Claes L, Wilke HJ. Influence of a dynamic stabilisation system on load bearing of a bridged disc: an in vitro study of intradiscal pressure. European spine journal 2006; 15(8): 1276-1285.

[12] Beastall J, Karadimas E, Siddiqui M, Nicol M, Hughes J, Smith F, Wardlaw D. The Dynesys Lumbar Spinal Stabilization System Imaging Findings. Spine 2007; 32(6): 685-690.

[13] Schmidt H, Heuer F, Wilke H-J. Which axial and bending stiffnesses of posterior implants are required to design a flexible lumbar stabilization system? Journal of Biomechanics 2009; 42(1): 48-54.

[14] Schulte TL, Hurschler C, Haversath M, Liljenqvist U, Bullmann V, Filler TJ, Osada N, Fallenberg EM, Hackenberg L. The effect of dynamic, semi-rigid implants on the range of motion of lumbar motion segments after decompression. Eur Spine J 2008; 17(8): 1057-65.

[15] Wilke H-J, Heuer F, Schmidt H. Prospective Design Delineation and Subsequent In Vitro Evaluation of a New Posterior Dynamic Stabilization System. Spine 2009; 34(3): 255-261.

[16] Hashimoto T, Oha F, Shigenobu K, Kanayama M, Harada M, Ohkoshi Y, Tada H, Yamamoto K, Yamane S. Mid-term clinical results of Graf stabilization for lumbar degenerative pathologies. a minimum 2-year follow-up. The spine journal 2001; 1(4): 283-289.

[17] Kanayama M, Hashimoto T, Shigenobu K. Rationale, biomechanics, and surgical indications for Graf ligamentoplasty. The Orthopedic clinics of North America 2005; 36(3): 373-377.

[18] Stoffel M, Behr M, Reinke A, Stüer C, Ringel F, Meyer B. Pedicle screw-based dynamic stabilization of the thoracolumbar spine with the Cosmic-system: a prospective observation. Acta neurochirurgica 2010; 152(5): 835-843.

[19] Meyers K, Tauber M, Sudin Y, Fleischer S, Arnin U, Girardi F, Wright T. Use of instrumented pedicle screws to evaluate load sharing in posterior dynamic stabilization systems. The Spine Journal 2008; 8(6): 926-932.

[20] Ozer A, Crawford N, Sasani M, Oktenoglu T, Bozkus H, Kaner T, Aydin S. Dynamic lumbar pedicle screw-rod stabilization: two-year follow-up and comparison with fusion. The open orthopeadics journal 2010; 4: 137-41.

[21] von Strempel A. Dynamic stabilisation: cosmic system. Interactive Surgery 2008; 3(4): 229-236.

[22] Smith ZA, Armin S, Raphael D, Khoo LT. A minimally invasive technique for percutaneous lumbar facet augmentation: Technical description of a novel device. Surgical Neurology International 2011; 2: 165.

[23] Masala S, Tarantino U, Nano G, Iundusi R, Fiori R, Da Ros V, Simonetti G. Lumbar Spinal Stenosis Minimally Invasive Treatment with Bilateral Transpedicular Facet Augmentation System. Cardiovascular and interventional radiology 2012; In press.

[24] Mandigo CE, Sampath P, Kaiser MG. Posterior dynamic stabilization of the lumbar spine: pedicle based stabilization with the AccuFlex rod system. Neurosurgical focus 2007; 22(1): E9: 1-4.

[25] Reyes-Sánchez A, Zárate-Kalfópulos B, Ramírez-Mora I, Rosales-Olivarez LM, Alpizar-Aguirre A, Sánchez-Bringas G. Posterior dynamic stabilization of the lumbar spine with the Accuflex rod system as a stand-alone device: experience in 20 patients with 2-year follow-up. European spine journal 2010; 19(12): 2164-2170.

[26] Cho BY, Murovic J, Park KW, Park J. Lumbar disc rehydration postimplantation of a posterior dynamic stabilization system. Journal of neurosurgery Spine 2010; 13(5): 576-580.

[27] Kondrashov DG, Hannibal M, Hsu KY, Zucherman JF. Interspinous Process Decompression With the X-STOP Device for Lumbar Spinal Stenosis. Journal of spinal disorders & techniques 2006; 19(5): 323-327.

[28] Lindsey DP, Swanson KE, Fuchs P, Hsu KY, Zucherman JF, Yerby Sa. The effects of an interspinous implant on the kinematics of the instrumented and adjacent levels in the lumbar spine. Spine 2003; 28(19): 2192-2197.

[29] Siddiqui M, Karadimas E, Nicol M, Smith FW, Wardlaw D. Effects of X-STOP device on sagittal lumbar spine kinematics in spinal stenosis. Journal of spinal disorders & techniques 2006; 19(5): 328-333.

[30] Richter A, Schütz C, Hauck M, Halm H. Does an interspinous device (Coflex) improve the outcome of decompressive surgery in lumbar spinal stenosis? One-year follow up of a prospective case control study of 60 patients. European Spine Journal 2010; 19(2): 283-289.

[31] Christie SD, Song JK, Fessler RG. Dynamic interspinous process technology. Spine 2005; 30(16S): S73-S78.

[32] Sénégas J. Mechanical supplementation by non-rigid fixation in degenerative intervertebral lumbar segments: the Wallis system. European Spine Journal 2002; 11(Suppl 2): S164-S169.

# Chapter 5:

## Determination of biomechanical effect of interspinous process device on implanted and adjacent lumbar spinal segments using a hybrid testing protocol: a finite element study[1]

[1]D. Erbulut, **I. Zafarparandeh**, C. Hassan, I. Lazoglu, and A. F. Ozer. Determination of biomechanical effect of interspinous process device on implanted and adjacent lumbar spinal segments using a hybrid testing protocol: a finite element study. Journal of Neurosurgery-Spine,

### 1. Introduction

Implantation of ISP devices is known to be useful as a surgical treatment for different types of spinal pathologies, such as spinal stenosis or facet arthritis.[1-3] The main design goal of such devices is to apply a distraction force to the processes and prevent further extension of the segment. As a result, ISP devices help to relieve the symptoms of neurogenic intermittent claudication associated with spinal stenosis. Further, these devices are designed to limit extension and expand the spinal column and foramen at the treated level. They are also designed to allow motion during flexion, lateral bending, and axial rotation at the treated segment, because of which they reduce the adjacent-level effects (ALEs).[1, 4]

From among all ISP devices, X-STOP (SFMT, Concord, CA, USA) has been documented most extensively in the literature.[5] It has two lateral wings to prevent unnecessary displacements.[6] The design of X-STOP is aimed mostly at preventing extension while allowing normal motion in other motion planes. In an *in vitro* study, Lindsey et al.[7]

investigated the effect of X-STOP implantation on the kinematics of implanted and adjacent segments and found that it significantly reduced the range of motion(ROM) in extension at the implanted level while retaining the ROM in flexion, axial rotation, and lateral bending. They also found that X-STOP did not affect the ROM of the adjacent segments in any motion direction. In another *in vivo* study, Siddiqui et al.[8] investigated the changes in the disc height and segmental and total lumbar rotation before and after X-STOP implantation and concluded that the disc height and sagittal kinematics of the lumbar spine are not significantly affected by X-STOP.

Wilke et al.[2] compared the effects of four interspinous implants—Coflex, Wallis, DIAM, and X-STOP—on the ROM and intradiscal pressure (IDP) in an *in vitro* test in which pure moments were applied on a functional spinal unit in flexion-extension, lateral bending, and axial rotation. Their results showed that all implants reduced the ROM in extension by about 50% of that in the intact model. However, none of them affected the ROM in other directions. Further, as was the case with the ROM, all the implants reduced the IDP in extension but did not have any effect on it in other directions. In another *in vitro* study, Hartmann et al.[4] studied the biomechanical effect of four interspinous implants— Aperius (Kyphon, Mannheim, Germany), In-Space (Synthes, Umkirch, Germany), X-STOP, and Coflex—on the ROM at implanted and adjacent levels using L1–L5 lumbar cadavers. They found that all four devices caused a significant reduction in the ROM in extension but did not affect it under pure moments in other directions. They also demonstrated that when a follower load was applied with pure moments, the ROM in flexion decreased for all four implants. Wiseman et al.[9] determined the effect of implantation of X-STOP on the facet load in extension at the index and adjacent segments of L2–L5 lumbar cadavers and found a

significant reduction in facet loads at the index level but no change in the loads at the adjacent level. Swanson et al.[10] investigated the influence of X-STOP implantation on the IDP at the index (L3-L4) and adjacent levels *in vitro*. They observed that the IDP was not significantly affected by the device at the adjacent level but it decreased considerably at the index level.

All the above-discussed studies were *in vitro* studies. However, *in vitro* investigations have several limitations; for example, as reported by Wilke et al.,[2] the IDP *in vitro* may not be calculated correctly with pressure transducers. However, finite element (FE) studies, unlike *in vitro* studies, can help researchers in examining the inner workings of the lumbar spine and studying the effects of an ISP device on the load sharing, stresses, and strains in the spine under different loading conditions. To this end, Lafage et al.[11] conducted a combined *in vitro* and FE study to investigate the effect of the Wallis implant on the ROM and the stress at the disc annulus and implant at the index and superior adjacent levels. They used the L3–L5 segments for cadaver and FE studies and observed a reduction in the motion and disc internal loads in the case of the implanted segment. However, their model was limited to studying the adjacent-segment effect since it had just two segments; furthermore, they applied a flexible protocol (load control) instead of the hybrid protocol (displacement control). The hybrid protocol is more anatomically relevant and can better represent the motion and loads experienced by the spine after surgical procedures and implantation.[12, 13]However, in the field of ISP devices, studies have rarely been conducted using the FE approach for performing a detailed biomechanical investigation of the effect of these devices on adjacent segments with hybrid protocol.

Therefore, the aim of the present FE study was to evaluate the effect of an ISP device on the biomechanical parameters of an implanted lumbar spine using a hybrid testing protocol. The biomechanical parameters considered were the ROM, IDP, and facet load at both the index level and the adjacent level. In addition, the stress in the ISP after implantation was evaluated.

## 2. Materials and methods

### 2.1. Intact model

A three-dimensional (3D) FE model of L1–L5 segments of the lumbar spine was developed. The geometry of the vertebrae was obtained from CT scan data of a healthy 35-year-old male. The lordosis curvature was measured to be 25° using Cobb method (Figure 23a). All cancellous, cortical, and posterior parts of the vertebrae were meshed using hexahedral elements (C3D8). The outer layer of the elements on each vertebra was considered as the cortical layer with a thickness of approximately 0.5mm.[14] Further, the adjacent level of the disc was considered as the endplate with an average thickness of 0.6mm, and the cancellous part of the vertebrae composed the inner mesh. The detailed meshing procedure has been reported in our previous study.[15] Three-dimensional gap contact elements (GAPUNI) were used to simulate the facet joints between the vertebrae. These elements transfer force between nodes in a single direction as a function of the specified gap between them. The behavior of the cartilaginous layers of the facet surfaces was simulated with a parameter called “softened contact” in the ABAQUS software (ABAQUS®, Version 6.10-2; Abaqus, Inc., Providence, RI, USA).

The circular mesh pattern[15] on the disc helped to model the concentric rings of the annulus ground substance. The rebar option of ABAQUS oriented ±30° to the horizontal plane was used to model the fibers in the annulus. The "no compression" option of the ABAQUS software was used to restrict the fibers only under tension loading. A hyperelastic material model was used to simulate the behavior of the annulus. Further, the fluid behavior of the nucleus was simulated using a hexahedral element assigned a very low stiffness (1 MPa) and near-incompressibility (Poisson's ratio υ=0.4999).

The ligaments were simulated using 3D truss elements, which were constrained to act nonlinearly only in tension. All seven major ligaments, i.e., the anterior longitudinal ligament (ALL), posterior longitudinal ligament(PLL), ligamentum flavum(LF), intertransverse ligament(ITL), interspinous ligament(ISL), supraspinous ligament(SSL), and capsular ligament(CL), were represented. The ligaments' behavior, namely, the change in their stiffness with strain, was simulated using a hypoelastic material model.

The complete model consisted of 72193 nodes and 55650 elements that represented the entire structure of the lumbar spine (Figure 23b). The material properties of various components of the lumbar model (Table 3) were obtained from the literature.[16]

**2.2. Boundary and loading conditions**

In all directions, the nodes lying on the upper endplate of L1 were coupled to a flying node (FN) higher than the surface of the L1 endplate; then, a pure moment was applied to the FN. The follower load was applied on each side of all segments such that the unwanted segmental rotation was less than 0.2°[17]The follower load was simulated using the

connector elements between each set of adjacent vertebrae. The nodes lying at the bottom endplate of L5 were constrained in all directions.

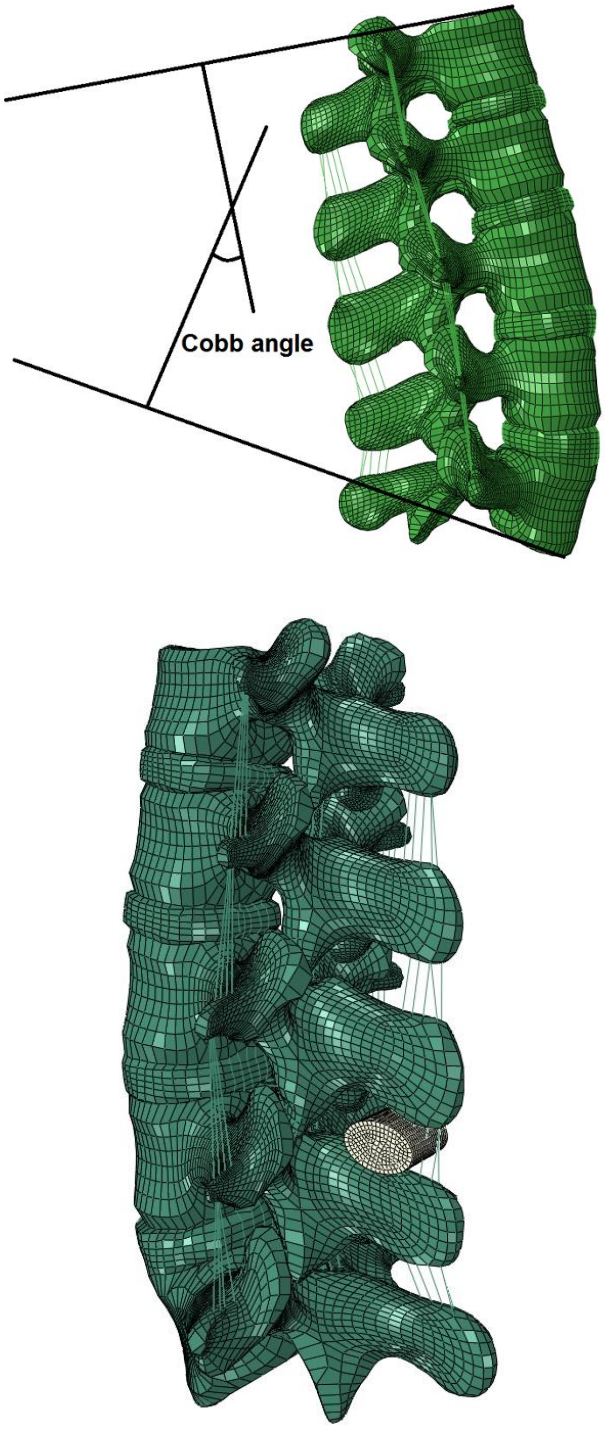


**Figure 23: Finite Element model of lumbar spine (L1-L5) instrumented with ISP device at L3-L4 segment.**

The intact L1–L5 lumbar model was validated against published *in-vitro* studies in three motion planes. The amount of rotation in each segment was compared with that reported in published *in vitro* studies. A pure moment of 10 Nm combined with an applied follower load of 400 N was used to simulate the model in flexion/extension and axial rotation, and the motion response was compared to those reported in the *in vitro* studies of Yamamoto et al.,[18] Schmoelz et al.,[19] Niosi et al.,[20] and Schilling et al.[21]

**2.3. Implanted model**

An ISP device was inserted between the ISPs of the L3 and L4 segments; the design of this device, which was of the static kind, was similar to X-Stop in that the cross-section of the device was oval (Figure 23b). The device had a core that could be accommodated between the processes without any injury to the ISL and SSL. Two wings were designed to keep the device in place. The upper elements of the device were coupled to adjacent elements on the processes of the corresponding vertebra. Titanium alloy was selected as the material for the device. The isotropic elastic formulation was used to simulate the material properties of titanium (Young's modulus: 115 GPa, Poisson's ratio: 0.3).

The implanted model was loaded in all three main directions: flexion/extension, lateral bending, and axial rotation. A hybrid protocol was used in all simulations. This hybrid protocol was implemented with the aim of examining adjacent-segment biomechanics by varying the moment until the overall deflection of the implanted L1–L5models equaled the predicted deflection for the intact model.[13, 17] The hybrid moment for the implanted model was14.5 Nm in extension. A bending moment of 10Nm was used in all other

directions because similar total ranges of motions were obtained in other motion directions.

## 3. Results

### 3.1. Validation

The FE model of the intact L1–L5 segments was validated against reported *in vitro* studies[18-21]in flexion/extension, axial rotation, and lateral bending. A precompression load of 400N and pure moment of 10Nm were applied to the FE model to predict the ROM values. Table 4 presents results of a comparison between the motion values predicted by the FE model and those reported in the published *in vitro* studies. The kinematic data predicted by the FE model were within the standard deviation or close to the average of the cadaver data obtained from the literature (Table 4). The small variations in the ROMs between the studies were observed only at the L1-L2 segment in flexion and axial rotation; these variations are attributed to the differences in the study methods and the loading conditions used in these studies. In this study, we used this validated FE model for evaluating the effect of ISP devices under hybrid loading in extension. A comparison of the ROM values at the L1-L2 segment predicted by the FE model with those obtained in the *in vitro* study of Yamamoto et al.[18] showed that the FE-model-predicted values in extension and axial rotation were in the range of those found in the *in vitro* study. In lateral bending and flexion, however, the ROM values were 25% higher and 41%lower, respectively, than

those in the *in vitro* study.[18] In other words, the FE-model-predicted motion values were lower in flexion but higher in lateral bending and axial rotation in comparison to the corresponding *in vitro* values.

### 3.2. ROM

Figure 24 shows the ROM at each lumbar level for both the intact and the implanted models in flexion, extension, lateral bending, and axial rotation. It can be seen that in the extension direction, the ROM at the L3-L4 segment decreased by 80.6% after implantation relative to the ROM at this segment in the intact lumbar spine. Further, the ROM values in adjacent segments—L2-L3 and L4-L5—increased by 29.7%and 21%, respectively, relative to those in the corresponding segments in the intact spine.

At the index level, the ROM changed by up to 8% and 3% in lateral bending and axial rotation, respectively, but it did not change in flexion. At the adjacent level, the change in the ROM was the same—by up to 2%—in flexion, lateral bending, and axial rotation.

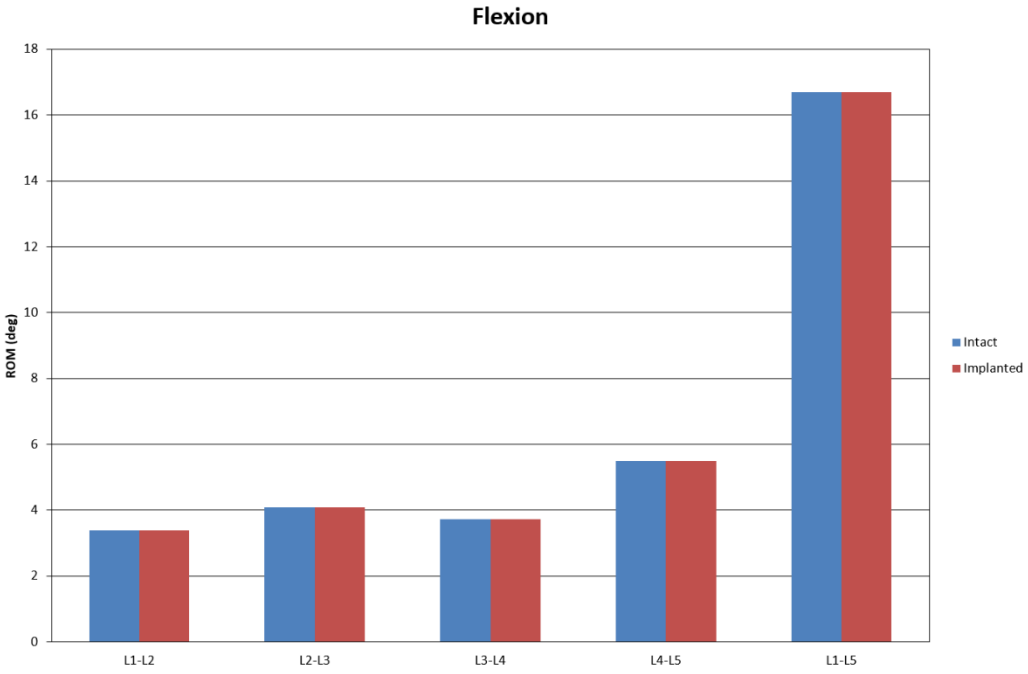
Flexion
ROM (deg)
18
16
14
12
10
8
6
4
2
0
L1-L2
L2-L3
L3-L4
L4-L5
L1-L5
Intact
Implanted

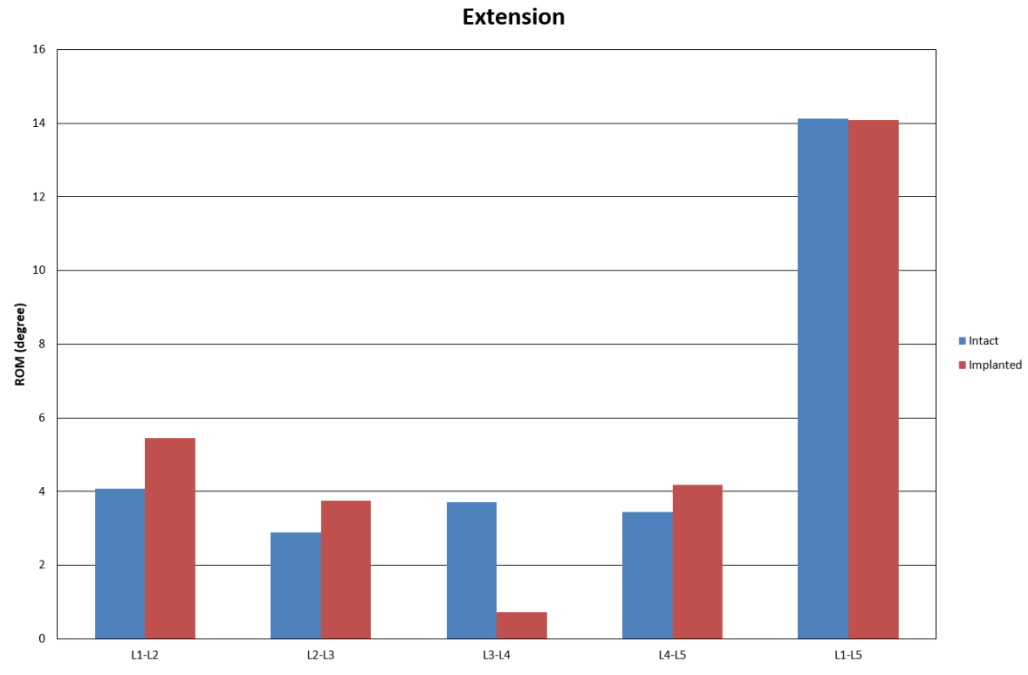
Extension
ROM (degree)
16
14
12
10
8
6
4
2
0
L1-L2
L2-L3
L3-L4
L4-L5
L1-L5
Intact
Implanted

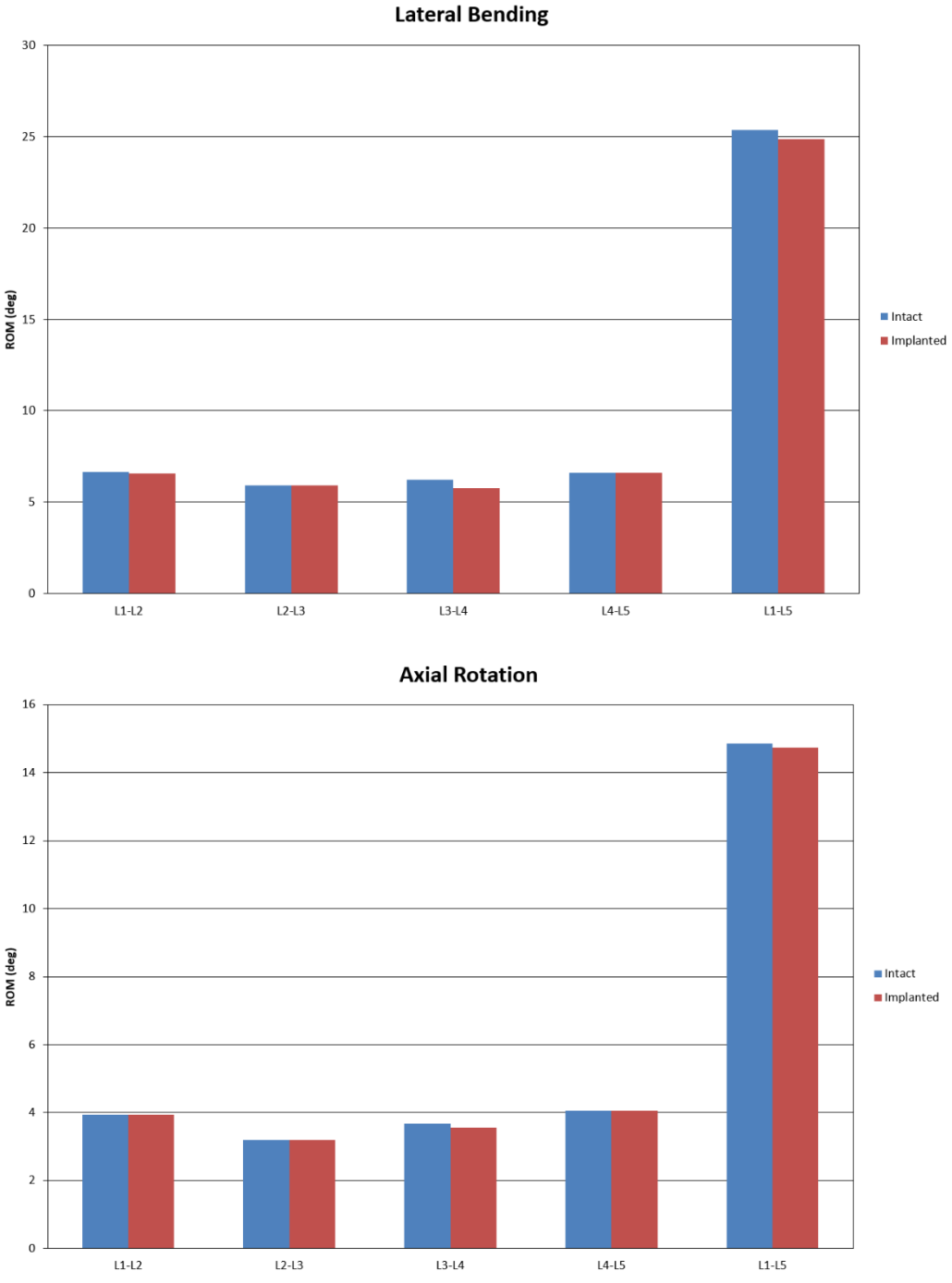


**Figure 24: The ROM for the intact and implanted lumbar model. 10 Nm bending moment and 400 N follower load applied to intact model in three main planes. 14.5 Nm hybrid moment and 400 N follower load applied to implanted model in extension and 10 Nm bending moment**

## 3.3. Facet loads

Table 5 lists the left and right facet loads at the index and adjacent levels. In extension, a comparison of facet loads at the index and adjacent levels in both the models reveals that at the index level in the implanted model, the facet loads decreased significantly—up to 99.9%—relative to the intact model. However, at the superior adjacent level (L2-L3) and the inferior adjacent level (L4-L5), the facet loads increased up to 51.9% and up to 60.3%, respectively.

At the index level, the facet load changed by up to 22% and 15% in lateral bending and axial rotation, respectively, but it did not change in flexion. At the adjacent level, the change in the facet load was the same—by up to 7%—in flexion, lateral bending, and axial rotation.

**3.4. IDP**

Table 6 presents the maximum IDP at the index and adjacent levels for both the intact and the implanted models. It can be seen that the predicted IDP at the index level in the intact model was 0.98MPa but it dropped by 52.6% after implantation. In contrast, the predicted IDP at the superior adjacent level in the intact model was 0.87 MPa but it increased significantly by 40% after implantation. Further, the predicted IDP at the inferior adjacent level in the intact model was 0.80MPa but it increased moderately by 6.6% after implantation.

At the index level, the IDP changed by 5% and 0.05% in lateral bending and axial rotation, respectively, but it did not change in flexion. At the adjacent level, the IDP was almost the same nearly similar to that in the intact model in flexion, lateral bending, and axial rotation.

### 3.5. Stress in spinous processes

Figure 25 shows the predicted von Mises stress distribution in spinous processes before and after implantation, in extension. The maximum von Mises stress in the L3 spinous process increased significantly (to 53MPa) after implantation. Similarly, the maximum predicted von Mises stress in the L4 spinous process was 48.2MPaafter implantation.

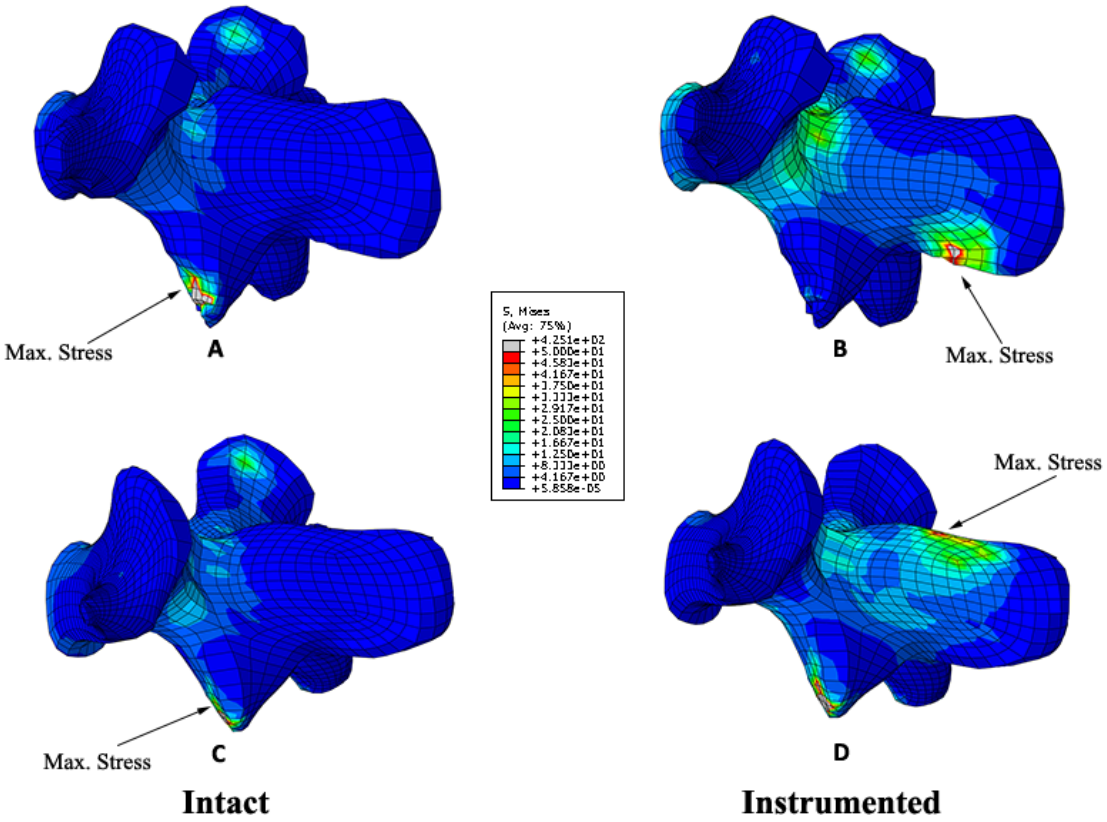


**Figure 25: Von Mises stress distribution at the posterior lumbar spine. A) Intact L3 posterior; B) implanted L3 posterior; C) Intact L4 posterior; D) implanted L4 posterior.**

## 4. Discussion

ISP devices are useful in the treatment of various lumbar spine pathologies. Several studies have investigated the effects of such devices on the biomechanical behavior of the lumbar

spine at both the index and the adjacent segments. However, none of these studies applied the hybrid protocol to investigate adjacent-segment effects. As suggested by Panjabi et al.,[13, 17] a hybrid approach gives results representing the actual scenario in clinical cases following surgical procedures and implantation. In particular, a hybrid testing protocol is appropriate for the biomechanical evaluation of spinal adjacent levels.[13] Studies have shown that the hybrid protocol is more anatomically relevant and can better represent the motion and loads experienced by the spine after surgical procedures and implantation.[12, 13]Therefore, we attempted to evaluate the biomechanical effect of ISP devices on adjacent and index segments using the hybrid protocol, which has rarely been attempted in the past in this field.

**Table 3: Mechanical Properties and element types of Lumbar FE model components**

| Component | Element Formulation | Modulus (MPa) | Poisson's Ratio |
|---|---|---|---|
| Vertebral Cancellous Bone | Isotropic, elastic hex elements | 450 | 0.25 |
| Vertebral Cortical Bone | Isotropic, elastic hex elements | 12000 | 0.3 |
| Posterior Bone | Isotropic, elastic hex elements | 3500 | 0.25 |
| Nucleus Pulposus | Isotropic, elastic hex elements | 9 | 0.4999 |
| Annulus (Ground) | Hyperelastic, Neo Hooke | C10=0.3448, D10=0.3 | |
| Annulus (Fiber) | Rebar | 357-550 | 0.3 |
| **Ligaments** | | | |
| Anterior Longitudinal | Truss elements | 7.8 (<12%), 20.0 (>12%) | 0.3 |
| Posterior Longitudinal | Truss elements | 10.0 (<11%), 20.0 (>11%) | 0.3 |
| Ligamentum Flavum | Truss elements | 15.0 (<6.2%), 19.5 (>6.2%) | 0.3 |
| Intertransverse | Truss elements | 10.0 (<18%), 58.7 (>18%) | 0.3 |
| Interspinous | Truss elements | 10.0 (<14%), 11.6 (>14%) | 0.3 |
| Supraspinous | Truss elements | 8.0 (<20%), 15.0 (>20%) | |
| Capsular | Truss elements | 7.5 (<25%), 32.9(25%) | 0.3 |
| Apophyseal Joints | GAPUNI | | |

The FE model (L1–L5) used in the study was successfully validated in all three main planes via a comparison of its results with those of various published *in vitro* studies. Specifically, the model was validated from the fact that the kinematic data predicted by the FE model in all segments were within the standard deviation or close to the average of the results of *in vitro* studies.

According to literature,[2, 3, 22] all commercially available ISP devices affect the biomechanics of the lumbar spine only in extension but not in flexion, lateral bending, and axial rotation. Therefore, we modeled an elliptic cylinder-shaped device with lateral wings that mimicked the X-STOP device and placed it between the L3 and L4 spinous processes of the FE model (L1–L5).

**Table 4: The predicted ROM by the intact FE model compared with the reported ROM from the in vitro studies.**

| | **Flexion** | **Extension** | **Lateral Bending** | **Axial Rotation** |
|---|---|---|---|---|
| **L1-L2** | | | | |
| Yamamoto et. al (Yamamoto et al., 1989), 10Nm | 5.8±0.6 | 4.3±0.5 | 4.7±0.4 (L)<br>5.2±0.4 (R) | 2.6±0.5 (L)<br>2.0±0.6 (R) |
| Present Study, 10Nm | 3.4 | 4.1 | 7.0 (L)<br>7.1 (R) | 3.9 (L)<br>3.5 (R) |
| **L2-L3** | | | | |
| Schmoelz et al (Schmoelz et al., 2003), 10Nm | 4.3±1.0 | 4.6±2.2 | 5.4±2.2 | 1.0±1.0 |
| Yamamoto et. al (Yamamoto et al., 1989), 10Nm | 6.5±0.3 | 4.3±0.3 | 7.0±0.6 (L)<br>7.0±0.6 (R) | 2.2±0.4 (L)<br>3.0±0.4 (R) |
| Present Study, 10Nm | 4.1 | 2.9 | 6.0 (L)<br>6.7 (R) | 3.2 (L)<br>3.4 (R) |
| **L3-L4** | | | | |
| Niosi et al (Niosi et al., 2006), 7.5Nm | 4.4 ±2.0 | 2.4 ± 0.9 | 2.4 ± 1.2 | 1.2 ±0.5 |
| Schilling et al (Schilling et al., 2011), 7.5Nm | 4.67±1.79 | 2.18±0.54 | 7.66 ±2.91 | 4.67 ±2.52 |
| Schmoelz et al (Schmoelz et al., 2003), 10Nm | 5.0±1.0 | 4.0±1.3 | 4.7±2.0 | 1.0±0.6 |
| Yamamoto et. al (Yamamoto et al., 1989), 10Nm | 7.5 ±0.8 | 3.7 ±0.3 | 5.7 ±0.3 (L)<br>5.8 ± 0.5 (R) | 2.7 ± 0.4 (L)<br>2.5 ±0.4 (R) |
| Present Study, 10Nm | 3.7 | 3.7 | 6.0 (L)<br>7.5 (R) | 3.7 (L)<br>3.8 (R) |

| **L4-L5** | | | | |
|---|---|---|---|---|
| Schilling et al (Schilling et al., 2011), 7.5Nm | 5.62 ±2.17 | 3.32 ±1.12 | 7.76 ±1.85 | 5.16±1.30 |
| Yamamoto et. al (Yamamoto et al., 1989), 10Nm | 8.9 ±0.7 | 5.8 ±0.4 | 5.5 ±0.5 (L)<br>5.9 ±0.5 (R) | 1.7±0.3 (L)<br>2.7±0.5 (R) |
| Present Study, 10Nm | 5.5 | 3.5 | 6.7 (L)<br>7.3 (R) | 4.1 (L)<br>4.0 (R) |

In our study, we simulated the implanted model in all motion directions. In general, the changes in the ROM, IDP, and facet loads were negligible in directions other than the extension direction, as reported in the literature [2, 4]. As expected, the IDP, facet load, and ROM decreased after ISP implantation in extension at the implanted level.

**Table 5: Comparison of the predicted facet load between the intact and instrumented FE models for the index and the adjacent segments.**

| | | Flexion | | | Extension | | | Lateral bending | | | Axial rotation | | |
|---|---|---|---|---|---|---|---|---|---|---|---|---|---|
| Segment | | L2-L3 | L3-L4 | L4-L5 | L2-L3 | L3-L4 | L4-L5 | L2-L3 | L3-L4 | L4-L5 | L2-L3 | L3-L4 | L4-L5 |
| Intact | Right | 45.63 | 76.68 | 25.89 | 127.13 | 147.36 | 120.37 | 29.40 | 54.67 | 76.17 | 0 | 0 | 0 |
| | Left | 54.40 | 77.44 | 19.46 | 151.72 | 156.99 | 194.33 | 37.51 | 59.35 | 21.93 | 172.11 | 175.72 | 214.00 |
| Implanted | Right | 45.66 | 76.68 | 25.89 | 184.02 | 0.06 | 192.95 | 29.84 | 66.32 | 73.95 | 0 | 0 | 0 |
| | Left | 54.40 | 77.44 | 19.46 | 230.38 | 11.06 | 299.92 | 37.53 | 46.12 | 23.55 | 172.16 | 150.12 | 215.17 |

Our kinematic results at the index level in extension were in agreement with the corresponding results in the literature.[2, 4, 7, 11]Specifically, our FE study predicted that the ROM reduced to 0.72° at the index level after implantation in extension, which is similar to the observed reduction of 0.5° ± 0.3° by Lindsey et al.[7] after ISP implantation, at the index level in extension. Another study[4] reported similar results, i.e., reduction in extension, after ISP implantation in flexion-extension. Although we applied the hybrid

protocol, which leads to higher loading (14.5Nm), the restriction of motion in extension at the implanted level was almost the same as that in the aforementioned studies, owing to the design of ISP devices that makes them restrict motion in extension.

The question then is whether ISP surgery affects the kinematics of adjacent segments. Lindsey et al.,[7] who determined the ROM at the adjacent levels (L2-L3 and L4-L5) after implantation of the ISP device X-Stop into a cadaver lumbar spine (L2-L5), reported that the ROM at adjacent segments was not significantly affected in flexion-extension. Similarly, Hartmann et al.[4] reported that there was no significant change in the ROM for all segments (L2–L5) in flexion-extension under a pure moment of 7.5 Nm and follower load of 400 N. However, they reported a significant increase in the ROM for an entire specimen (L2–L5) during lateral bending and rotation after implantation of four different ISP devices, and they suggested further investigation of ISP devices for determining ALEs.

In contrast to these findings, our present FE model predicted increased motion in the superior and inferior adjacent segments after ISP implantation in extension under hybrid loading (pure moment of 14.5Nm) and follower load of 400N. Although an increase in motion may not lead to adjacent-segment hypermobility because of changes in extension only and is possibly not clinically significant, it may be useful to investigate the effect of motion changes on other components at adjacent levels, such as facet joints and intervertebral discs.

Further, the facet loads predicted by the FE model in this study for the intact model at the implanted segment were consistent with those reported in the literature.[16] After implantation of the ISP device, the facet load reduced at the index level in extension. Similar

findings were reported by Wiseman et al.:[9] they also reported ALEs after implantation and found an increase in the facet load (by 10%)at the superior adjacent level and a decrease in the facet load (by 17%) at the inferior adjacent level. However, they also reported that the changes were not significantly different between the intact and implanted specimens. In contrast to their results, our FE model predicted that the facet load increased by up to 60% in extension at both the superior and the inferior adjacent levels. This contrast in results can be explained as follows. Wiseman et al. placed a pressure-sensitive film in the facet joint to investigate the load values and compared them between the intact and implanted specimens at the adjacent and implanted levels using a load control protocol. However, this approach has some drawbacks: a ±15% error, which is associated with the pressure measurement; variation in the contact area of the pressure sensor; and unsuitability of the load control protocol for adjacent-level investigations. In comparison, the hybrid protocol is more appropriate for evaluating ALEs after implantation of a healthy lumbar FE model. Therefore, our results suggest that after ISP implantation, the adjacent-level facet joint will be affected over the long term and should be subjected to further investigation. At the index level, the facet loads changed by up to 22% and 15% in lateral bending and axial rotation, respectively. These changes were attributed to the wings of the ISP device, which limit the motion in these directions. However, the total facet load in the index segment remained similar to that in the intact model, and only the load sharing between the right and left facets changed. In contrast, in extension, the total facet load changed, i.e., decreased.

ISP devices prevent motion in extension and unload the intervertebral disc, resulting in an enlargement of the central canal for the treatment of neurogenic intermittent claudication.

As expected, the FE model predicted that the ISP device would release the IDP at the index level in extension. This result was in agreement with cadaver studies in literature.[2, 10] However, the FE model predicted that the IDP at the superior adjacent segment, L2-L3,increased by almost 40% after ISP implantation and that this IDP was very close to that in the intact case at the inferior adjacent segment, L4-L5, in extension. Unfortunately, these results disagree with those of a cadaver study by Swanson et al.[10] One of the reasons for this disagreement is that Swanson et al. performed load control (i.e., a flexibility test) instead of displacement control (i.e., a hybrid test) for adjacent-level investigation. Another reason is that, as mentioned in the previous paragraph when discussing the results of facet loads, Swanson et al. used a pressure transducer, which may not measure the IDP correctly, as suggested by Wilke et al.[2] Therefore, the efficiency of intended use of ISP devices may not be correctly interpreted by flexible testing.

Although successful outcomes have been reported pertaining to the use of ISP devices in the treatment of lumbar spine diseases,[23, 24] a few cases of ISP failure after ISP surgery have also been reported. For example, Miller et al.[25] reported two cases of ISP failure, in which gradual erosion of the spinous processes occurred because of consistent motion at the spacer–bone interface. Furthermore, Bowers et al.[26] published medical records of complications associated with implantation of the X-Stop device. They reported the fracture of spinous processes of 3 out of 13 patients and suggested possible causes of fracture, including the degree of osteoporosis and over-distraction of the interspinous space with an oversized implant. Kim et al.[27] reported a high rate (52%) of spinous process fracture associated with IPS surgery carried out on 39 patients at their institution. One of the main reasons for spinous process fracture would be the stress concentration at the bone after ISP

implantation. Our FE study drew a clear conclusion in this regard and showed that the stress distribution in the spinous processes at the index level changed significantly after implantation. In the intact model, most of the stresses were concentrated at the facet joints. After implantation, however, a greater part of the stress was transferred to the implanted region (Figure 25). Similarly, other studies[11] reported an increase in the load transmitted through spinous processes. Spinous processes may be strong enough to withstand the stresses after implantation,[28] but ISP devices may cause gradual erosion at the bone–implant interface under constant stress and motion, thereby increasing the recurrence probability of preoperative symptoms. In addition, the success rate of the outcome of lumbar treatment by an ISP device also depends largely on the bone density[27] and the overall lumbar scoliosis[29] of patients.

Like any other numerical study, this study has certain limitations: unlike cadaver studies, FE models do not account for the variation in material properties or geometry. Furthermore, some assumptions and simplifications in the model may not represent real values for the human spine. Nevertheless, the predicted data for the intact case are in agreement with the results of cadaver studies.

## 5. References

[1] Erbulut DU, Zafarparandeh I, Ozer aF, Goel VK. Biomechanics of posterior dynamic stabilization systems. Adv Orthop 2013; 2013: 1-6.

[2] Wilke H-J, Drumm J, Häussler K, Mack C, Steudel W-I, Kettler A. Biomechanical effect of different lumbar interspinous implants on flexibility and intradiscal pressure. Eur Spine J 2008; 17(8): 1049-1056.

[3] Bono CM, Vaccaro AR. Interspinous process devices in the lumbar spine. J Spinal Disord Tech 2007; 20(3): 255-261.

[4] Hartmann F, Dietz S-O, Hely H, Rommens PM, Gercek E. Biomechanical effect of different interspinous devices on lumbar spinal range of motion under preload conditions. Arch Orthop Trauma Surg 2011; 131(7): 917-926.

[5] Sangiorgio SN, Sheikh H, Borkowski SL, Khoo L, Warren CR, Ebramzadeh E. Comparison of three posterior dynamic stabilization devices. Spine 2011; 36(19): E1251-E1258.

[6] Kondrashov DG, Hannibal M, Hsu KY, Zucherman JF. Interspinous Process Decompression With the X-STOP Device for Lumbar Spinal Stenosis. J Spinal Disord Tech 2006; 19(5): 323-327.

[7] Lindsey DP, Swanson KE, Fuchs P, Hsu KY, Zucherman JF, Yerby Sa. The effects of an interspinous implant on the kinematics of the instrumented and adjacent levels in the lumbar spine. Spine 2003; 28(19): 2192-2197.

[8] Siddiqui M, Karadimas E, Nicol M, Smith FW, Wardlaw D. Effects of X-STOP device on sagittal lumbar spine kinematics in spinal stenosis. J Spinal Disord Tech 2006; 19(5): 328-333.

[9] Wiseman CM, Lindsey DP, Fredrick AD, Yerby Sa. The effect of an interspinous process implant on facet loading during extension. Spine 2005; 30(8): 903-7.

[10] Swanson KE, Lindsey DP, Hsu KY, Zucherman JF, Yerby Sa. The effects of an interspinous implant on intervertebral disc pressures. Spine 2003; 28(1): 26-32.

[11] Lafage V, Gangnet N, Sénégas J, Lavaste F, Skalli W. New interspinous implant evaluation using an in vitro biomechanical study combined with a finite-element analysis. Spine 2007; 32(16): 1706-1713.

[12] Goel VK, Grauer JN, Patel TC, Biyani A, Sairyo K, Vishnubhotla S, Matyas A, Cowgill I, Shaw M, Long R, Dick D, Panjabi MM, Serhan H. Effects of charité artificial disc on the implanted and adjacent spinal segments mechanics using a hybrid testing protocol. Spine 2005; 30(24): 2755-2764.

[13] Panjabi M. Hybrid multidirectional test method to evaluate spinal adjacent-level effects. Clin Biomech 2007; 22(3): 257-265.

[14] Panjabi MM, Chen NC, Shin E, Wang J-L. The cortical shell architecture of human cervical vertebral bodies. Spine 2001; 26(22): 2478-2484.

[15] Erbulut DU, Zafarparandeh I, Lazoglu I, Ozer AF. Application of an asymmetric finite element model of the C2-T1 cervical spine for evaluating the role of soft tissues in stability. Med Eng Phys 2014.

[16] Kiapour A, Ambati D, Hoy RW, Goel VK. Effect of graded facetectomy on biomechanics of Dynesys dynamic stabilization system. Spine 2012; 37(10): E581-E589.

[17] Panjabi M, Malcolmson G, Teng E, Tominaga Y, Henderson G, Serhan H. Hybrid Testing of Lumbar CHARITE Versus Fusions. Spine 2007; 32(9): 959-966.

[18] Yamamoto I, Panjabi MM, Crisco T, Oxland T. Three-Dimensional Movements of the Whole Lumbar Spine and Lumbosacral Joint. Spine 1989; 14(11): 1256-1260.

[19] Schmoelz W, Huber JF, Nydegger T, Dipl-Ing, Claes L, Wilke HJ. Dynamic stabilization of the lumbar spine and its effects on adjacent segments: an in vitro experiment. J Spinal Disord Tech 2003; 16(4): 418-423.

[20] Niosi Ca, Zhu Qa, Wilson DC, Keynan O, Wilson DR, Oxland TR. Biomechanical characterization of the three-dimensional kinematic behaviour of the Dynesys dynamic stabilization system: an in vitro study. Eur Spine J 2006; 15(6): 913-922.

[21] Schilling C, Kru¨ger S, Grupp TM, Duda GN, Blo¨mer W, Rohlmann A. The effect of design parameters of dynamic pedicle screw systemson kinematics and load bearing: an in vitro study. Eur Spine J 2011; 20(2): 297-307.

[22] Richards JC, Majumdar S, Lindsey DP, Beaupré GS, Yerby Sa. The treatment mechanism of an interspinous process implant for lumbar neurogenic intermittent claudication. Spine 2005; 30(7): 744-749.

[23] Zucherman JF, Hsu KY, Hartjen CA, Mehalic TF, Implicito DA, Martin MJ, Johnson DRI, Skidmore GA, Vessa PP, Dwyer JW, Puccio ST, Cauthen JC, Ozuna RM. A Multicenter, Prospective, Randomized Trial Evaluating the X STOP Interspinous Process Decompression System for the Treatment of Neurogenic Intermittent Claudication: Two-Year Follow-Up Results. Spine 2005; 30(12): 1351-1358

[24] Lee J, Hida K, Seki T, Iwasaki Y, Minoru A. An Interspinous Process Distractor (X STOP) for Lumbar Spinal Stenosis in Elderly Patients: Preliminary Experiences in 10 Consecutive Cases. J Spinal Disord Tech 2004; 17(1): 72-77.

[25] Miller JD, Miller MC, Lucas MG. Erosion of the spinous process: a potential cause of interspinous process spacer failure. J Neurosurg Spine 2010; 12(2): 210-3.

[26] Bowers C, Amini A, Dailey AT, Schmidt MH. Dynamic interspinous process stabilization: review of complications associated with the X-Stop device. Neurosurg Focus 2010; 28(6): E8.

[27] Kim DH, Shanti N, Tantorski ME, Shaw JD, Li L, Martha JF, Thomas AJ, Parazin SJ, Rencus TC, Kwon B. Association between degenerative spondylolisthesis and spinous process fracture after interspinous process spacer surgery. Spine J 2012; 12(6): 466-72.

[28] Shepherd DE, Leahy JC, Mathias KJ, Wilkinson SJ, Hukins DW. Spinous process strength. Spine 2000; 25(3): 319-23.

[29] Rolfe KW, Zucherman JF, Kondrashov DG, Hsu KY, Nosova E. Scoliosis and interspinous decompression with the X-STOP: prospective minimum 1-year outcomes in lumbar spinal stenosis. Spine J 2010; 10(11): 972-8.

# Chapter 6:

# Conclusions

In summary, a novel method was used tconstruct the FE model of the cervical and lumbar spines. Using the novel method, it was possible to create a fine hexahedral mesh on the vertebrae and discs while keeping them integrated in their interface. Compared to the models in the literature, both models had the exact geometry of the human spine with hexahedral mesh.

The models were validated with previously proposed models in the literature. The range of motion was compared in the three main motion planes. For the cervical spine, the moment-rotation curves were created. The predicted response followed the results of the in vitro studies reasonably. The cervical FE model predicted coupled motion for the lateral bending and the axial rotation. The asymmetry nature of the cervical spine was considered in the modeling.

The application of each model was studied by adding different types of implants to the models. Using the hybrid protocol for the first time in the literature the effect of X-STOP device was studies. The results showed that although the device works well for limiting the motion in extension direction, the adjacent levels' effect was considerable. Also, there was stress concentration on the bone and the device interface.

In general, the proposed models can be used for other application in human spine biomechanics. Namely, whiplash trauma can simulated with the proposed FE model of the cervical spine.